ADVANCES IN PHYSICS, 1994, VOL. 43, NO. 3, 357–459

Theory of phase-ordering kinetics

By A. J. BRAY
Department of Theoretical Physics, The University,
Manchester M13 9PL, England

[Received 23 May 1994; accepted 29 September 1994]

Abstract

The theory of phase-ordering dynamics, that is the growth of order through domain coarsening when a system is quenched from the homogeneous phase into a broken-symmetry phase, is reviewed, with the emphasis on recent developments. Interest will focus on the scaling regime that develops at long times after the quench. How can one determine the growth laws that describe the time dependence of characteristic length scales, and what can be said about the form of the associated scaling functions? Particular attention will be paid to systems described by more complicated order parameters than the simple scalars usually considered, for example vector and tensor fields. The latter are needed, for example, to describe phase ordering in nematic liquid crystals, on which there have been a number of recent experiments. The study of topological defects (domain walls, vortices, strings and monopoles) provides a unifying framework for discussing coarsening in these different systems.

Contents

0001–8732/94 $25·00

1. Introduction

The theory of phase-ordering kinetics or 'domain coarsening' following a temperature quench from a homogeneous phase into a two-phase region has a history going back more than three decades to the pioneering work of Lifshitz [1], Lifshitz and Slyozov [2] and Wagner [3]. Since that time, many excellent reviews have appeared,

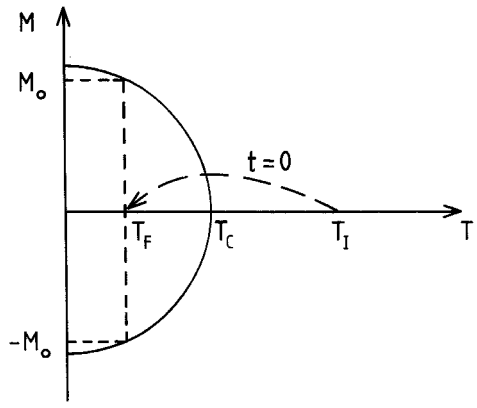

Figure 1. Magnetization of the Ising model in zero applied field as a function of temperature (schematic), showing spontaneous symmetry breaking at T_C. The arrow indicates a temperature quench, at time $t = 0$, from T_I to T_F.

including those by Gunton *et al.* [4], Binder [5], Furukawa [6] and Langer [7]. In the present article, I shall not therefore attempt to cover the complete history of the field. Rather, I shall concentrate on some of the recent developments, over the past 5 years or so, which in my view are interesting and represent significant advances or new directions of research, for example the recent interest in systems with non-scalar order parameters. The fundamental concepts and background material necessary for the understanding and appreciation of these new developments will, nevertheless, be discussed in some detail. It follows that, while this article does not aim to be a complete or comprehensive account, it does aspire to be self-contained and comprehensive to non-experts. By adopting a fairly pedagogical approach, I hope that the article may also serve as a useful introduction to the field.

In order to keep the length of the article within reasonable bounds, I shall concentrate primarily on theoretical developments, although important results from experiment and simulations will be cited as appropriate. For the same reason, I apologise in advance to all those authors whose work has not been explicitly discussed.

Systems quenched from a disordered phase into an ordered phase do not order instantaneously. Instead, the length scale of ordered regions grows with time as the different broken-symmetry phases compete to select the equilibrium state. To fix our ideas, it is helpful to consider the simplest, and most familiar, system: the ferromagnetic Ising model. Figure 1 shows the spontaneous magnetization as a function of temperature. The arrow indicates a temperature quench, at time $t = 0$, from an initial temperature T_I above the critical point T_C to a final temperature T_F below T_C. At T_F there are two equilibrium phases, with magnetization $\pm M_0$. Immediately after the quench, however, the system is in an unstable disordered state corresponding to equilibrium at temperature T_I. The theory of phase ordering kinetics is connected with the dynamical evolution of the system from the initial disordered state to the final equilibrium state.

Part of the fascination of the field, and the reason why it remains a challenge more than three decades after the first theoretical papers appeared, is that, in the thermodynamic limit, final equilibrium is never achieved! This is because the longest relaxation time diverges with the system size in the ordered phase, reflecting the broken ergodicity. Instead, a network of domains of the equilibrium phases develops, and the typical length scale associated with these domains increases with time t. This situation

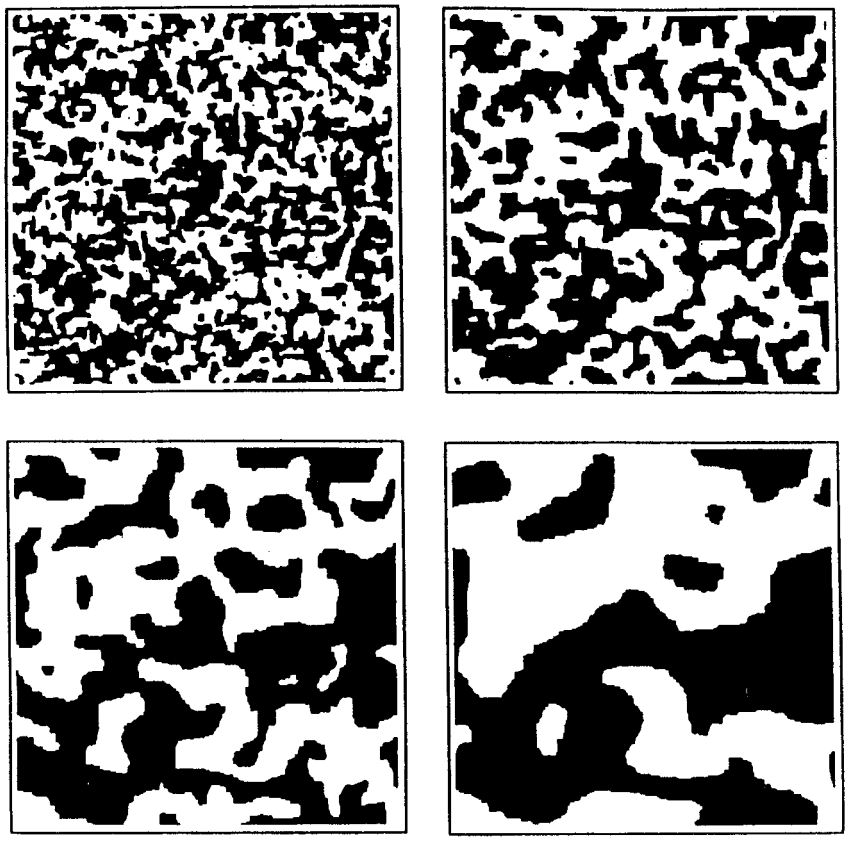

Figure 2. Monte Carlo simulation of domain growth in the $d = 2$ Ising model at $T = 0$ (taken from Kissner [8]). The system size is 256×256, and the snapshots correspond to 5, 15, 60 and 200 Monte Carlo steps per spin after a quench from $T = \infty$.

is illustrated in figure 2, which shows a Monte Carlo simulation of a two-dimensional Ising model, quenched from $T_I = \infty$ to $T_F = 0$. Inspection of the time sequence may persuade the reader that domain growth is a *scaling* phenomenon; the domain patterns at later times look statistically similar to those at earlier times, apart from a global change of scale. This 'dynamic scaling hypothesis' will be formalized below.

For pedagogical reasons, we have introduced domain growth in the context of the Ising model and shall continue to use magnetic language for simplicity. A related phenomenon that has been studied for many decades, however, by metallurgists, is the spinodal decomposition of binary alloys, where the late stages of growth are known as Ostwald ripening. Similar phenomena occur in the phase separation of fluids or binary liquids, although in these cases the phase separation is accelerated by the Earth's gravitational field, which severely limits the temporal duration of the scaling regime. The gravitational effect can be moderated by using density-matched binary liquids and/or performing the experiments under microgravity. All the above systems, however, contain an extra complication not present in the Ising ferromagnet. This is most simply seen by mapping an AB alloy onto an Ising model. If we represent an A atom by an up spin, and a B atom by a down spin, then the *equilibrium* properties of the alloy can be modelled very nicely by the Ising model. There is one important feature of the alloy, however, that is not captured by the Ising model with conventional Monte

Carlo dynamics. Flipping a single spin in the Ising model corresponds to converting an A atom to a B atom (or vice versa), which is inadmissible. The dynamics must conserve the number of A and B atoms separately, that is the magnetization (or order parameter) of the Ising model should be *conserved*. This will influence the form of the coarse-grained equation of motion, as discussed in section 2 and lead to slower growth than for a non-conserved order parameter.

In all the systems mentioned so far, the order parameter (e.g. the magnetization of the Ising model) is a scalar. In the last few years, however, there has been increasing interest in systems with more complex order parameters. Consider, for conceptual simplicity, a planar ferromagnet, in which the order parameter is a vector confined to a plane. After a quench into the ordered phase, the magnetization will point in different directions in different regions of space, and singular lines (vortex lines) will form at which the direction is not well defined. These 'topological defects' are the analogue of domain walls for the scalar systems. We shall find that, quite generally, an understanding of the relevant topological defects in the system, combined with the scaling hypothesis, will take us a long way towards understanding the forms of the growth laws and scaling functions for phase ordering in a wide variety of systems.

The article is organized as follows. The following section introduces most of the important concepts, presents dynamical models appropriate to the various phase-ordering systems and analyses these models using simple physical arguments. Section 3 broadens the discussion to more general phase-ordering systems, with non-scalar order parameters and introduces the key concept of topological defects which, in later sections, will provide a unifying framework for analytical treatments. Section 4 involves a temporary excursion to the realm of exactly soluble models. These models, although of interest in their own right, unfortunately lack many of the physical features of more realistic models. In section 5, approximate analytical treatments are presented for the more physical models introduced in sections 2 and 3. Finally, sections 6–8 present some exact results for the short-distance behaviour and the growth laws for these systems and make some observations concerning universality classes for the dynamics of phase ordering.

2. Dynamical models

It is convenient to set up a continuum description in terms of a coarse-grained order-parameter field (e.g. the magnetization density) $\phi(\mathbf{x}, t)$, which we shall initially take to be a scalar field. A suitable Landau free-energy functional to describe the ordered phase is

$$F[\phi] = \int \mathrm{d}^d x \, [\tfrac{1}{2}|\nabla\phi|^2 + V(\phi)], \tag{1}$$

where the potential $V(\phi)$ has a double-well structure, for example $V(\phi) = (1 - \phi^2)^2$. We shall take the minima of $V(\phi)$ to occur at $\phi = \pm 1$ and adopt the convention that $V(\pm 1) = 0$. The potential $V(\phi)$ is sketched in figure 3. The two minima of V correspond to the two equilibrium states, while the gradient-squared term in equation (1) associates an energy cost with an interface between the phases.

In the case where the order parameter is not conserved, an appropriate equation for the time evolution of the field ϕ is

$$\frac{\partial\phi}{\partial t} = -\frac{\delta F}{\delta\phi} = \nabla^2\phi - V'(\phi), \tag{2}$$

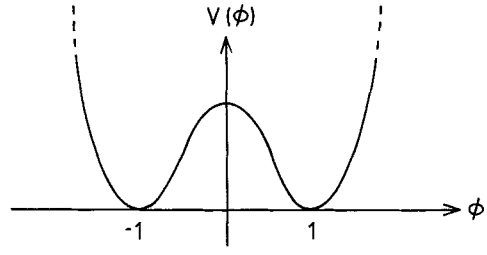

Figure 3. Typical form of the symmetric double-well potential $V(\phi)$ in equation (2). The detailed functional form of $V(\phi)$ is not important.

where $V'(\phi) \equiv \mathrm{d}V/\mathrm{d}\phi$. A kinetic coefficient Γ, which conventionally multiplies the right-hand side of equation (2), has been absorbed into the time scale. Equation (2), a simple reaction–diffusion equation, corresponds to simple gradient descent, that is the rate of change in ϕ is proportional to the gradient of the free-energy functional in function space. This equation provides a suitable coarse-grained description of the Ising model, as well as alloys that undergo an order–disorder transition on cooling through T_C, rather than phase separating. Such alloys form a two-sublattice structure, with each sublattice occupied predominantly by atoms of one type. In Ising model language, this corresponds to antiferromagnetic ordering. The magnetization is no longer the order parameter, but a 'fast mode', whose conservation does not significantly impede the dynamics of the important 'slow modes'.

When the order parameter is conserved, as in phase separation, different dynamics are required. In the alloy system, for example, it is clear physically that A and B atoms can exchange only locally (not over large distances), leading to diffusive transport of the order parameter, and an equation of motion of the form

$$\frac{\partial \phi}{\partial t} = \nabla^2 \frac{\delta F}{\delta \phi}$$
$$= -\nabla^2[\nabla^2 \phi - V'(\phi)], \tag{3}$$

which can be written in the form of a continuity equation, $\partial_t \phi = -\nabla \cdot \mathbf{j}$, with current $\mathbf{j} = \lambda \nabla(\delta F/\delta \phi)$. In equation (3), we have absorbed the transport coefficient λ into the time scale.

Equations (2) and (3) are sometimes called the time-dependent Ginzburg–Landau (TDGL) equation and the Cahn–Hilliard equation respectively. A more detailed discussion of them in the present context can be found in the lectures by Langer [7]. The same equations with additional Langevin noise terms on the right-hand sides are familiar from the theory of critical dynamics, where they are called model A and model B respectively in the classification of Hohenberg and Halperin [9].

The absence of thermal noise terms in equations (2) and (3) indicates that we are effectively working at $T = 0$. A schematic renormalization group (RG) flow diagram for T is given in figure 4, showing the three RG fixed points at 0, T_C and ∞, and the RG flows. Under coarse graining, temperatures above T_C flow to infinity, while those below T_C flow to zero. We therefore expect the final temperature T_F to be an irrelevant variable (in the scaling regime) for quenches into the ordered phase. This can be shown explicitly for systems with a conserved order parameter [10, 11]. For this case the thermal fluctuations at T_F simply renormalize the bulk order parameter and the surface tension of the domain walls; when the characteristic scale of the domain pattern is large

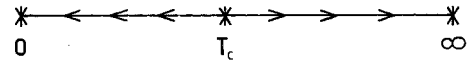

Figure 4. Schematic RG flow diagram, with fixed points at $T = 0$, T_C and ∞. All $T > T_C$ are equivalent to $T = \infty$ and all $T < T_C$ to $T = 0$, as far as large length-scale properties are concerned.

compared with the domain wall thickness (i.e. the bulk correlation length in equilibrium), the system behaves *as if* it were $T = 0$, with the temperature dependence entering through T-dependent model parameters.

In a similar way, any short-range correlations present at T_I should be irrelevant in the scaling regime, that is all initial temperatures are equivalent to $T_I = \infty$. Therefore we shall take the *initial conditions* to represent a completely disordered state. For example, one could choose the 'white-noise' form

$$\langle \phi(\mathbf{x}, 0)\phi(\mathbf{x}', 0)\rangle = \Delta\delta(\mathbf{x} - \mathbf{x}'), \tag{4}$$

where $\langle \ldots \rangle$ represents an average over an ensemble of initial conditions, and Δ controls the size of the initial fluctuations in ϕ. The above discussion, however, indicates that the precise form of the initial conditions should not be important, as long as only short-range spatial correlations are present.

The challenge of understanding phase-ordering dynamics therefore can be posed as finding the nature of the late-time solutions of deterministic differential equations such as equations (2) and (3), subject to random initial conditions. A physical approach to this formal mathematical problem is based on studying the structure and dynamics of the topological defects in the field ϕ. This is approach that we shall adopt. For scalar fields, the topological defects are just domain walls.

2.1. *The scaling hypothesis*

Although originally motivated by experimental and simulation results for the structure factor and pair correlation function [12–14], for ease of presentation it is convenient to introduce the scaling hypothesis first, and then to discuss its implications for growth laws and scaling functions. Briefly, the scaling hypothesis states that there exists, at late times, a single characteristic length scale $L(t)$ such that the domain structure is (in a statistical sense) independent of time when lengths are scaled by $L(t)$. It should be stressed that scaling has not been proved, except in some simple models such as the one-dimensional Glauber model [15] and the n-vector model with $n = \infty$ [16]. However, the evidence in its favour in compelling (see, for example, figure 5).

We shall find, in section 7, that the scaling hypothesis, together with a result derived in section 6 for the tail of the structure factor, is sufficient to determine the form of $L(t)$ for most cases of interest.

Two commonly used probes of the domain structure are the equal time pair correlation function

$$C(\mathbf{r}, t) = \langle \phi(\mathbf{x} + \mathbf{r}, t)\phi(\mathbf{x}, t)\rangle, \tag{5}$$

and its Fourier transform, the equal-time structure factor,

$$S(\mathbf{k}, t) = \langle \phi_{\mathbf{k}}(t)\phi_{-\mathbf{k}}(t)\rangle. \tag{6}$$

Here angular brackets indicate an average over initial conditions. The structure factor can, of course, be measured in scattering experiments. The existence of a single

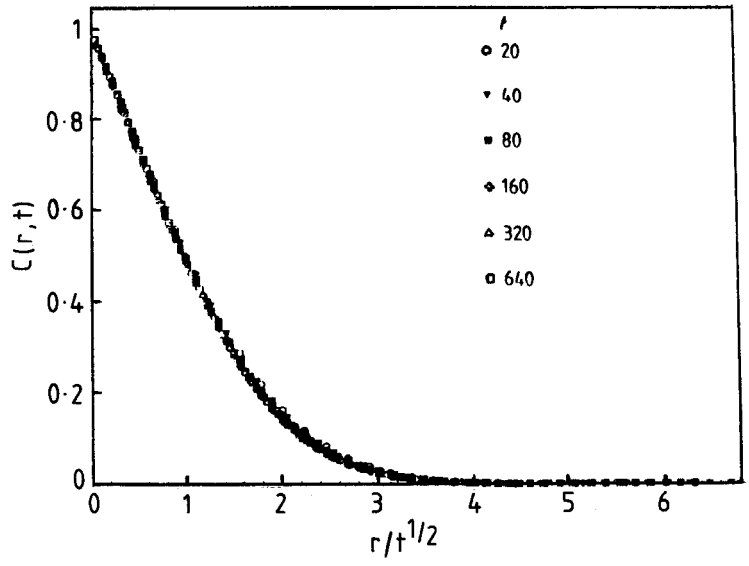

Figure 5. Scaling function $f(x)$ for the pair correlation function of the $d = 2$ Ising model with non-conserved order parameter (from [17]). The time t is the number of Monte Carlo steps per spin.

characteristic length scale, according to the scaling hypothesis, implies that the pair correlation function and the structure factor have the scaling forms

$$C(\mathbf{r}, t) = f\left(\frac{r}{L}\right), \qquad S(\mathbf{k}, t) = L^d g(kL), \tag{7}$$

where d is the spatial dimensionality, and $g(y)$ is the Fourier transform of $f(x)$. Note that $f(0) = 1$, since (at $T = 0$) there is perfect order within a domain.

At general temperatures $T < T_C$, $f(0) = M^2$, where M is the equilibrium value of the order parameter. (Note that the *scaling limit* is defined by $r \gg \xi, L \gg \xi$, with r/L arbitrary, where ξ is the equilibrium correlation length.) Alternatively, we can extract the factor M^2 explicitly by writing $C(\mathbf{r}, t) = M^2 f(r/L)$. The statement that T is irrelevant then amounts to asserting that any remaining temperature dependence can be absorbed into the domain scale L, such that the function $f(x)$ is independent of T.

The scaling forms (7) are well supported by simulation data and experiment. As an example, figure 5 shows the scaling plot for $f(x)$ for the two-dimensional Ising model, with $x = r/t^{1/2}$.

For future reference, we note that the different-time correlation function, defined by $C(\mathbf{r}, t, t') = \langle \phi(\mathbf{x} + \mathbf{r}, t)\phi(\mathbf{x}, t') \rangle$, can also be written in scaling form. A simple generalization of equation (7) gives [18]

$$C(\mathbf{r}, t, t') = f\left(\frac{r}{L}, \frac{r}{L'}\right), \tag{8}$$

where L and L' stand for $L(t)$ and $L(t')$. Especially interesting is the limit $L \gg L'$ when

equation (8) takes the form

$$C(\mathbf{r}, t, t') \to \left(\frac{L'}{L}\right)^{\bar{\lambda}} h\left(\frac{r}{L}\right), \quad L \gg L' \tag{9}$$

where the exponent $\bar{\lambda}$, first introduced by Fisher and Huse [19] in the context of non-equilibrium relaxation in spin glasses, is a non-trivial exponent associated with phase-ordering kinetics [20]. (Note that our exponent $\bar{\lambda}$ is called λ in [19].) It has recently been measured in an experiment on twisted nematic liquid crystal films [21]. The *autocorrelation* function $A(t) = C(\mathbf{0}, t, t')$ is therefore a function only of the ratio L'/L, with $A(t) \sim (L'/L)^{\bar{\lambda}}$ for $L \gg L'$.

In the following sections, we explore the forms of the scaling functions in more detail. For example, the linear behaviour of $f(x)$, for small scaling variable x in figure 5, is a generic feature for scalar fields, both conserved and non-conserved. We shall see that it is a simple consequence of the existence of 'sharp' (in a sense to be clarified) well defined domain walls in the system. A corollary that we shall demonstrate is that the structure factor scaling function $g(y)$ exhibits a power-law tail $g(y) \sim y^{-(d+1)}$ for $y \gg 1$, a result known as the Porod law [22, 23]. In section 7 we shall show that this result and its generalization to more complex fields, together with the scaling hypothesis, are sufficient to determine the growth law for $L(t)$.

2.2. *Domain walls*

It is instructive first to look at the properties of a flat equilibrium domain wall. From equation (2) the wall profile is the solution of the equation

$$\frac{\mathrm{d}^2\phi}{\mathrm{d}g^2} = V'(\phi), \tag{10}$$

with boundary conditions $\phi(\pm\infty) = \pm 1$, where g is a coordinate normal to the wall. We can fix the 'centre' of the wall (defined by $\phi = 0$) to be at $g = 0$ by the extra condition $\phi(0) = 0$. Integrating equation (10) once, and imposing the boundary conditions, gives $(\mathrm{d}\phi/\mathrm{d}g)^2 = 2V(\phi)$. This result can be used in equation (1) to give the energy per unit area of wall, that is the surface tension, as

$$\sigma = \int_{-\infty}^{\infty} \mathrm{d}g \left(\frac{\mathrm{d}\phi}{\mathrm{d}g}\right)^2 = \int_{-1}^{1} \mathrm{d}\phi\, [2V(\phi)]^{1/2}. \tag{11}$$

Note that, for scalar fields, the two terms in equation (1) contribute equally to the wall energy.

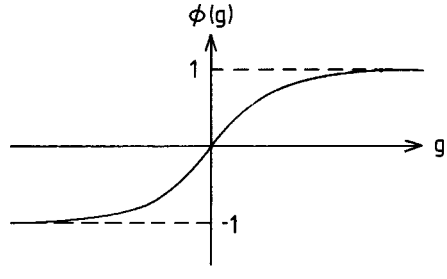

Figure 6. Domain-wall profile function $\phi(g)$ (schematic).

The profile function $\phi(g)$ is sketched in figure 6. For $g \to \pm\infty$, linearizing equation (10) around $\phi = \pm 1$ gives

$$1 \mp \phi \sim \exp - [V''(\pm 1)]^{1/2}|g|, \quad g \to \pm\infty, \tag{12}$$

that is the order parameter saturates exponentially away from the walls. It follows that the excess energy is localized in the domain walls, and that the driving force for the domain growth is the wall curvature, since the system energy can only decrease through a reduction in the total wall area. The growth mechanism is rather different, however, for conserved and non-conserved fields.

2.3. *Non-conserved fields: the Allen–Cahn equation*

The existence of a surface tension implies a force per unit area, proportional to the mean curvature, acting at each point on the wall. The calculation is similar to that of the excess pressure inside a bubble. Consider, for example, a spherical domain of radius R, in three dimensions. If the force per unit area is F, the work done by the force in decreasing the radius by $\mathrm{d}R$ is $4\pi FR^2\mathrm{d}R$. Equating this to the decrease in surface energy, $8\pi\sigma R\,\mathrm{d}R$, gives $F = 2\sigma/R$. For model A dynamics, this force will cause the walls to move, with a velocity proportional to the local curvature. If the friction constant for domain-wall motion is η, then this argument gives $\eta\,\mathrm{d}R/\mathrm{d}t = -2\sigma/R$. For general dimension d, the factor 2 on the right is replaced by $d-1$.

It is interesting to see how this result arises directly from the equation of motion (2). We consider a single spherical domain of (say) $\phi = -1$ immersed in a sea of $\phi = +1$. Exploiting the spherical symmetry, equation (2) reads

$$\frac{\partial\phi}{\partial t} = \frac{\partial^2\phi}{\partial r^2} + \frac{d-1}{r}\frac{\partial\phi}{\partial r} - V'(\phi). \tag{13}$$

Provided that the droplet radius R is much larger than the interface width ξ, we expect a solution of the form

$$\phi(r,t) = f[r - R(t)]. \tag{14}$$

Inserting this in equation (13) gives

$$0 = f'' + \left(\frac{d-1}{r} + \frac{\mathrm{d}R}{\mathrm{d}t}\right)f' - V'(f). \tag{15}$$

The function $f(x)$ changes from -1 to 1 in a small region of width ξ near $x = 0$. Its derivative is therefore sharply peaked near $x = 0$ (i.e. near $r = R(t)$). Multiplying equation (15) by f' and integrating through the interface gives

$$0 = \frac{d-1}{R} + \frac{\mathrm{d}R}{\mathrm{d}t}, \tag{16}$$

where we have used $f' = 0$ far from the interface, and $V(f)$ has the same value on both sides of the interface (in the absence of a bulk driving force, i.e. a magnetic field). Integrating equation (16) gives $R^2(t) = R^2(0) - 2(d-1)t$, that is the collapse time scales with the initial radius at $t \sim R^2(0)$. Equation (16) is identical with our previous result obtained by considering the surface tension as the driving force, provided that the surface tension σ and friction constant η are equal. This we show explicitly below.

The result for general curved surfaces was derived by Allen and Cahn [24], who noted that, close to a domain wall, one can write $\nabla\phi = (\partial\phi/\partial g)_t\hat{\mathbf{g}}$, where $\hat{\mathbf{g}}$ is a unit vector normal to the wall (in the direction of increasing ϕ), and so $\nabla^2\phi = (\partial^2\phi/\partial g^2)_t + (\partial\phi/\partial g)_t\nabla\cdot\hat{\mathbf{g}}$. Noting also the relation $(\partial\phi/\partial t)_g = -(\partial\phi/\partial g)_t(\partial\dot{g}/\partial t)_\phi$, equation (2) can be

recast as

$$-\left(\frac{\partial\phi}{\partial g}\right)_t\left(\frac{\partial g}{\partial t}\right)_\phi = \left(\frac{\partial\phi}{\partial g}\right)_t \nabla\cdot\hat{\mathbf{g}} + \left(\frac{\partial^2\phi}{\partial g^2}\right)_t - V'(\phi). \tag{17}$$

On the assumption that, for gently curving walls, the wall profile is given by the equilibrium condition (10), the final two terms in equation (17) cancel. Noting also that $(\partial g/\partial t)_\phi$ is just the wall velocity v (in the direction of increasing ϕ), equation (17) simplifies to

$$v = -\nabla\cdot\hat{\mathbf{g}} = -K, \tag{18}$$

the Allen–Cahn equation, where $K \equiv \nabla\cdot\hat{\mathbf{g}}$ is $d-1$ times the mean curvature. For brevity, we shall call K simply the curvature. An alternative derivation of equation (18) follows the approach used for the spherical domain, that is we multiply equation (17) by $(\partial\phi/\partial g)_t$ and integrate (with respect to g) through the interface. This gives the same result.

Equation (18) is an important result, because it establishes that the motion of the domain walls is determined (for non-conserved fields) purely by the local curvature. In particular, the detailed shape of the potential is not important; the main role of the double-well potential $V(\phi)$ is to establish (and maintain) well-defined domain walls. (Of course, the well depths must be equal, or there would be a volume driving force.) We shall exploit this insensitivity to the potential, by choosing a particularly convenient form for $V(\phi)$, in section 5.

For a spherical domain, the curvature K is $(d-1)/R$, and equation (18) reduces to equation (16). Our explicit treatment of the spherical domain verifies the Allen–Cahn result, and, in particular, the independence from the potential of the interface dynamics.

A second feature of equation (18) is that the surface tension σ (which *does* depend on the potential) does not explicitly appear. How can this be, if the driving force on the walls contains a factor σ? The reason, as we have already noted, is that one also needs to consider the *friction constant* η per unit area of wall. The equation of motion for the walls in this dissipative system in $\eta v = -\sigma K$. Consistency with equation (18) requires that $\eta = \sigma$. In fact, η can be calculated independently, as follows. Consider a plane wall moving uniformly (under the influence of some external driving force) at speed v. The rate energy dissipation per unit area is

$$\begin{aligned}\frac{\mathrm{d}E}{\mathrm{d}t} &= \int_{-\infty}^{\infty} \mathrm{d}g \,\frac{\delta F}{\delta\phi}\frac{\partial\phi}{\partial t} \\ &= -\int_{-\infty}^{\infty} \mathrm{d}g \left(\frac{\partial\phi}{\partial t}\right)^2,\end{aligned} \tag{19}$$

using equation (2). The wall profile has the form $\phi(g,t) = f(g-vt)$, where the profile function f will, in general, depend on v. Putting this form into equation (19) gives

$$\frac{\mathrm{d}E}{\mathrm{d}t} = -v^2\int \mathrm{d}g \left(\frac{\partial\phi}{\partial g}\right)^2 = -\sigma v^2, \tag{20}$$

where the definition (11) of the surface tension σ was used in the final step, and the profile function $f(x)$ replaced by its $v=0$ form to lowest order in v. By definition, however, the rate of energy dissipation is the product of the frictional force ηv and the velocity: $\mathrm{d}E/\mathrm{d}t = -\eta v^2$. Comparison with equation (20) gives $\eta = \sigma$. We conclude that, notwithstanding some contrary suggestions in the literature, the Allen–Cahn equation is completely consistent with the idea that domain growth is driven by the surface tension of the walls.

2.4. *Conserved fields*

For conserved fields the interfaces cannot move independently. At late times the dominant growth mechanism is the transport of the order parameter from interfaces of high curvature to regions of low curvature by diffusion through the intervening bulk phases. To see how this works, we first linearize equation (3) in one of the bulk phases, with say $\phi \approx 1$. Putting $\phi = 1 + \tilde{\phi}$ in equation (3) and linearizing in $\tilde{\phi}$ give

$$\frac{\partial \tilde{\phi}}{\partial t} = -\nabla^4 \tilde{\phi} + V''(1)\nabla^2 \tilde{\phi}. \tag{21}$$

Since the characteristic length scales are large at late times, the ∇^4 term is negligible and equation (21) reduces to the diffusion equation, with diffusion constant $D = V''(1)$. The interfaces provide the boundary conditions, as we shall see. However, we can first make a further simplification. Owing to the conservation law, the interfaces move little during the time that it takes the diffusion field $\tilde{\phi}$ to relax. If the characteristic domain size is L, the diffusion field relaxes on a time scale $t_D \sim L^2$. We shall see below, however, that a typical interface velocity is of order $1/L^2$; so the interfaces only move a distance of order unity (i.e. much less than L) in the time t_D. This means that the diffusion field relaxes quickly compared with the rate at which the interfaces move and is essentially always in equilibrium with the interfaces. The upshot is that the diffusion equation can be replaced by Laplace's equation $\nabla^2 \tilde{\phi} = 0$ in the bulk.

To derive the boundary conditions at the interfaces, it is convenient to work not with $\tilde{\phi}$ directly, but with the chemical potential $\mu \equiv \delta F/\delta\phi$. In terms of μ, equation (3) can be written as a continuity equation

$$\frac{\partial \phi}{\partial t} = -\nabla \cdot \mathbf{j}, \tag{22}$$

$$\mathbf{j} = -\nabla \mu, \tag{23}$$

$$\mu = V'(\phi) - \nabla^2 \phi. \tag{24}$$

In the bulk, μ and $\tilde{\phi}$ are proportional to each other, because equation (24) can be linearized to give $\mu = V''(1)\tilde{\phi} - \nabla^2 \tilde{\phi}$, and the ∇^2 term is again negligible. Therefore μ also obeys Laplace's equation

$$\nabla^2 \mu = 0 \tag{25}$$

in the bulk.

The boundary conditions are derived by analysing equation (24) near an interface. As in the derivation of the Allen–Cahn equation, we consider surfaces of constant ϕ near the interface and introduce a Cartesian coordinate system at each point, with a coordinate g normal to the surface (and increasing with increasing ϕ). Then equation (24) becomes (compare equation (17))

$$\mu = V'(\phi) - \left(\frac{\partial \phi}{\partial g}\right)_t K - \left(\frac{\partial^2 \phi}{\partial g^2}\right)_t \tag{26}$$

near the interface, where $K = \nabla \cdot \hat{\mathbf{g}}$ is the curvature. The value of μ at the interface can be obtained (just as in our treatment of the spherical domain in section 2.3), by multiplying through by $(\partial\phi/\partial g)_t$, which is sharply peaked at the interface, and integrating over g through the interface. Noting that μ and K vary smoothly through the interface, this gives the completely general relation

$$\mu \, \Delta\phi = \Delta V - \sigma K \tag{27}$$

at the interface, where $\Delta\phi$ is the change in ϕ across the interface, and ΔV is the difference in the minima of the potential for the two bulk phases. In deriving equation (27), we have used $(\partial\phi/\partial g)_t \to 0$ far from the interface and made the identification $\int \mathrm{d}g\,(\partial\phi/\partial g)_t^2 = \sigma$, as in equation (11), with σ the surface tension. Simplifying to the case where the minima have equal depth (we shall see that the general case introduces no new physics) and taking the minima to be at $\phi = \pm 1$ as usual give $\Delta V = 0$ and $\Delta\phi = 2$. Then equation (27) becomes

$$\mu = -\frac{\sigma K}{2}. \tag{28}$$

This (or, more generally, equation (27)) is usually known as the Gibbs–Thomson boundary condition. Note that we have assumed that the order parameter takes its equilibrium value (± 1) in both bulk phases. This is appropriate to the late stages of growth in which we are primarily interested.

To summarize, equation (28) determines μ on the interfaces in terms of the curvature. Between the interfaces, μ satisfies the Laplace equation (25). The final step is to use equation (23) to determine the motion of the interfaces. An interface moves with a velocity given by the imbalance between the current flowing into and out of it:

$$v\,\Delta\phi = j_{\mathrm{out}} - j_{\mathrm{in}} = -\left[\frac{\partial\mu}{\partial g}\right] = -[\hat{\mathbf{g}}\cdot\nabla\mu], \tag{29}$$

where v is the speed of the interface in the direction of increasing ϕ, g is the usual coordinate normal to interface, [...] indicates the discontinuity across the interface, and we have assumed as usual that $\phi \approx \pm 1$ in the bulk phases.

To illustrate how equations (25), (28) and (29) are used, we consider again the case of a single spherical domain of negative phase ($\phi = -1$) in an infinite sea of positive phase ($\phi = +1$). We restrict ourselves to $d = 3$ for simplicity. The definition of μ (equation (24)) gives $\mu = 0$ at infinity. Let the domain have radius $R(t)$. The solution of equation (25) that obeys the boundary conditions $\mu = 0$ at infinity and equation (28) at $r = R$, and respects the spherical symmetry is (using $K = 2/R$ for $d = 3$) $\mu = -\sigma/r$ for $r \geqslant R$. Inside the domain, the $1/r$ term must be absent to avoid an unphysical singularity at $r = 0$. The solution of equation (25) in this region is therefore $\mu =$ constant. The boundary condition (28) gives $\mu = -\sigma/R$.

To summarize,

$$\mu = \begin{cases} -\dfrac{\sigma}{R}, & r \leqslant R, \\ -\dfrac{\sigma}{r}, & r \geqslant R. \end{cases} \tag{30}$$

Using equation (29), with $\Delta\phi = 2$, then gives

$$\frac{\mathrm{d}R}{\mathrm{d}t} = v = -\frac{1}{2}\left[\frac{\partial\mu}{\partial r}\right]_{R-\epsilon}^{R+\epsilon} = -\frac{\sigma}{2R^2}, \tag{31}$$

and hence $R^3(t) = R^3(0) - 3\sigma t/2$. We conclude that a domain of initial radius $R(0)$ evaporates in a time proportional to $R^3(0)$. This contrasts with the $R^2(0)$ result obtained for a non-conserved order parameter. In the non-conserved case, of course, the domain

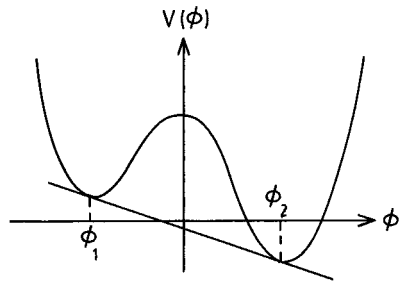

Figure 7. Asymmetrical potential $V(\phi)$ for a conserved order parameter, showing the common-tangent construction that determines the compositions of the separated phases.

simply shrinks under the curvature forces, whereas for the conserved case it evaporates by the diffusion of material to infinity.

We now briefly discuss the case where the potential minima have unequal depths, as sketched in figure 7. Consider first a planar interface separating the two equilibrium phases, with order parameter values ϕ_1 and ϕ_2. Since no current flows, $\mathbf{j} = -\nabla\mu = 0$ gives $\mu =$ constant. From the definition (24) of μ, and the fact that $\nabla^2\phi$ vanishes far from the interface, it follows that $\mu = V'(\phi_1) = V'(\phi_2)$. On the other hand, the Gibbs–Thomson boundary condition (27) for a flat interface ($K = 0$) gives $\mu = \Delta V/\Delta\phi$. Combining these two results gives

$$V'(\phi_1) = V'(\phi_2) = \frac{\Delta V}{\Delta\phi}, \tag{32}$$

leading to the common tangent construction, shown in figure 7, that determines ϕ_1 and ϕ_2 as the points where the common tangent touches the potential. If one now repeats the calculation for a spherical drop, with a domain with $\phi = \phi_1$ immersed in a sea with $\phi = \phi_2$, one obtains the equation of motion for the radius, $\mathrm{d}R/\mathrm{d}t = -2\sigma/(\Delta\phi)^2R^2$, a simple generalization of equation (31). Henceforth, we shall consider only the case of degenerate minima.

2.5. *Growth laws*

The scaling hypothesis suggests intuitive derivation of the 'growth laws' for $L(t)$, which are really just generalizations of the calculations for isolated spherical domains. For model A, we can estimate both sides of the Allen–Cahn equation (18) as follows. If there is a single characteristic scale L, then the wall velocity $v \sim \mathrm{d}L/\mathrm{d}t$, and the curvature $K \sim 1/L$. Equating and integrating gives $L(t) \sim t^{1/2}$ for non-conserved scalar fields.

For conserved fields (model B), the argument is slightly more subtle. We shall follow the approach of Huse [25]. From equation (28), the chemical potential has a typical value $\mu \sim \sigma/L$ on interfaces and varies over a length scale of order L. The current, and therefore the interface velocity v, scale as $|\nabla\mu| \sim \sigma/L^2$, giving $\mathrm{d}L/\mathrm{d}T \sim \sigma/L^2$ and $L(t) \sim (\sigma t)^{1/3}$. A more compelling argument for this result will be given in section 7. We note, however, that the result is supported by evidence from computer simulations [25, 26] (which usually require, however, some extrapolation into the asymptotic scaling regime) as well as a RG treatment [10, 11]. In the limit that one phase occupies an infinitesimal volume fraction, the original Lifshitz–Slyozov–Wagner (LSW) theory convincingly demonstrates a $t^{1/3}$ growth. This calculation, whose physical mechanism

is the evaporation of material (or magnetization) from small droplets and condensation onto larger droplets, will be discussed briefly in the following section.

It is interesting that these growth laws can also be obtained using naive arguments based on the results for single spherical domains [7]. For non-conserved dynamics, we know that a domain of radius R collapses in a time of order R^2. Therefore, crudely speaking, after time t there will be no domains smaller than $t^{1/2}$; so the characteristic domain size is $L(t) \sim t^{1/2}$. Of course, this is an oversimplification, but it captures the essential physics. For conserved dynamics, the same line of argument leads to $t^{1/3}$ growth. This approach can be used rather generally, for a variety of systems [27], and gives results which agree, in nearly all cases, with the exact growth laws that will be derived in section 7.

2.6. *The Lifshitz–Slyozov–Wagner theory*

In their seminal work, Lifshitz and Slyozov [2], and independently Wagner [3], derived some exact results in the limit that the minority phase occupies a negligible volume fraction. In particular, they showed that the characteristic size of the minority phase droplets increases as $t^{1/3}$.

We begin by considering again a single spherical droplet of minority phase ($\phi = -1$), or radius R, immersed in a sea of majority phase, but now we let the majority phase have order parameter $\phi = \phi_0 < 1$ at infinity, that is the majority phase is supersaturated with the dissolved minority species. If the minority droplet is sufficiently large, it will grow by absorbing material from the majority phase. Otherwise it will shrink by evaporation as before. A critical radius R_c separates these two regimes.

With the convention that $V(\pm 1) = 0$, the boundary condition (27) at $r = R$ becomes $(1 + \phi_0)\mu = V(\phi_0) - 2\sigma/R$, while the boundary condition at infinity is $\mu = V'(\phi_0)$. Solving the Laplace equation for μ with these boundary conditions gives

$$\mu = \begin{cases} V'(\phi_0) + \left(\dfrac{V(\phi_0)}{1+\phi_0} - V'(\phi_0)\right)\dfrac{R}{r} - \dfrac{2\sigma}{1+\phi_0}\dfrac{1}{r}, & r \geqslant R, \quad (33) \\ \dfrac{V(\phi_0)}{1+\phi_0} - \dfrac{2\sigma}{1+\phi_0}\dfrac{1}{R}, & r \leqslant R. \quad (34) \end{cases}$$

Equation (29) gives the interface velocity,

$$\frac{dR}{dt} = \left(\frac{V(\phi_0)}{(1+\phi_0)^2} - \frac{V'(\phi_0)}{1+\phi_0}\right)\frac{1}{R} - \frac{2\sigma}{(1+\phi_0)^2}\frac{1}{R^2}. \quad (35)$$

Now consider the limit of small supersaturation, $\phi_0 = 1 - \epsilon$ with $\epsilon \ll 1$. To leading non-trivial order in ϵ, the velocity is

$$\frac{dR}{dt} = \frac{\sigma}{2R}\left(\frac{1}{R_c} - \frac{1}{R}\right), \quad (36)$$

where $R_c = \sigma/V''(1)\epsilon$ is the critical radius.

In the LSW theory, an assembly of drops is considered. Growth proceeds by evaporation of drops with $R < R_c$ and condensation on to drops with $R > R_c$. The key is to use the time-dependent supersaturation $\epsilon(t)$ as a kind of mean field, related to the time-dependent critical radius via $R_c(t) = \sigma/V''(1)\epsilon(t)$, and to use equation (36) with the time-dependent R_c for the dynamics of a given drop.

So far the discussion has been restricted to spatial dimension $d = 3$. However, a result of the form (36) can be derived (with a d-dependent numerical constant

multiplying the right-hand side) for general $d > 2$. The next step is to write down a scaling distribution of droplet radii,

$$n(R,t) = \frac{1}{R_c^{d+1}} f\left(\frac{R}{R_c}\right), \tag{37}$$

obeying the continuity equation

$$\frac{\partial n}{\partial t} + \frac{\partial}{\partial R}[v(R)n(R)] = 0, \tag{38}$$

where $v(R)$ is just the velocity $\mathrm{d}R/\mathrm{d}t$.

Suppose that the spatial average of the order parameter is $1 - \epsilon_0$. At late times the supersaturation $\epsilon(t)$ tends to zero, giving the constraint

$$\epsilon_0 = 2V_d \int_0^\infty \mathrm{d}R\, R^d n(R,t) = 2V_d \int_0^\infty \mathrm{d}x\, x^d f(x), \tag{39}$$

where V_d is the volume of the d-dimensional unit sphere. Equation (39) fixes the normalization of $f(x)$. A linear equation for $f(x)$ can be derived by inserting the scaling form (37) into the continuity equation (38) and using equation (36) for $v(R)$, which we write in the form (valid for general $d > 2$)

$$v(R) = \frac{\alpha_d}{R}\left(\frac{1}{R_c} - \frac{1}{R}\right), \tag{40}$$

where $\alpha_3 = \sigma/2$. This procedure gives

$$\frac{\dot{R}_c}{R_c^{d+2}}[(d+1)f + xf'] = \frac{\alpha_d}{R_c^{d+4}}\left[\left(\frac{2}{x^3} - \frac{1}{x^2}\right)f + \left(\frac{1}{x} - \frac{1}{x^2}\right)f'\right], \tag{41}$$

where $\dot{R}_c \equiv \mathrm{d}R_c/\mathrm{d}t$ and $f' \equiv \mathrm{d}f/\mathrm{d}x$. A consistent solution requires that the R_c dependence drops out from this equation. This means that $R_c^2 \dot{R}_c = \alpha_d \gamma$, a constant, giving

$$R_c(t) = (3\alpha_d \gamma t)^{1/3}. \tag{42}$$

Integrating equation (41) then gives

$$\ln[f(x)] = \int^x \frac{\mathrm{d}y}{y} \frac{2 - y - \gamma(d+1)y^3}{\gamma y^3 - y + 1}. \tag{43}$$

It is clear that $f(x)$ cannot be non-zero for arbitrarily large x, or one would have the asymptotic behaviour $f(x) \sim x^{-(d+1)}$, and the normalization integral (39) would not exist. Therefore $f(x)$ must vanish for x greater than some value $x_{\max}$, which must be the first pole of the integrand on the positive real axis. The existence of such a pole requires $\gamma \leq \frac{4}{27}$. Lifshitz and Slyozov argue that the only physically acceptable solution is $\gamma = \gamma_0 = \frac{4}{27}$, corresponding to a double pole at $x_{\max} = \frac{3}{2}$. The argument is as follows. In terms of the scaled radius $x = R/R_c$, equation (40) and (42) imply that

$$\begin{aligned} \frac{\mathrm{d}x}{\mathrm{d}t} &= \frac{1}{3\gamma t}\left(\frac{1}{x} - \frac{1}{x^2} - \gamma x\right) \\ &= \frac{1}{3\gamma t}\, g(x), \end{aligned} \tag{44}$$

the last equality defining the function $g(x)$. The form of $g(x)$ is sketched in figure 8, where the arrows indicate the flow of x under the dynamics (44). From figure 8 (*a*) it

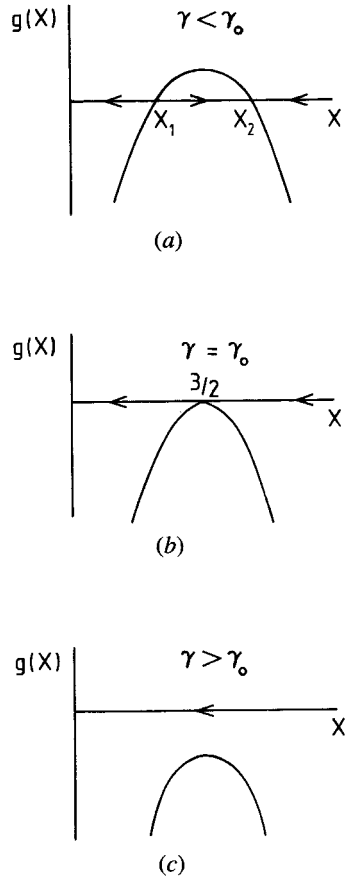

Figure 8. Sketch of the function $g(x)$, given by equation (44), for different γ, where $\gamma_0 = \frac{4}{27}$.

is clear that, for $\gamma < \gamma_0$, all drops with $x > x_1$ will asymptotically approach the size $x_2 R_c(t)$, which tends to ∞ with t. Therefore it will not be possible to satisfy the condition (39) which imposes the conservation of the order parameter. Similarly, figure 8 (*c*) shows that, for $\gamma > \gamma_0$, all points move to the origin and the conservation condition again cannot be satisfied. The only possibility is that γ tends to γ_0 asymptotically from above (it cannot reach γ_0 in finite time; otherwise all drops with $x > \frac{3}{2}$ would eventually arrive at $x = \frac{3}{2}$ and become stuck, much like the case $\gamma < \gamma_0$).

Evaluating the integral (43) with $\gamma = \gamma_0 = \frac{4}{27}$ gives the scaling function for the droplet size distribution:

$$f(x) = \text{constant} \times x^2(3+x)^{-1-4d/9}(\tfrac{3}{2}-x)^{-2-5d/9} \exp\left(-\frac{d}{3-2x}\right) \qquad (45)$$

for $x < \frac{3}{2}$, and $f(x) = 0$ for $x \geqslant \frac{3}{2}$. The constant pre-factor is fixed by the normalization integral (39).

Lifshitz and Slyozov have shown that the above scaling solution is obtained for generic initial conditions in the limit of small volume fraction v of the minority phase. The general-d form (45) for $f(x)$ has been derived by Yao *et al.* [28]. Note that the method described above only works for $d > 2$; it is easy to show that the constant α_d

in equation (40), which sets the time scale for the growth via equation (42), vanishes linearly with $d-2$ for $d \to 2$, reflecting the singular nature of the Green function for the Laplacian in $d=2$. The general expression in $\alpha_d = (d-1)(d-2)\sigma/4$. Working in the limit of strictly vanishing v, Rogers and Desai [29] found the same scaling form (45) for $d=2$, but with $R_c \sim (t/\ln t)^{1/3}$. For small but non-zero v, Yao *et al.* [28] find that $R_c \sim (t/|\ln v|)^{1/3}$. The two results correspond to taking the limit $v \to 0$ before [29] or after [28] the limit $t \to \infty$.

Many groups have attempted, with varying degrees of success, to extend the LSW treatment to non-zero v, either by expanding in v (actually, $v^{1/2}$) [30, 31], or by the use of physically motivated approximation schemes and/or numerical methods [28, 32–37]. When v is of order unity, however, such that both phases are continuous, different techniques are required, discussion of which will be postponed to section 5.

2.7. *Binary liquids*

The phase separation of binary liquids is a phenomenon of considerable experimental interest. Model B is inappropriate for this system, since it takes no account of the transport of the order parameter by hydrodynamic flow. Here we briefly review the modifications to model B needed to describe binary liquids.

The principal new ingredient is 'advection' of the order parameter by the fluid. The appropriate modification of equation (3) is

$$\frac{\partial \phi}{\partial t} + \mathbf{v} \cdot \nabla \phi = \lambda \nabla^2 \mu, \tag{46}$$

where $\mathbf{v}$ is the (local) fluid velocity, and we have reinstated the transport coefficient λ. The velocity obeys the Navier–Stokes equation which, with the simplification that the fluid is incompressible, reads

$$\rho\left(\frac{\partial \mathbf{v}}{\partial t} + (\mathbf{v} \cdot \nabla)\mathbf{v}\right) = \eta \nabla^2 \mathbf{v} - \nabla p - \phi \nabla \mu, \tag{47}$$

where p is the pressure, η is the viscosity, and the density ρ is constant. The final term in equation (47) arises from the free-energy change $\phi\,\delta\mu$ per unit volume that accompanies the transport of a fluid region with order parameter ϕ over a distance for which the change in the chemical potential is $\delta\mu$: chemical potential gradients act as a driving force on the fluid.

In the overdamped limit appropriate to most experimental systems, the left-hand side of equation (47) can be set to zero. The velocity is then 'slaved to the order parameter' [38, 39]. The resulting linear equation for $\mathbf{v}$ can be solved in Fourier space:

$$v_\alpha(\mathbf{k}) = \frac{1}{\eta k^2}[-\mathrm{i}k_\alpha p(\mathbf{k}) + F_\alpha(\mathbf{k})], \tag{48}$$

where $\mathbf{F} = -\phi \nabla \mu$. The incompressibility condition $\mathbf{k} \cdot \mathbf{v}(\mathbf{k}) = 0$ determines the pressure. Putting the result into equation (48) gives, with the summation convention for repeated indices,

$$v_\alpha(\mathbf{k}) = T_{\alpha\beta}(\mathbf{k}) F_\beta(\mathbf{k}),$$

$$T_{\alpha\beta}(\mathbf{k}) = \frac{1}{\eta k^2}\left(\delta_{\alpha\beta} - \frac{k_\alpha k_\beta}{k^2}\right), \tag{49}$$

where T is the Oseen tensor. In real space (for $d = 3$),

$$T_{\alpha\beta}(\mathbf{r}) = \frac{1}{8\pi\eta r}\left(\delta_{\alpha\beta} + \frac{r_\alpha r_\beta}{r^2}\right). \tag{50}$$

Putting everything together gives the equation of motion in real space,

$$\frac{\partial\phi}{\partial t} = \lambda\nabla^2\mu - \int \mathrm{d}\mathbf{r}'\,[\nabla\phi(r)\cdot T(\mathbf{r}-\mathbf{r}')\cdot\nabla'\phi(\mathbf{r}')]\mu(\mathbf{r}'), \tag{51}$$

where we recall that $\mu(\mathbf{r}) = \delta F/\delta\phi(\mathbf{r})$. In deriving the final form (51), integration by parts (exploiting the transverse property, $T_{\alpha\beta}(\mathbf{k})k_\beta = 0$, of the Oseen tensor) was used to convert $\phi(\mathbf{r}')\nabla'\mu(\mathbf{r}')$ to $-\mu(\mathbf{r}')\nabla'\phi(\mathbf{r}')$ inside the integral.

It should be emphasized that, as usual, thermal fluctuations have been neglected in equation (51). We have previously argued, on rather general grounds, that these are negligible at late times, because the coarsening is controlled by a strong coupling RG fixed point (see, in particular, the discussion in section 8). For binary liquids, however, a rather subtle situation can arise when the nominally dominant coarsening mechanism does not operate. Then thermal fluctuations do contribute. We shall enlarge on this below.

We can use dimensional arguments to estimate the sizes of the two terms on the right-hand side of equation (51). Using $\mu \sim \sigma/L$, $T \sim 1/\eta L$ and $\nabla\phi \sim 1/L$ gives $\lambda\sigma/L^3$ for the first ('diffusive') term and $\sigma/\eta L$ for the second ('advective') term. Advective transport of the order parameter therefore dominates over diffusion for $L \gg (\lambda\eta)^{1/2}$. To determine $L(t)$ in this regime, we use the expression for the fluid velocity:

$$\mathbf{v}(\mathbf{r}) = \int \mathrm{d}\mathbf{r}'\,[T(\mathbf{r}-\mathbf{r}')\cdot\nabla\phi(\mathbf{r}')]\mu(\mathbf{r}'). \tag{52}$$

Using the same dimensional arguments as before, and also $v \sim L/t$, gives $L(t) \sim \sigma t/\eta$, a result first derived by Siggia [40]. This result has been confirmed by experiments [41] and by numerical simulations [42–44]. Because the inertial terms are negligible compared with the viscous force here, we shall call this the viscous hydrodynamic (or just viscous) regime.

Under what conditions is it correct to ignore the inertial terms on the left-hand side of (47)? Using dimensional arguments again, we see that these terms are of order $\rho L/t^2$. Comparing this with the driving term $\phi\,\nabla\mu \sim \sigma/L^2$ on the right (the viscous term $\eta\,\nabla^2 v$ is of the same order in the viscous regime) and using the result derived above, $t \sim \eta L/\sigma$, for this regime show that the inertial terms are negligible when $L \ll \eta^2/\sigma\rho$. At sufficiently late times, when this inequality is violated, the inertial terms will therefore be important. In this inertial regime, $L(t)$ is determined by equating the inertial terms, which scale as $\rho L/t^2$, to the driving term $\phi\,\nabla\mu$, which scales as σ/L^2 (and the viscous term is negligible) to give $L \sim (\sigma t^2/\rho)^{1/3}$. The $t^{2/3}$ growth in the inertial regime was first predicted by Furukawa [45].

To summarize, there are in principle three growth regimes for phase separation in binary liquids, after a deep quench, with the growth laws

$$L(t) \sim \begin{cases} (\lambda\sigma t)^{1/3}, & L \ll (\lambda\eta)^{1/2}, \quad \text{(diffusive)}, & (53) \\ \dfrac{\sigma t}{\eta}, & (\lambda\eta)^{1/2} \ll L \ll \dfrac{\eta^2}{\rho\sigma}, \quad \text{(viscous hydrodynamic)} & (54) \\ \left(\dfrac{\sigma t^2}{\rho}\right)^{1/3}, & L \gg \dfrac{\eta^2}{\rho\sigma}, \quad \text{(inertial hydrodynamic)}. & (55) \end{cases}$$

The results basically follow from dimensional analysis. The inertial hydrodynamic regime has not, to my knowledge, been observed experimentally and we shall not consider it further. However, a $t^{2/3}$ regime has been observed at late times in simulations of two-dimensional binary liquids [44, 46].

Siggia [40] has discussed the physical origin of the linear growth in the 'viscous hydrodynamic' regime. He argues that the essential mechanism is the hydrodynamic transport of fluid along the interface driven by the surface tension. This mechanism, however, can only operate if both phases are continuous. If, by contrast, the minority phase consists of independent droplets (which occurs for volume fractions less than about 15%), this mechanism tends to make the droplets spherical but does not lead to any coarsening (it is easy to show, for example, that the hydrodynamic term in equation (51) vanishes for a single spherical droplet). In the absence of thermal fluctuations therefore the Lifshitz–Slyozov evaporation–condensation mechanism determines the growth even beyond the nominal cross-over length given above. Thermal fluctuations, however, facilitate a second coarsening mechanism, namely droplet coalescence driven by Brownian motion of the droplets. Again, Siggia has given the essential argument. The mobility μ of a droplet of size L is of order $1/\eta L$; so the diffusion constant is given by the Einstein relation as $D = \mu k_B T \sim k_B T/\eta L$, where k_B is Boltzmann's constant. The time for the droplet to diffuse a distance of order L (and to coalesce with another droplet) is $t \sim L^2/D \sim \eta L^3/k_B T$, which gives $L \sim (k_B T t/\eta)^{1/3}$.

The presence of two different mechanisms leading to the same growth exponent suggests a 'marginal operator' in the theory, and the RG treatment in section 8 lends support to this view. The RG approach also shows how, in this case, a nominally irrelevant variable (temperature) can affect the late-stage growth in a non-trivial way. From a physical point of view, it seems plausible that the presence of competing mechanisms will lead to a late-stage morphology that depends on the ratio of the amplitudes derived for the two mechanisms, that is that scaling functions will depend continuously on this ratio. This could be tested by numerical simulations, where the transport coefficient λ and viscosity η can be independently varied. In real binary liquids, however, these coefficients are related, and the ratio of amplitudes for the two mechanisms depends only on the volume fraction v (see [40] and the discussion in section 8.4). Note that, even without hydrodynamics, the scaling functions will depend on v, since the morphology does. The role of the Lifshitz–Slyozov mechanism can be enhanced by going to small v, since the growth rate due to evaporation–condensation is independent off v for small v. By contrast, the coalescence rate increases with increasing v. To see this, we refine the argument given in the previous paragraph. (I thank Andrew Rutenberg for a useful discussion of this point.)

Let R be a typical droplet radius. Then the droplet number density is $n \sim v/R^3$. The time for a droplet to diffuse a distance of order its radius is $t_R \sim R^2/D$. The volume swept out by the drop in time t (for $t > t_R$) is of order $R^3\, t/t_R \sim RDt$. In a 'coalescence time' t_c the expected number of drops in this volume is of order unity, that is $nRDt_c \sim 1$, giving $t_c \sim R^2/vD \sim \eta R^3/vk_B T$, where we used $D \sim k_B T/\eta R$ in the last step. This implies that R grows with time as $R \sim (vk_B T t/\eta)^{1/3}$, a result first given by Siggia [40].

3. Topological defects

The domain walls discussed in the previous section are the simplest form of topological defect and occur in systems described by scalar fields (for a general discussion of topological defects, see for example [47]). They are surfaces on which the order parameter vanishes and which separate domains of the two equilibrium phases.

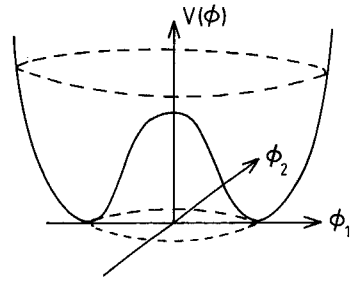

Figure 9. The 'Mexican hat' potential $V(\vec{\phi})$ for the O(n) model with $n = 2$.

A domain wall is topologically stable: local changes in the order parameter can move the wall but cannot destroy it. For an isolated flat wall, the wall profile function is given by the solution of equation (10), with the appropriate boundary conditions, as discussed in section 2.2 (and sketched in figure 6). For the curved walls present in the phase-ordering process, this will still be an approximate solution locally, provided that the typical radius L of curvature is large compared with the intrinsic width (or core size) ξ of the walls. (This could be defined from equation (12) as $\xi = [V''(1)]^{-1/2}$, say.) The same condition, $L \gg \xi$, ensures that typical wall separations are large compared with their width.

Let us now generalize the discussion to vector fields. The O(n) model is described by an n-component vector field $\vec{\phi}(\mathbf{x}, t)$, with a free-energy functional $F[\vec{\phi}]$ that is invariant under global rotations of $\vec{\phi}$. A suitable generalization of equation (1) is

$$F[\vec{\phi}] = \int \mathrm{d}^d x \, [\tfrac{1}{2}(\nabla\vec{\phi})^2 + V(\vec{\phi})], \tag{56}$$

where $(\nabla\vec{\phi})^2$ means $\Sigma_{i=1}^{d}\Sigma_{a=1}^{n}(\partial_i\phi^a)^2$ (i.e. a scalar product over both spatial and 'internal' coordinates), and $V(\vec{\phi})$ is the 'Mexican hat' (or 'wine bottle') potential, such as $(1-\vec{\phi}^2)^2$, whose general form is sketched in figure 9. It is clear that $F[\vec{\phi}]$ is invariant under global rotations of $\vec{\phi}$ (a continuous symmetry), rather than just the inversion symmetry ($\phi \to -\phi$, a discrete symmetry) of the scalar theory. We shall adopt the convention that V has its minimum for $\vec{\phi}^2 = 1$.

For non-conserved fields, the simplest dynamics (model A) is a straightforward generalization of equation (2), namely

$$\frac{\partial\vec{\phi}}{\partial t} = \nabla^2\vec{\phi} - \frac{\mathrm{d}V}{\mathrm{d}\vec{\phi}}. \tag{57}$$

For conserved fields (model B), we simply add another $-\nabla^2$ in front of the right-hand side.

Stable topological defects for vector fields can be generated, in analogy to the scalar case, by seeking stationary solutions of equation (57) with appropriate boundary conditions. For the O(n) theory in d-dimensional space, the requirement that all n components of $\vec{\phi}$ vanish at the defect core defines a surface of dimension $d-n$ (e.g. a domain wall is a surface of dimension $d-1$; the scalar theory corresponds to $n = 1$). The existence of such defects therefore requires that $n \leqslant d$. For $n = 2$ these defects are points ('vortices') for $d = 2$ or lines ('strings' or 'vortex lines') for $d = 3$. For $n = 3$, $d = 3$, they are points ('hedgehogs' or 'monopoles'). The field configurations for these defects are sketched in figures 10(a)–(d). Note that the forms shown are radially

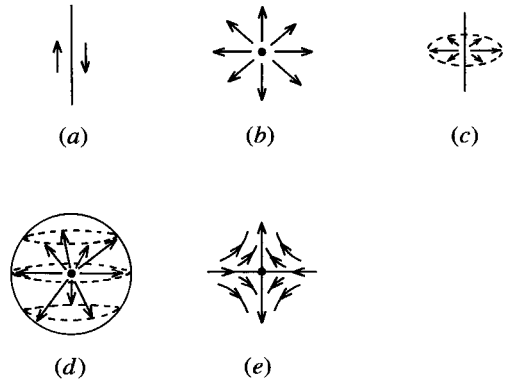

Figure 10. Types of topological defect in the O(n) model: (a) domain wall ($n = 1$); (b) vortex ($n = 2 = d$); (c) string ($n = 2$; $d = 3$); (d) monopole or 'hedgehog' ($n = 3 = d$); (e) antivortex.

symmetric with respect to the defect core; any configuration obtained by a global rotation is also acceptable. For $n < d$, the field $\vec{\phi}$ only varies in the n dimensions 'orthogonal' to the defect core and is uniform in the remaining $d - n$ dimensions 'parallel' to the core.

For $n < d$, the defects are spatially extended. Coarsening occurs by a 'straightening out' (or reduction in typical radius of curvature) as sharp features are removed, and by the shrinking and disappearance of small domain bubbles or vortex loops. These processes reduce the total area of domain walls, or length of vortex line, in the system. For point defects ($n = d$), coarsening occurs by the mutual annihilation of defect–anti-defect pairs. The antidefect for a vortex (antivortex) is sketched in figure 10 (e). Note that the antivortex is *not* obtained by simply reversing the directions of the arrows in figure 10 (b); this would correspond to a global rotation through π. Rather, the vortex and antivortex have different 'topological charges'; the fields rotate by 2π or -2π respectively on encircling the defect. By contrast, an antimonopole *is* generated by reversing the arrows in figure 10 (d); the reversed configuration cannot be generated by a simple rotation in this case.

For the radially symmetrical defects illustrated in figures 10 (b)–(d), the field $\vec{\phi}$ has the form $\vec{\phi}(\mathbf{r}) = \hat{\mathbf{r}} f(r)$, where $\hat{\mathbf{r}}$ is a unit vector in the radial direction and $f(r)$ is the profile function. Inserting this form into equation (57), with the time derivative set to zero, gives the equation

$$\frac{\mathrm{d}^2 f}{\mathrm{d}r^2} + \frac{n-1}{r}\frac{\mathrm{d}f}{\mathrm{d}r} - \frac{n-1}{r^2} f - V'(f) = 0, \tag{58}$$

with boundary conditions $f(0) = 0$, $f(\infty) = 1$. Of special interest is the approach to saturation at large r. Putting $f(r) = 1 - \epsilon(r)$ in equation (58) and expanding to first order in ϵ yields

$$\epsilon(r) \approx \frac{n-1}{V''(1)}\frac{1}{r^2}, \quad r \to \infty. \tag{59}$$

This should be contrasted with the exponential approach to saturation (equation (12)) for scalar fields. A convenient definition of the core size ξ is through $f \approx 1 - \xi^2/r^2$ for large r. This gives $\xi = [(n-1)/V''(1)]^{1/2}$ for $n > 1$.

3.1. *Defect energetics*

Consider an isolated equilibrium defect of the O(n) model in d-dimensional space (with, of course, $n \leqslant d$). For a radially symmetrical defect, $\vec{\phi}(\mathbf{r}) = f(r)\hat{\mathbf{r}}$, the energy per unit core volume (e.g. per unit area for a wall, per unit length for a line, or per defect for a point) is, from equation (56),

$$E = S_n \int \mathrm{d}r\, r^{n-1} \left(\frac{n-1}{2r^2} f^2 + \tfrac{1}{2}|\nabla f|^2 + V(f) \right), \tag{60}$$

where $S_n = 2\pi^{n/2}/\Gamma(n/2)$ is the surface area of an n-dimensional sphere.

For scalar fields ($n = 1$), we have seen (section 2.2) that the terms in $|\nabla f|^2$ and $V(f)$ contribute equally to the wall energy. For $n \geqslant 2$, the first term in equation (60) dominates the other two because, from equation (59), the three terms in the integrand fall off with distance as r^{-2}, r^{-6} and $V(f) \sim V''(1)(1-f)^2 \sim r^{-4}$ respectively as $r \to \infty$. For $n \geqslant 2$, therefore, the first term gives a divergent integral which has to be cut off as the system size L_{sys}, that is $E \sim \ln(L_{\mathrm{sys}}/\xi)$ for $n = 2$ and $E \sim L_{\mathrm{sys}}^{n-2}$ for $n > 2$. Actually, the second and third terms give divergent integrals for $n \geqslant 6$ and $n \geqslant 4$ respectively, but these are always subdominant compared with the first term.

The above discussion concerns an *isolated* defect. In the phase-ordering system the natural cut-off is not L_{sys} but $L(t)$, the characteristic scale beyond which the field of a single defect will be screened by the other defects. Of particular interest are the dynamics of defect structures much smaller than $L(t)$. These are the analogues of the small domains of the scalar system. For $d = n = 2$, these are vortex–antivortex pairs; for $d = 3$, $n = 2$, they are vortex rings; for $d = 3 = n$, they are monopole–antimonopole pairs. For such a structure, the pair separation r (for point defects) or ring radius r (for a vortex loop) provides the natural cut-off. Including the factor r^{d-n} for the volume of defect core, the energy of such a structure is

$$E \sim \begin{cases} r^{d-2} \ln \dfrac{r}{\xi}, & d \geqslant n = 2, \\ r^{d-2}, & d \geqslant n > 2. \end{cases} \tag{61}$$

The derivative with respect to r of this energy provides the driving force $-\mathrm{d}E/\mathrm{d}r$ for the collapse of the structure. Dividing by r^{d-n} gives the force F acting on a unit volume of core (i.e. per unit length for strings, per point for points, etc.):

$$F(r) \sim \begin{cases} -r^{-1}, & d = n = 2, \\ -r^{n-3} \ln\left(\dfrac{r}{\xi}\right), & d > n = 2, \\ -r^{n-3}, & d \geqslant n > 2. \end{cases} \tag{62}$$

In order to calculate the collapse time we need the analogue of the friction constant η (see section 2.3) for vector fields. This we calculate in the next section. Before doing so, we compute the total energy density ϵ for vector fields. This can be obtained by putting $r \sim L(t)$ in equation (61), and dividing by a characteristic volume $L(t)^d$ (since there will typically be of order one defect structure, with size of order $L(t)$, per scale

volume $L(t)^d$),

$$\epsilon \sim \begin{cases} L(t)^{-2} \ln\left(\dfrac{L(t)}{\xi}\right), & d \geqslant n = 2, \\ L(t)^{-2}, & d \geqslant n > 2. \end{cases} \tag{63}$$

For scalar systems, of course, $\epsilon \sim L(t)^{-1}$.

As a caveat to the above discussion, we note that we have explicitly assumed that the individual defects possess an approximate radial symmetry on scales small compared with $L(t)$. It has been known for some time (for example [48]), however, that an isolated point defect for $d > 3$ can lower its energy by having the field uniform (pointing 'left', say) over most of space, with a narrow 'flux tube' of field in the opposite direction (i.e. pointing 'right'). The energy is then linear in the size of the system, $E \sim L_{\rm sys}\xi^{d-3}$, which is smaller than the energy, $E \sim L_{\rm sys}^{d-2}$, of the spherically symmetric defect, for $d > 3$. A defect–antidefect pair with separation r, connected by such a flux tube, has an energy $E \sim r\xi^{d-3}$, which implies an r-independent force for all $d \geqslant 3$, in contrast with equation (62).

How relevant are these considerations in the context of phase-ordering dynamics? These single-defect and defect-pair calculations treat the field as completely relaxed with respect to the defect cores. If this were true, we could estimate the energy density for typical defect spacing $L(t)$ as $\xi^{d-3}L(t)^{1-d}$ for $d > 3$. However, the smooth variation ('spin waves') of the field between the defects gives a contribution to the energy density of $|\nabla\phi|^2 \sim L(t)^{-2}$, which dominates over the putative defect contribution for $d > 3$. Under these circumstances, we would not expect a strong driving force for point defects to adopt the flux-tube configuration, since the energy is dominated by spin waves. Rather, our tentative picture is of the point defects 'riding' on the evolving spin-wave structure for $d > 3$, although this clearly requires further work. Note, however, that these concerns are only relevant for $d > 3$; equation (62) is certainly correct for the physically relevant cases $d \leqslant 3$.

3.2. *Defect dynamics*

Here we shall consider only non-conserved fields. Using the methods developed in section 7, however, it is possible to generalize the results to conserved fields [27]. The caveats for $d > 3$ discussed in the previous section also apply here.

The calculation of the friction constant η proceeds as in section 2.3. Consider an isolated equilibrium defect, that is a vortex for $d = n = 2$, a monopole for $n = d = 3$, a straight vortex line for $n = 2$, $d = 3$, etc. Set up a Cartesian coordinate system $x_1, \ldots, x_d$. For extended defects, let the defect occupy the (hyper)plane defined by the last $d - n$ Cartesian coordinates and move with speed v in the x_1 direction. Then $\vec{\phi}$ depends only on coordinates $x_1, \ldots, x_n$, and the rate of change in the system energy per unit volume of defect core is

$$\begin{aligned} \frac{\mathrm{d}E}{\mathrm{d}t} &= \int \mathrm{d}x_1 \ldots \mathrm{d}x_n \frac{\delta F}{\delta \vec{\phi}} \cdot \frac{\partial \vec{\phi}}{\partial t} \\ &= -\int \mathrm{d}x_1 \ldots \mathrm{d}x_n \left(\frac{\partial \vec{\phi}}{\partial t}\right)^2. \end{aligned} \tag{64}$$

The defect profile has the form $\vec{\phi}(x_1, \ldots, x_n) = \vec{f}(x_1 - vt, x_2, \ldots, x_n)$, where the function

$\vec{f}$ depends on v in general. Putting this into equation (64) gives

$$\frac{dE}{dt} = -v^2 \int dx_1 \dots dx_n \left(\frac{\partial \vec{\phi}}{\partial x_1}\right)^2$$

$$= -\frac{v^2}{n} \int d^n r (\nabla \vec{\phi})^2 = -\eta v^2, \tag{65}$$

where the function $\vec{f}$ has been replaced by its $v = 0$ form to lowest order in v, and η is the friction constant per unit core volume. The final expression follows from symmetry. It follows that η is (up to constants) equal to the defect energy per unit core volume. In particular, it diverges with the system size for $n \geqslant 2$. For a small defect structure of size r, we expect the divergence to be effectively cut off at r. This gives a scale-dependent friction constant

$$\eta(r) \sim \begin{cases} r^{n-2} \ln \dfrac{r}{\xi}, & d \geqslant n = 2, \\ r^{n-2}, & d \geqslant n > 2. \end{cases} \tag{66}$$

Invoking the scaling hypothesis, we can now determine the growth laws for non-conserved vector systems. Equations (62) and (66) give the typical force and friction constant per unit core volume as $F(L)$ and $\eta(L)$. Then a typical velocity is $v \sim dL/dt \sim F(L)/\eta(L)$, which can be integrated to give, asymptotically,

$$L(t) \sim \begin{cases} \left(\dfrac{t}{\ln t}\right)^{1/2}, & d = n = 2, \\ t^{1/2}, & \text{otherwise.} \end{cases} \tag{67}$$

The result for $n = d = 2$ was derived by Pargellis *et al.* [49], and checked numerically by Yurke *et al.* [50]. The method used here follows their approach (I am grateful to N. Turok for a useful discussion of this approach.). The key concept of a scale-dependent friction constant has been discussed by a number of authors [51]. A detailed analysis of monopole–antimonopole annihilation, in the context of nematic liquid crystals, has been given by Pisman and Rubinstein [52].

A more general and powerful method for deriving growth laws, valid for both conserved and non-conserved systems, is the subject of section 7. The results agree with the intuitive arguments presented so far, with the possible exception of the case $n = d = 2$, for which evidence suggestive of scaling violations will be presented.

3.3. *The Porod law*

The presence of topological defects, seeded by the initial conditions, in the system undergoing phase ordering has an important effect on the short-distance form of the pair correlation function $C(\mathbf{r}, t)$, and therefore on the large-momentum form of the structure factor $S(\mathbf{k}, t)$. To see why this is so, we note that, according to the scaling hypothesis, we would expect a typical field gradient to be of order $|\nabla \vec{\phi}| \sim 1/L$. At a distance r from a defect core, however, with $\xi \ll r \ll L$, the field gradient is much larger, of order $1/r$ (for a vector field), because $\vec{\phi} = \hat{\mathbf{r}}$ implies that $(\nabla \vec{\phi})^2 = (n-1)/r^2$. Note that we require $r \gg \xi$ for the field to be saturated, and $r \ll L$ for the defect field to be largely unaffected by other defects (which are typically a distance L away). This gives a meaning to short distances ($\xi \ll r \ll L$), and large momenta ($L^{-1} \ll k \ll \xi^{-1}$). The large field gradients near defects leads to a non-analytic behaviour at $x = 0$ of the scaling function $f(x)$ for pair correlations.

We start by considering scalar fields. Consider two points $\mathbf{x}$ and $\mathbf{x}+\mathbf{r}$, with $\xi \ll r \ll L$. The product $\phi(\mathbf{x})\phi(\mathbf{x}+\mathbf{r})$ will be -1 if a wall passes between them, and $+1$ if there is no wall. Since $r \ll L$, the probability of finding more than one wall can be neglected. The calculation amounts to finding the probability that a randomly placed rod of length r cuts a domain wall. The probability is of order r/L; so we estimate

$$C(\mathbf{r},t) \approx (-1)\frac{r}{L} + (+1)\left(\frac{1-r}{L}\right)$$

$$= 1 - \frac{2r}{L}, \quad r \ll L. \tag{68}$$

The factor 2 in this result should not be taken seriously.

The important result is that equation (68) is non-analytic in $\mathbf{r}$ at $\mathbf{r}=\mathbf{0}$, since it is linear in $r \equiv |\mathbf{r}|$. Technically, of course, this form breaks down inside the core region, when $r < \xi$. We are interested, however, in the scaling limit defined by $r \gg \xi, L \gg \xi$, with $x = r/L$ arbitrary. The non-analyticity is really in the scaling variable x.

The non-analytic form (68) implies a power-law tail in the structure factor, which can be obtained from equation (68) by simple power counting:

$$S(\mathbf{k},t) \sim \frac{1}{Lk^{d+1}}, \quad kL \gg 1, \tag{69}$$

a result known universally as the Porod law. It was first written down in the general context of scattering from two-phase media [22]. Again, one requires $k\xi \ll 1$ for the scaling regime. Although the k dependence of equation (69) is what is usually referred to as the Porod law, the L dependence is equally interesting. The factor $1/L$ is simply (up to constants) the total area of domain wall per unit volume, a fact appreciated by Porod, who proposed structure factor measurements as a technique for determining the area of interface in the two-phase medium [22]. On reflection, the factor $1/L$ is not so surprising. For $kL \gg 1$, the scattering function is probing structure on scales much shorter than the typical interwall spacing or radius of curvature. In this regime we would expect the structure factor to scale as the total wall area since each element of wall with linear dimension large compared with $1/k$ contributes essentially independently to the structure factor.

This observation provides the clue to how to generalize equation (69) to vector (and other) fields [53, 54]. The idea is that, for $kL \gg 1$, the structure factor should scale as the total volume of defect core. Since the dimension of the defects is $d-n$, the amount of defect per unit volume scales as L^{-n}. Extracting this factor from the general scaling form (7) yields

$$S(\mathbf{k},t) \sim \frac{1}{L^n k^{d+n}}, \quad kL \gg 1, \tag{70}$$

for the O(n) theory, a generalized Porod law.

Equation (70) was first derived from approximate treatments of the equation of motion (57) for non-conserved fields [55–58]. In these derivations, however, the key role of topological defects was far from transparent. The above heuristic derivation suggests that the result is in fact very general (e.g. it should hold equally well for conserved fields), with extensions beyond simple O(n) models. The appropriate techniques, which also enable the amplitude of the tail to be determined, were developed by Bray and Humayun [54] and will be discussed in detail in section 6.

3.4. *Nematic liquid crystals*

Liquid crystals have been a fertile area for recent experimental work on the kinetics of phase ordering, largely because of the efforts of Yurke and coworkers [21, 49, 59–61]. Here we shall concentrate on the simplest liquid crystal phase, the nematic. In a simple picture which captures the orientational degrees of freedom of the nematic, the liquid crystal can be thought of as consisting of rod-like molecules (for example [62]) which have a preferential alignment with the 'director' $\mathbf{n}$ in the ordered phase. Because the molecules have a head–tail symmetry, however, the free energy is invariant under the local transformation $\mathbf{n} \to -\mathbf{n}$. As a result, the nematic is usually described by a tensor order parameter Q that is invariant under this local transformation, and has in the ordered phase the representation

$$Q_{ab} = S(n_a n_b - \tfrac{1}{3}\delta_{ab}). \tag{71}$$

Note that Q is a traceless symmetric tensor. The simplest free-energy functional is one that is invariant under global rotations of the field $n(\mathbf{r})$. It has the form [62]

$$F[Q] = \int \mathrm{d}^3x \left(\tfrac{1}{2} \operatorname{Tr}(|\nabla Q|^2) + \frac{r}{2} \operatorname{Tr} Q^2 - \frac{w}{3} \operatorname{Tr} Q^3 + \frac{u}{4} (\operatorname{Tr} Q^2)^2 \right), \tag{72}$$

where we have retained only terms up to order Q^4, and the lowest order term involving spatial gradients. (Note that $\operatorname{Tr} Q^4 = \frac{1}{2}(\operatorname{Tr} Q^2)^2$ for a 3×3 traceless symmetric tensor; so we do not include this term separately.) The presence of the cubic term, allowed by symmetry, leads to a first-order phase transition in mean-field theory [62]. In experimental systems the transition is weakly first order.

The free-energy functional (72) is an idealization of real nematics, in the spirit of the Lebwohl–Lasher, lattice Hamiltonian $H_{\mathrm{LL}} = -J\Sigma_{\langle i,j \rangle}(\mathbf{n}_i \cdot \mathbf{n}_j)^2$, where $\mathbf{n}_i$ is the local director at site i. Both models are invariant under global rotations of $\mathbf{n}$, as well as local inversions $\mathbf{n} \to -\mathbf{n}$. The gradient terms in equation (72) can be written, using equation (71), as (ignoring constants) $\Sigma_{i,a}(\partial n^a / \partial x_i)^2$, that is as $(\nabla \vec{n})^2$, which continuum version of H_{LL}.The overarrow on $\vec{n}$ here indicates that, in these models, the spatial and 'internal' spaces can be considered as distinct (much as in the O(n) model, where n and d can be different). In real nematics, however, these spaces are coupled. An appropriate gradient energy density is the Frank energy

$$E_{\mathrm{F}} = K_1(\nabla \cdot \mathbf{n})^2 + K_2(\mathbf{n} \cdot \nabla \times \mathbf{n})^2 + K_3|\mathbf{n} \times (\nabla \times \mathbf{n})|^2, \tag{73}$$

where the Frank constants K_1, K_2 and K_3 are associated with 'splay', 'twist' and 'bend' of the director [62]. The isotropic models discussed above correspond to the case $K_1 = K_2 = K_3$, the much-used equal-constant approximation. We shall limit our considerations exclusively to this case.

In a similar spirit, we adopt the simplest possible dynamics, namely the purely relaxational dynamics of model A. This captures correctly the non-conserved nature of the dynamics but ignores possible complications due to hydrodynamic interactions. Recent work comparing experimental results with simulations based on relaxational dynamics provides some justification for this approach [63]. The equation of motion is $\partial Q / \partial t = -\delta G[Q]/\delta Q$, where $G[Q] = F[Q] - \int \mathrm{d}^3x\, \lambda(\mathbf{x}) Q(\mathbf{x})$ and λ is a Lagrange multiplier introduced to maintain the condition $\operatorname{Tr} Q = 0$. Imposing the constraint to eliminate λ gives

$$\frac{\partial Q}{\partial t} = \nabla^2 Q - rQ + w(Q^2 - \tfrac{1}{3} I \operatorname{Tr} Q^2) - uQ \operatorname{Tr} Q^2, \tag{74}$$

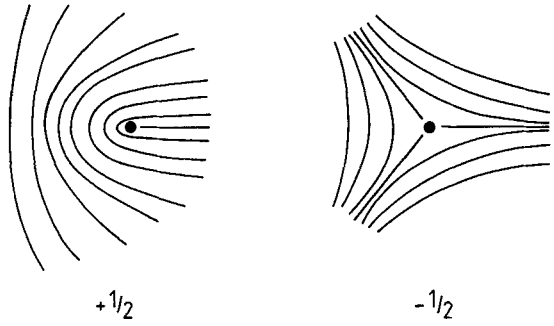

Figure 11. Cross-section of $\pm\frac{1}{2}$-string configurations for a nematic liquid crystal.

where I is the unit tensor. This equation will be discussed in more detail in section 5.4.

Owing to the extra local symmetry (compared with O(3) models) under $\mathbf{n} \rightarrow -\mathbf{n}$, nematic liquid crystals support a number of defect types [47]. In the present context, the most important are string defects, or 'disclinations', in which the director rotates through $\pm\pi$ on encircling the string, as sketched in figure 11. The $\pm\frac{1}{2}$ strings are topologically stable in contrast with ± 1 string configurations (in nematics and the O(3) model) which can be relaxed by smoothly canting the order parameter towards the string axis ('escape in the third dimension'). The presence of string defects (which have been observed by Yurke's group [59]), makes the nematic more akin to the O(2) model than to the O(3) model as far as its ordering kinetics are concerned. In particular, if we make the natural assumption that the total string length decreases as L^{-2}, a Porod law of the form (70) with $n = 2$ is predicted. Scattering data were originally interpreted as being consistent with $n = 3$-like behaviour, that is an effective exponent $d + n = 6{\cdot}0 \pm 0{\cdot}3$ in equation (70) was observed [60], but it is not clear whether the appropriate region of the structure factor tail was fitted [64]. Numerical simulations of a 'soft-spin' version of the Lebwohl–Lasher model [65] are fully consistent with a tail exponent of 5 [64]. We shall return to this point in section 5.4.

4. Exactly soluble models

There are few exactly solved models of phase-ordering dynamics and, unfortunately, these models are quite far from describing systems of physical interest. However, the models are not without interest, as some qualitative features survive in more physically relevant models. In particular, such models are the only cases in which the hypothesized scaling property has been explicitly established.

We begin by discussing phase ordering of a vector field in the limit that the number n of vector components of the field tends to infinity. This limit has been studied, mostly for non-conserved fields, by a large number of workers [16, 20, 66–69]. (A rather complete discussion of growth kinetics in the large-n limit, for both conserved and non-conserved dynamics is contained in [67].) In principle, the solution is the starting point for a systematic treatment in powers of $1/n$. In practice, the calculation of the $O(1/n)$ terms is technically difficult [20, 69]. (Note that [69] corrects an error in [20].) Moreover, some important physics is lost in this limit. In particular, there are no topological defects, since clearly $n > d + 1$ for any d as $n \rightarrow \infty$. As a consequence, the Porod law (70), for example, is not found. It turns out, however, that similar techniques can be applied for any n after a preliminary transformation from the physical order parameter field $\vec{\phi}$ to a suitably chosen 'auxiliary field' $\vec{m}$. This is discussed in

section 5. The topological defects are incorporated through the functional dependence of $\vec{\phi}$ on $\vec{m}$, and the Porod law is recovered.

4.1. *The large-*n *limit: non-conserved fields*

Although not strictly necessary, it is convenient to choose in equation (57) the familiar 'ϕ^4' potential, in the form $V(\vec{\phi}) = (n - \vec{\phi}^2)^2/4n$, where the explicit n-dependence is for later convenience in taking the limit $n \to \infty$. With this potential, equation (57) becomes

$$\frac{\partial \vec{\phi}}{\partial t} = \nabla^2 \vec{\phi} + \vec{\phi} - \frac{1}{n}(\vec{\phi}^2)\vec{\phi}. \tag{75}$$

The simplest way to take the limit is to recognize that, for $n \to \infty$, $\vec{\phi}^2/n$ can be replaced by its average, to give

$$\frac{\partial \phi}{\partial t} = \nabla^2 \phi + a(t)\phi, \tag{76}$$

$$a(t) = 1 - \langle \phi^2 \rangle, \tag{77}$$

where ϕ now stands for (any) one of the components of $\vec{\phi}$. Equation (76) can alternatively be derived by standard diagrammatic techniques [20]. Equation (76) can be solved exactly for arbitrary time t after the quench. However, we are mainly interested in late times (i.e. the scaling regime), when the solution simplifies. After Fourier transformation, the formal solution of equation (76) is

$$\phi_{\mathbf{k}}(t) = \phi_{\mathbf{k}}(0) \exp[-k^2 t + b(t)], \tag{78}$$

$$b(t) = \int_0^t \mathrm{d}t'\, a(t'), \tag{79}$$

giving

$$a(t) = \frac{\mathrm{d}b}{\mathrm{d}t} = 1 - \Delta \sum_{\mathbf{k}} \exp[-2k^2 t + 2b(t)], \tag{80}$$

where equation (4) has been used to eliminate the initial condition. Since we shall find *a posteriori* that $a(t) \ll 1$ at late times, the left-hand side of equation (80) is negligible for $t \to \infty$. Using $\Sigma_{\mathbf{k}} \exp(-2k^2 t) = (8\pi t)^{-d/2}$ gives $b(t) \to (d/4)\ln(t/t_0)$, where

$$t_0 = \Delta^{2/d}/8\pi. \tag{81}$$

Therefore $a(t) \to d/4t$ for $t \to \infty$, and the solution of equation (78), valid at late times, is

$$\phi_{\mathbf{k}}(t) = \phi_{\mathbf{k}}(0)\left(\frac{t}{t_0}\right)^{d/4} \exp(-k^2 t). \tag{82}$$

Using equation (4) once more, we obtain the structure factor and its Fourier transform, the pair correlation function, as

$$S(\mathbf{k}, t) = (8\pi t)^{d/2} \exp(-2k^2 t), \tag{83}$$

$$C(\mathbf{r}, t) = \exp\left(-\frac{r^2}{8t}\right). \tag{84}$$

The results exhibit the expected scaling forms (7), with length scale $L(t) \propto t^{1/2}$. Note that

the structure factor has a Gaussian tail, in contrast with the power-law tail (70) found in systems with $n \leq d$. It might be hoped, however, that the large-n forms (83) and (84) would be qualitatively correct in systems with no topological defects, that is for $n > d + 1$. These cases will be discussed in section 6.

4.2. *Two-time correlations*

Within the large-n solution, we can also calculate two-time correlations to test the scaling form (8). It turns out (although this becomes apparent only at O($1/n$)) [20, 69] that there is a new non-trivial exponent associated with the limit when the two times are well separated. (A similar exponent has been introduced in the context of non-equilibrium *critical* dynamics by Janssen *et al.* [70].)

From equation (82) it follows immediately that

$$S(\mathbf{k}, t, t') \equiv \langle \phi_{\mathbf{k}}(t) \phi_{-\mathbf{k}}(t') \rangle = [8\pi(tt')^{1/2}]^{d/2} \exp[-k^2(t+t')], \tag{85}$$

$$C(\mathbf{r}, t, t') \equiv \langle \phi(\mathbf{r}, t) \phi(\mathbf{0}, t') \rangle = \left(\frac{4tt'}{(t+t')^2}\right)^{d/4} \exp\left[-\frac{r^2}{4(t+t')}\right]. \tag{86}$$

Equation (86) indeed has the expected form (8). In the limit $t \gg t'$, equation (86) becomes

$$C(\mathbf{r}, t, t') = \left(\frac{4t'}{t}\right)^{d/4} \exp\left(-\frac{r^2}{4t}\right) \tag{87}$$

$$= \left(\frac{L'}{L}\right)^{\bar{\lambda}} h\left(\frac{r}{L}\right), \tag{88}$$

where the last equation defines the exponent $\bar{\lambda}$ through the dependence on the *later* time t. Clearly, $\bar{\lambda} = d/2$ for $n = \infty$. When the O($1/n$) correction is included, however, an entirely non-trivial result is obtained [20, 69].

It is interesting to consider the special case where the earlier time t' is zero. Then $C(\mathbf{r}, t, 0)$ is just the correlation with the initial condition. This quantity is often studied in numerical simulations as a convenient way to determine the exponent $\bar{\lambda}$. Within the large-n solution, equations (82) and (81) give, in Fourier and real space,

$$S(\mathbf{k}, t, 0) = [8\pi(tt_0)^{1/2}]^{d/2} \exp(-k^2 t), \tag{89}$$

$$C(\mathbf{r}, t, 0) = \left(\frac{4t_0}{t}\right)^{d/4} \exp\left(-\frac{r^2}{4t}\right). \tag{90}$$

This is just what one gets by replacing t' by t_0 in equations (85) and (86) (with t_0 playing the role of a short-time cut-off), and then neglecting t_0 compared with t.

A related function is the *response* to the initial condition, defined by

$$G(\mathbf{k}, t) = \left\langle \frac{\partial \phi_{\mathbf{k}}(t)}{\partial \phi_{\mathbf{k}}(0)} \right\rangle. \tag{91}$$

Within the large-n solution, equation (82) gives immediately

$$G(\mathbf{k}, t) = \left(\frac{t}{t_0}\right)^{d/4} \exp(-k^2 t). \tag{92}$$

Comparing equations (89) and (92) and using equation (81) once more give the relation.

$$S(\mathbf{k}, t, 0) = \Delta G(\mathbf{k}, t). \tag{93}$$

This is an exact result, valid beyond the large-n limit, as may be proved easily using integration by parts on the Gaussian distribution for $\{\phi_{\mathbf{k}}(0)\}$. The general scaling form for $G(\mathbf{k}, t)$, namely

$$G(\mathbf{k}, t) = L^{\lambda} g_R(kL), \tag{94}$$

defines a new exponent λ, equal to $d/2$ for $n = \infty$. Since, however, the correlation with the initial condition has the scaling form $C(\mathbf{r}, t, 0) = L^{-\bar{\lambda}} f(r/L)$, the identity (93) gives immediately†

$$\bar{\lambda} = d - \lambda. \tag{95}$$

(The symbol λ is also used for the transport coefficient in systems with conserved dynamics. This should not be a source of confusion, as the meaning will be clear from the context.)

Before leaving this section, it is interesting to consider to what extent the results depend on the specific form (4) chosen for the correlator of the initial conditions. Let us replace the right-hand side of equation (4) by a function $\Delta(|\mathbf{x} - \mathbf{x}'|)$, with Fourier transform $\Delta(k)$. Then $\Delta(k)$ will appear inside the sum over $\mathbf{k}$ in equation (80). The dominant k values in the sum, however, are of order $t^{-1/2}$; so for late times we can replace $\Delta(k)$ by $\Delta(0)$, provided that the latter exists. The means that universal results are obtained when only *short-range* spatial correlations are present at $t = 0$. For sufficiently *long-range* correlations, however, such that $\Delta(k)$ diverges for $k \to 0$, new universality classes are obtained. We shall return to the role of initial conditions, from a more general perspective, in section 8.

4.3. *The large-*n *limit: conserved fields*

For conserved fields, the calculation proceeds as before, but with an extra $-\nabla^2$ on the right-hand side of the equation of motion. Making as before, the replacement $\vec{\phi}^2/n \to \langle \phi^2 \rangle$ for $n \to \infty$, where ϕ is (any) one component of $\vec{\phi}$, one obtains

$$\frac{\partial \phi}{\partial t} = -\nabla^4 \phi - a(t) \nabla^2 \phi, \tag{96}$$

with $a(t)$ still given by equation (77). Transforming to Fourier space, the solution is

$$\phi_{\mathbf{k}}(t) = \phi_{\mathbf{k}}(0) \exp[-k^4 t + k^2 b(t)]. \tag{97}$$

The function $b(t)$, defined as in equation (79), satisfies the equation

$$a(t) = \frac{\mathrm{d}b}{\mathrm{d}t} = 1 - \Delta \sum_{\mathbf{k}} \exp[-2k^4 t + 2k^2 b(t)]. \tag{98}$$

This equation was solved by Coniglio and Zannetti [16], by first expressing the sum over $\mathbf{k}$ as a parabolic cylinder function and then taking the large-t limit. Here we shall take the large-t limit from the outset and recognize that the sum can then be evaluated using steepest descents. Just as for the non-conserved case, we can show *a posteriori* that $\mathrm{d}b/\mathrm{d}t \ll 1$ at late times, so that this term can be dropped from equation (98). After

† The exponent λ defined here (and in earlier papers by the present author) differs from that defined in [19] and in Mazenko's papers. Their λ is our $\bar{\lambda}$.

the change of variable $\mathbf{k} = [b(t)/t]^{1/2}\mathbf{x}$, we obtain

$$1 = \Delta C_d \left(\frac{b}{t}\right)^{d/2} \int_0^\infty x^{d-1}\,dx \exp\left[2\beta(x^2 - x^4)\right], \tag{99}$$

where C_d is an uninteresting constant, and

$$\beta(t) = \frac{b^2(t)}{t}. \tag{100}$$

Providing $\beta(t) \to \infty$ for $t = \infty$ (which can be verified *a posteriori*), the integral on the right of equation (99) can be evaluated by steepest descents. Including the Gaussian fluctuations around the maximum of the integrand at $x = 1/2^{1/2}$ gives

$$1 = \text{constant}\, \Delta \beta^{-1/2} \left(\frac{\beta}{t}\right)^{d/4} \exp\left(\frac{\beta}{2}\right), \tag{101}$$

with asymptotic solution

$$\beta \approx \frac{d}{2} \ln t, \quad t \to \infty, \tag{102}$$

justifying the use of the steepest-descents method for large t. Putting this result into equation (97) gives the final result for the structure factor [16]

$$S(\mathbf{k}, t) \approx t^{(d/4)\phi(k/k_m)} \tag{103}$$

$$k_m \approx \left(\frac{d}{8} \frac{\ln t}{t}\right)^{1/4} \tag{104}$$

$$\phi(x) = 1 - (1 - x^2)^2. \tag{105}$$

Here $k_m(t)$ is the position of the maximum in $S(\mathbf{k}, t)$. A slightly more careful treatment (retaining the leading subdominant term in equation (102)), gives an additional logarithmic pre-factor, of order $(\ln t)^{(2-d)/4}$, in equation (103), such that (asymptotically in time) $\Sigma_{\mathbf{k}} S(\mathbf{k}, t) = 1$.

Equation (103) is interesting because, in contrast with the non-conserved result (83), it does not have the conventional scaling form. Rather it exhibits 'multiscaling' [16]. In particular there are two, logarithmically different length scales k_m^{-1} and $L = t^{1/4}$. For simple scaling, these two scales would be the same. Furthermore, for fixed scaling variable, which can be written as k/k_m, the structure factor would vary as $L(t)^d$, with a *pre-factor* depending on the scaling variable. In the multiscaling form (103), for fixed scaling variable, $S(\mathbf{k}, t) \sim L^{d\phi(k/k_m)}$, that is the *exponent* depends continuously on the scaling variable.

After the discovery of multiscaling in the $n \to \infty$ limit, some effort was devoted to looking for similar phenomena at finite n, notably for scalar systems [71], but also for $n = 2$ [72, 73] and $n = 3$ [74]. However, no evidence was found for any departure from simple scaling for any finite n. At the same time, Bray and Humayun [75] showed, within the context of an approximate calculation based on an idea of Mazenko, that simple scaling is recovered asymptotically for any finite n. This result is discussed in detail in section 5.

4.4. *The one-dimensional Ising model*

An exceptionally simple system that can be solved exactly [15] is the Ising model in one dimension with Glauber dynamics. It is defined by the Glauber equation for the spin probability weight:

$$\frac{\mathrm{d}}{\mathrm{d}t}P(S_1,\ldots,S_N;t) = -P(S_1,\ldots,S_N;t)\sum_i\left(\frac{1-S_i\tanh(\beta h_i)}{2}\right) + \sum_i P(S_1,\ldots,-S_i,\ldots,S_N;t)\left(\frac{1+S_i\tanh(\beta h_i)}{2}\right), \quad (106)$$

where $\beta = 1/T$, $h_i = J(S_{i-1} + S_{i+1})$ is the local field at site i, and periodic boundary conditions $S_{i+N} = S_i$ have been adopted.

From equation (106), it is straightforward to derive the equation of motion for the pair correlation function $C_{ij}(t) = \langle S_i(t)S_j(t)\rangle$, where the angular brackets indicate an average over the distribution P. After averaging also over the initial conditions, C_{ij} depends only on the difference $r = |i-j|$ if the ensemble of initial conditions is invariant under translations. Then one obtains

$$\frac{\mathrm{d}}{\mathrm{d}t}C(r,t) = C(r+1,t) - 2C(r,t) + C(r-1,t), \quad r \neq 0, \quad (107)$$

For $r = 0$, one has trivially $C(0,t) = 1$ for all t. To solve for C in the scaling limit, it is simplest to take the continuum limit, when equation (107) reduces to the diffusion equation, $\partial C/\partial t = \partial^2 C/\partial r^2$, with constraint $C(0,t) = 1$. A scaling solution obviously requires $L(t) = t^{1/2}$. Inserting $C(r,t) = f(r/t^{1/2})$ in the diffusion equation gives $f'' = -(x/2)f'$, which can be integrated with boundary conditions $f(0) = 1, f(\infty) = 0$ to give $f(x) = \mathrm{erfc}\,(x/2)$, where erfc is the complementary error function. Thus the scaling solution is

$$C(r,t) = \mathrm{erfc}\left(\frac{r}{2t^{1/2}}\right). \quad (108)$$

In particular, the solution exhibits the expected Porod regime

$$C = 1 - r/(\pi t)^{1/2} + \mathrm{O}(r^3/t^{3/2})$$

at short distances. A more complete discussion can be found in [15].

The scalar TDGL equation (2) is also soluble in one dimension, in the sense that the scaling functions can be exactly calculated [76]. When $L(t) \gg \xi$, neighbouring domain walls interact only weakly, with a force of order $\exp(-L/\xi)$, leading to a logarithmic growth law $L \sim \xi \ln t$. Moreover, in the limit $L/\xi \to \infty$, the closest pair of domain walls interact strongly compared with other pairs, so that the other walls can be treated as stationary while the closest pair annihilate. This leads to a simple recursion for the domain size distribution, with a scaling solution [76]. It is interesting that the fraction of the line which has never been traversed by a wall decays with a non-trivial power of the mean domain size [77]. A similar phenomenon (but with a different power) occurs for Glauber dynamics [78].

4.5. *The one-dimensional XY model*

As our final example of a soluble model, we consider the case $d = 1$, $n = 2$, with non-conserved order parameter. The solution, first given by Newman *et al.* [68], is interesting for the 'anomalous' growth law obtained, namely $L(t) \sim t^{1/4}$. Here we shall give a more detailed discussion than appears in [68], emphasizing the scaling violations exhibited by, in particular, the two-time correlation function. In section 7, we shall present a general technique, developed by Bray and Rutenberg (BR) [79], for determining growth laws for phase-ordering systems. The scaling form (8) plays an

important role in the derivation. For the $d = 1, n = 2$, model, however, our method fails to predict the correct $t^{1/4}$ growth. The reason is precisely the unconventional form (i.e. different from equation (8)) of the two-time correlation function for this system.

It is simplest to work with 'fixed-length' fields, that is $\vec{\phi}^2 = 1$, with Hamiltonian $F = \frac{1}{2}\int dx\,(\partial\vec{\phi}/\partial x)^2$. The constraint can be eliminated by the representation $\vec{\phi} = (\cos\theta, \sin\theta)$, where θ is the phase angle, to give $F = \frac{1}{2}\int dx\,(\partial\theta/\partial x)^2$. The 'model A' equation of motion, $\partial\theta/\partial t = -\partial F/\delta\theta$, becomes

$$\frac{\partial\theta}{\partial t} = \frac{\partial^2\theta}{\partial x^2}, \tag{109}$$

that is a simple diffusion equation for the phase. In general dimensions, it is difficult to include vortices, which are singularities in the phase field, in a simple way. Such singularities, however, are absent for $d = 1$.

Equation (109) has to be supplemented by suitable initial conditions. It is convenient to choose the probability distribution for $\theta(r, 0)$ to be Gaussian; in Fourier space

$$P(\{\theta_k(0)\}) \propto \exp\left(-\sum_k \frac{\beta_k}{2}\theta_k(0)\theta_{-k}(0)\right). \tag{110}$$

Then the real-space correlation function at $t = 0$ is readily evaluated using the Gaussian property of the $\{\theta_k(0)\}$:

$$\begin{aligned} C(r,0) &= \langle\cos[\theta(r,0) - \theta(0,0)]\rangle \\ &= \exp\{-\tfrac{1}{2}\langle[\theta(r,0) - \theta(0,0)]^2\rangle\} \\ &= \exp\left(-\sum_k \frac{1-\cos(kr)}{\beta_k}\right). \end{aligned} \tag{111}$$

The choice $\beta_k = (\xi/2)k^2$ yields $C(r, 0) = \exp(-|r|/\xi)$, appropriate to a quench from a disordered state with correlation length ξ.

The general two-time correlation function can be calculated in the same way [80]. Using $\beta_k = (\xi/2)k^2$, and the solution $\theta_k(t) = \theta_k(0)\exp(-k^2t)$ of equation (109), gives

$$\begin{aligned} C(r,t_1,t_2) &= \langle\cos[\theta(r,t_1) - \theta(0,t_2)]\rangle \\ &= \exp\{-\tfrac{1}{2}\langle[\theta(r,t_1) - \theta(0,t_2)]^2\rangle\} \\ &= \exp\Bigg(-\sum_k \frac{1}{\xi k^2}\{[\exp(-k^2t_1) - \exp(-k^2t_2)]^2 \\ &\qquad + 2[1-\cos(kr)]\exp[-k^2(t_1+t_2)]\}\Bigg). \end{aligned} \tag{112}$$

Since we shall find that r is scaled by $(t_1 + t_2)^{1/4}$, we can take $kr \ll 1$ in the summand for the r values of interest, that is we can replace $1 - \cos(kr)$ by $(kr)^2/2$. Evaluation of the sums then gives

$$C(r,t_1,t_2) = \exp\left[-\frac{1}{\xi\pi^{1/2}}\left(\frac{r^2}{2(t_1+t_2)^{1/2}} + 2(t_1+t_2)^{1/2} - (2t_1)^{1/2} - (2t_2)^{1/2}\right)\right]. \tag{113}$$

For the special case $t_1 = t_2 = t$, equation (113) reduces to

$$C(r,t,t) = \exp[-r^2/2\xi(2\pi t)^{1/2}],$$

which has the standard scaling form (7), with growth law $L(t) \sim t^{1/4}$. This growth law is unusual; we shall show in section 7 that the generic form for non-conserved fields

is $L(t) \sim t^{1/2}$, just as in the large-n result (84). Another, related feature of equation (113) is the explicit appearance of ξ, the correlation length for the initial condition. The large-n solution, for example, becomes independent of ξ for $L(t) \gg \xi$. The most striking feature of equation (113), however, is the breakdown of the scaling form (8) for the two-time correlations. It is this feature that invalidates the derivation of the result $L(t) \sim t^{1/2}$ given in section 7. It is possible that a similar anomalous scaling is present in the *conserved* $d = 1$ *XY* model, for which simulation results [72, 74] suggest $L(t) \sim t^{1/6}$, instead of the $t^{1/4}$ growth derived in section 7 assuming simple scaling for two-time correlations. Unfortunately, an exact solution for the conserved case in non-trivial.

The explicit dependence of equation (113) on ξ suggests an unusual sensitivity to the initial conditions in this system. A striking manifestation of this is obtained by choosing initial conditions with a non-exponential decay of correlations. For example, choosing $\beta_k \sim |k|^\alpha$ for small $|k|$ in equation (110) gives, via equation (111), $C(r, 0) \sim \exp(\text{constant } |r|^{\alpha-1})$ for large $|r|$, provided that $1 < \alpha < 3$. The calculation of the pair correlation function is again straightforward. For example the equal-time function has a scaling form given by $C(r, t) = \exp(\text{constant } r^2/t^{(3-\alpha)/2})$, implying a growth law $L(t) \sim t^{(3-\alpha)/4}$, but the two-time correlation still does not scale properly.

An especially interesting case is $\alpha = 1$, which generates power-law spatial correlations in the initial condition. Thus we choose $\beta_k = |k|/\gamma$ for $|k| \leq \Lambda$, and $\beta_k = \infty$ for $|k| > \Lambda$, where Λ is an ultraviolet cut-off. Then the initial-condition correlator has the form $C(r, 0) \sim (\Lambda r)^{-\gamma/\pi}$ for $\Lambda r \gg 1$. The general two-time correlation function now has the conventional scaling form (8), with $L(t) \sim t^{1/2}$. Its form is

$$C(r, t_1, t_2) = f\left(\frac{r}{(t_1 + t_2)^{1/2}}\right)\left(\frac{4t_1 t_2}{(t_1 + t_2)^2}\right)^{\gamma/4\pi}, \tag{114}$$

where $f(x)$ is the equal-time correlation function. In particular, for $t_2 \gg t_1$ this gives $C(r, t_1, t_2) \approx f(r/t_2^{1/2})\,(4t_1/t_2)^{\gamma/4\pi}$; so the exponent $\bar{\lambda}$ defined by equation (9) is $\gamma/2\pi$ for this model. Also the large-distance behaviour of the equal-time correlation function is $f(x) \sim x^{-\gamma/\pi}$, exhibiting the same power-law decay as the initial condition. These two results are in complete agreement with the general treatment [81] of initial conditions with power-law correlations, given in section 8.3.1.

5. Approximate theories for scaling functions

While the determination of growth laws (i.e. the form of $L(t)$) has proved possible using fairly simple arguments (as in section 2.5), which can be made precise by the use of exact relations between correlation functions (section 7), or RG methods (section 8), the calculation of scaling functions, for example the pair correlation scaling function $f(x)$ (see equation (7)), has been a long-standing challenge. In the previous section we have shown that this function can be calculated exactly in a number of soluble models. With the exception of the $1-d$ Glauber model, however, the models lack the topological defects that play such an important role in realistic models. In particular, these defects are responsible for the power-law tail (70) in the structure factor.

In this section we shall review some of the approximate theories that have been put forward for the scaling function $f(x)$ of the pair correlation function. The most successful by far are theories for non-conserved fields. Even these, however, are not quite as good as has been believed, as we shall show. We shall propose a new approach which can in principle lead to systematically improvable calculations of scaling functions for non-conserved fields. For conserved fields the theory is in a less

satisfactory state. We shall try to give some indication of why this is so. Finally we emphasize that the discussion is limited throughout to the late-stage scaling regime.

5.1. *Non-conserved fields*

A number of approximate scaling functions have been proposed for non-conserved fields, but in my view none of them is completely satisfactory. The most physically appealing approach for scalar fields is that of Ohta, Jasnow and Kawasaki (OJK) [82], which starts from the Allen–Cahn equation (18) for the interfaces. Below we will review the OJK method, as well as an earlier approach by Kawasaki, Yalabik and Gunton (KYG) [83], and more recent work by Mazenko [84–86]. Finally we discuss in detail a new approach [52] which has the virtue that it can, in principle, be systematically improved.

5.1.1. *The Ohta–Jasnow–Kawasaki theory*

A common theme, introduced by OJK, in the approximate theories of scaling functions is the replacement of the physical field $\phi(\mathbf{x}, t)$, which is ± 1 everywhere except at domain walls, where it varies rapidly, by an auxiliary field $m(\mathbf{x}, t)$, which varies smoothly in space. This is achieved by using a non-linear function $\phi(m)$ with a 'sigmoid' shape (such as $\tanh m$). In the OJK theory, the dynamics of the domain walls themselves, defined by the zeros of m, are considered. The normal velocity of a point on the interface is given by the Allen–Cahn equation (9), $v = -K = -\nabla \cdot \mathbf{n}$, where K is the curvature, and $\mathbf{n} = \nabla m/|\nabla m|$ is a unit vector normal to the wall. This gives

$$v = \frac{-\nabla^2 m + n_a n_b \nabla_a \nabla_b m}{|\nabla m|}. \tag{115}$$

In a frame of reference comoving with the interface,

$$\frac{\mathrm{d}m}{\mathrm{d}t} = 0 = \frac{\partial m}{\partial t} + \mathbf{v} \cdot \nabla m. \tag{116}$$

However, since $\mathbf{v}$ is parallel to ∇m (and defined in the same direction), $\mathbf{v} \cdot \nabla m = v|\nabla m|$; so

$$v = -\frac{1}{|\nabla m|} \frac{\partial m}{\partial t}. \tag{117}$$

Eliminating v between equations (115) and (117) gives the OJK equation

$$\frac{\partial m}{\partial t} = \nabla^2 m - n_a n_b \nabla_a \nabla_b m. \tag{118}$$

Since $\mathbf{n} = \nabla m/|\nabla m|$, this equation is nonlinear. To make further progress, OJK made the simplifying approximation of replacing $n_a n_b$ by its spherical average δ_{ab}/d, obtaining the simple diffusion equation

$$\frac{\partial m}{\partial t} = D \nabla^2 m, \tag{119}$$

with diffusion constant $D = (d-1)/d$.

Provided that there are no long-range correlations present, we do not expect the form of the random initial conditions to play an important role in the late-stage scaling. A convenient choice is a Gaussian distribution for the field $m(\mathbf{x}, 0)$, with mean zero

and correlator

$$\langle m(\mathbf{x},0)m(\mathbf{x}',0)\rangle = \Delta\delta(\mathbf{x}-\mathbf{x}'). \tag{120}$$

Then the linearity of equation (119) ensures that the field $m(\mathbf{x},t)$ has a Gaussian distribution at all times. Solving equation (119) and averaging over initial conditions using equation (120) give the equal-time correlation function

$$\langle m(1)m(2)\rangle = \frac{\Delta}{(8\pi Dt)^{d/2}}\exp\left(-\frac{r^2}{8Dt}\right), \tag{121}$$

where 1 and 2 represent space points separated by r. Of special relevance in what follows is the normalized correlator

$$\gamma(12) \equiv \frac{\langle m(1)m(2)\rangle}{\langle m(1)^2\rangle^{1/2}\langle m(2)^2\rangle^{1/2}} = \exp\left(-\frac{r^2}{8Dt}\right). \tag{122}$$

The generalization to different times is straightforward [88] and will be given explicitly below.

To calculate the pair correlation function of the original field ϕ, we need to know the joint probability distribution for $m(1)$ and $m(2)$. For a Gaussian field this can be expressed in terms of the second moments of m:

$$P(m(1),m(2)) = N\exp\left[-\frac{1}{2(1-\gamma^2)}\left(\frac{m(1)^2}{S_0(1)}+\frac{m(2)^2}{S_0(2)}-2\gamma\frac{m(1)m(2)}{[S_0(1)S_0(2)]^{1/2}}\right)\right], \tag{123}$$

where $\gamma = \gamma(12)$, and

$$S_0(1) = \langle m(1)^2\rangle,\ S_0(2) = \langle m(2)^2\rangle,\ N = (2\pi)^{-1}[(1-\gamma^2)S_0(1)S_0(2)]^{-1/2}. \tag{124}$$

Note that equation (123) is a general expression for the joint probability distribution of a Gaussian field, with γ defined by the first part of (122). Now 1 and 2 represent arbitrary space–time points. For the special case where m obeys the diffusion equation (119), γ is given by

$$\gamma = \left(\frac{4t_1t_2}{(t_1+t_2)^2}\right)^{d/4}\exp\left(-\frac{r^2}{4D(t_1+t_2)}\right), \tag{125}$$

a simple generalization of equation (122).

The pair correlation function is given by $C(\mathbf{r},t) = \langle\phi(m(1))\phi(m(2))\rangle$. In the scaling regime, one can replace the function $\phi(m)$ by $\operatorname{sgn}(m)$, because the walls occupy a negligible volume fraction. In a compact notation,

$$C(12) = \langle\operatorname{sgn}[m(1)]\operatorname{sgn}[m(2)]\rangle = \frac{2}{\pi}\sin^{-1}(\gamma). \tag{126}$$

The Gaussian average over the field m required in equation (126) is standard (for example [89]). Equations (122) and (126) define the OJK scaling function for equal-time pair correlations. Note that (apart from the trivial dependence through D) it is independent of the spatial dimension d. We shall present arguments that it becomes exact in the large-d limit. The OJK function fits experiment and simulation data very well. As an example, we show the function $f(x)$ for the $d=2$ scalar theory in figure 12.

The general two-time correlation function is especially interesting in the limit $t_1 \gg t_2$ that defines (see, for example, equation (88)) the exponent $\bar{\lambda}$. Since $\gamma \ll 1$ in this limit, equation (126) can be linearized in γ to give $C(\mathbf{r},t_1,t_2) \sim (4t_1/t_2)^{d/4}\exp(-r_2/4Dt_2)$, that is $\bar{\lambda} = d/2$ within the OJK approximation.

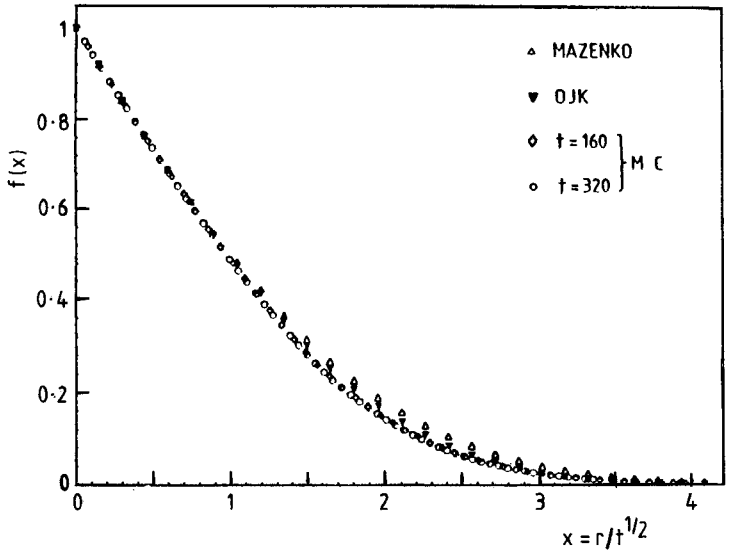

Figure 12. Scaling function $f(x)$ for the non-conserved $d = 2$ Ising model, showing Monte Carlo data (MC) from figure 5, and the approximations of OJK [82] and Mazenko [85]. The scaling lengths $L(t)$ for the theoretical curves were chosen to give the same slope as the data in the linear Porod regime at small x (from [90]).

5.1.2. *The Kawasaki–Yalabik–Gunton method*

An earlier approach, due to KYG, building on still earlier work of Suzuki [91], was based on an approximate resummation of the direct perturbation series in the nonlinearity, for the quartic potential $V(\phi) = \frac{1}{4}(1 - \phi^2)^2$. The equation of motion (2) for this potential is

$$\frac{\partial \phi}{\partial t} = \nabla^2 \phi + \phi - g\phi^3, \tag{127}$$

with $g = 1$. The basic idea is to treat g as small, to expand in powers of g, to extract the leading asymptotic (in t) behaviour of each term in the series and to set $g = 1$ at the end. However, an uncontrolled approximation is made in simplifying the momentum dependence of each term (the expansion is performed in Fourier space). After setting $g = 1$, the final result can be expressed in terms of the mapping

$$\phi(m) = \frac{m}{(1 + m^2)^{1/2}}. \tag{128}$$

It is found that m obeys the equation

$$\frac{\partial m}{\partial t} = \nabla^2 m + m, \tag{129}$$

instead of equation (119), which gives an exponential growth superimposed on the diffusion. After the replacement $\phi(m) \to \mathrm{sgn}(m)$, however, this drops out; the OJK scaling function (126) is recovered, with γ given by equation (122) (but with $D = 1$).

The nature of the approximation involved can be clarified by putting equation (128) into equation (127) (with $g = 1$) to derive the exact equation satisfied by m:

$$\frac{\partial m}{\partial t} = \nabla^2 m + m - 3\frac{m|\nabla m|^2}{1 + m^2}. \tag{130}$$

In contrast with a claim made in [83], there is no reason to neglect the final term. On a physical level, the fact that this approach gives the correct growth law $L(t) \sim t^{1/2}$ seems to be fortuitous (see the discussion in section 7). In particular, the crucial role of the interfacial curvature in driving the growth is not readily apparent in this method. By contrast the OJK approach, while giving the same final result, clearly contains the correct physics.

Despite its shortcomings, the KYG method has the virtue that it can be readily extended to vector fields [55, 92]. Equation (129) is again obtained, but with m replaced by a vector auxiliary field $\vec{m}$, with $\vec{\phi} = \vec{m}/(1 + \vec{m}^2)^{1/2}$. At late times, $\vec{\phi} \to \hat{\mathbf{m}}$, a unit vector, almost everywhere and $C(12) = \langle \hat{\mathbf{m}}(1) \cdot \hat{\mathbf{m}}(2) \rangle$. Taking Gaussian initial conditions for $\vec{m}$, the resulting scaling function is [55], with γ again given by equation (122) (but with $D = 1$),

$$C(12) = \frac{n\gamma}{2\pi}\left[B\left(\frac{n+1}{2}, \frac{1}{2}\right)\right]^2 F\left(\frac{1}{2}, \frac{1}{2}; \frac{n+2}{2}; \gamma^2\right), \tag{131}$$

where $B(x, y)$ is the beta function and $F(a, b; c; z)$ the hypergeometric function ${}_2F_1$. The same scaling function was obtained independently by Toyoki [56]. We shall call it the Bray–Puri–Toyoki (BPT) scaling function. The result (122) for γ implies $L(t) \sim t^{1/2}$ for all n within this approximation.

Both equations (119) and (129) suffer from the weakness that (for scalar fields) the width of the interface changes systematically with time. Since $\phi(m)$ is linear in m for small m, and $|\nabla\phi|$ is fixed (by the interface profile function) in the interface, we expect $\langle|\nabla m|^2\rangle$ = constant. Equations (119) and (129), however, give $\langle|\nabla m|^2\rangle \sim t^{-(d+2)/2}$ and $\langle|\nabla m|^2\rangle \sim \exp(2t)/t^{(d+2)/2}$ for this quantity, corresponding to increasing and decreasing interface widths respectively. Oono and Puri [89] showed that this unphysical feature can be eliminated by introducing an extra term $h(t)m$ in equation (119). Since this term vanishes at the interfaces, where $m = 0$, its inclusion does not change the underlying physics. Fixing $h(t)$ by the requirement $\langle|\nabla m|^2\rangle$ = constant gives $h(t) \approx (d + 2)/4t$ at late times. The scaling function (126), however, is unaffected by the presence of the extra term. In section 5.2 we shall find that the Oono–Puri result arises naturally within a systematic treatment of the problem.

5.1.3. *The Mazenko method*

In an interesting series of papers, Mazenko [84–86] has introduced a new approach that deals with the interface in a natural way. This approach combines a clever choice for the function $\phi(m)$ with the minimal assumption that the field m is Gaussian. Specifically $\phi(m)$ is chosen to be the *equilibrium interface profile function*, defined by (compare equation (10))

$$\phi''(m) = V'(\phi), \tag{132}$$

with boundary conditions $\phi(\pm\infty) = \pm 1$, $\phi(0) = 0$. The field m then has a physical interpretation, near walls, as a coordinate normal to the wall. Note that this mapping transforms a problem with *two* length scales, the domain scale $L(t)$ and the interface width ξ, into one with only a *single* length scale, namely $L(t)$ (figure 13). With the choice (132) for $\phi(m)$, the TDGL equation (2) becomes

$$\partial_t\phi = \nabla^2\phi - \phi''(m). \tag{133}$$

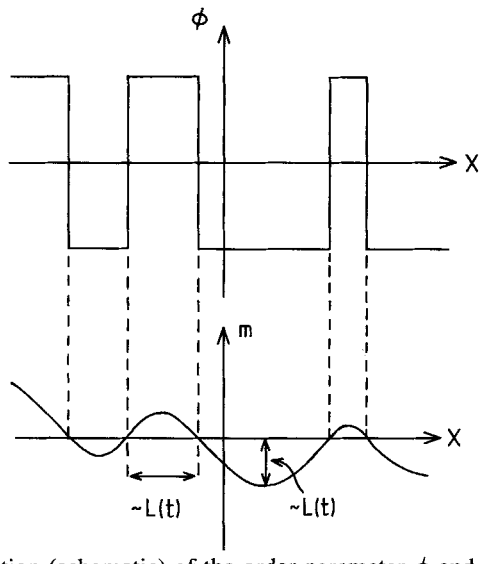

Figure 13. Spatial variation (schematic) of the order parameter ϕ and the auxiliary field m, defined by equation (132).

Multiplying by ϕ at a different space point and averaging over initial conditions gives

$$\tfrac{1}{2}\partial_t C(12) = \nabla^2 C(12) - \langle \phi''(m(1))\phi(m(2))\rangle. \tag{134}$$

So far this is exact. In order to simplify the final term in equation (134), Mazenko assumes that m can be treated as a Gaussian field. Then the final term can be expressed in terms of $C(12)$ itself as follows, exploiting the Fourier decomposition of $\phi(m)$ and the Gaussian property of m [85]:

$$\begin{aligned}\langle \phi''(m(1))\phi(m(2))\rangle &= \sum_{k_1,k_2} \phi_{k_1}\phi_{k_2}(-k_1^2)\langle \exp[ik_1 m(1) + ik_2 m(2)]\rangle \\ &= \sum_{k_1,k_2} \phi_{k_1}\phi_{k_2}(-k_1^2)\exp\left(-\frac{k_1^2 S_0(1)}{2} - \frac{k_2^2 S_0(2)}{2} - k_1 k_2 C_0(12)\right) \\ &= 2\frac{\partial C(12)}{\partial S_0(1)},\end{aligned} \tag{135}$$

where $S_0(1)$ and $S_0(2)$ are given by equation (124) and $C_0(12) = \langle m(1)m(2)\rangle$. The derivative in equation (135) is taken holding $S_0(2)$ and $C_0(12)$ fixed. Since, from the definition (122), $\gamma(12) = C_0(12)/[S_0(1)S_0(2)]^{1/2}$, the general result (126) for Gaussian fields implies that

$$\begin{aligned}2\frac{\partial C(12)}{\partial S_0(1)} &= 2\frac{dC(12)}{d\gamma(12)}\frac{\partial \gamma(12)}{\partial S_0(1)} \\ &= a(t)\gamma(12)\frac{dC(12)}{d\gamma(12)},\end{aligned} \tag{136}$$

where

$$a(t) = \frac{1}{S_0(1)} = \langle m(1)^2\rangle^{-1}. \tag{137}$$

Putting it all together, and suppressing the arguments, the final equation for C is

$$\tfrac{1}{2}\partial_t C = \nabla^2 C + a(t)\gamma \frac{\mathrm{d}C}{\mathrm{d}\gamma}. \tag{138}$$

Using equation (126) for $C(\gamma)$ gives $\gamma\,\mathrm{d}C/\mathrm{d}\gamma = (2/\pi)\tan[(\pi/2)C]$. Then equation (138) becomes a closed nonlinear equation for C. For a scaling solution, one requires $L(t) \sim t^{1/2}$ and $a(t) = \lambda/2t$ for large t in equation (138), so that each of the terms scales as $1/t$ times a function of the scaling variable $r/t^{1/2}$. Setting $C(\mathbf{r}, t) = f(r/t^{1/2})$ gives the equation

$$0 = f'' + \left(\frac{d-1}{x} + \frac{x}{4}\right) f' + \frac{\lambda}{\pi}\tan\left(\frac{\pi}{2} f\right) \tag{139}$$

for the scaling function $f(x)$. The constant λ is fixed by the requirement that the large-distance behaviour of C be physically reasonable [85]. Linearization of equation (139) (valid for large x) leads to two linearly independent large-x solutions with Gaussian and power-law tails. The constant λ is chosen to eliminate the 'unphysical' power-law term.

It is straightforward to adapt this approach to nonconserved vector fields [57, 58]. A significant simplification is that, for Gaussian fields, the joint probability distribution for $\vec{m}(1)$ and $\vec{m}(2)$ factors into a product of separate distributions of the form (123) for each component. This results is an equation of form (138) for any n, but with the function $C(\gamma)$ given by equation (131) for general n instead of equation (126). Again, $a(t) = \lambda/2t$, with λ chosen to eliminate the power-law tail in the scaling function $f(x)$. The values λ for various n and d are given in the table.

It is interesting that the 'unphysical' power-law tails in real space become physical when sufficiently long-range spatial correlations are present in the initial state. This will be shown using RG arguments [81] in section 8.3.1. It also emerges within the Mazenko treatment [90].

The general two-time correlation function $C(\mathbf{r}, t_1, t_2)$ can also be evaluated within this scheme [57, 58]. It is given by a simple generalization of equation (138), namely

$$\partial_{t_1} C = \nabla^2 C + a(t_1)\gamma \frac{\mathrm{d}C}{\mathrm{d}\gamma}, \tag{140}$$

with $a(t_1) = \lambda/2t_1$. This equation simplifies for $t_1 \gg t_2$, because C is then small and the linear relation between C and γ for small C (see equation (131)) implies that $\gamma\,\mathrm{d}C/\mathrm{d}\gamma = C$, that is

$$\partial_{t_1} C = \nabla^2 C + \frac{\lambda}{2t_1} C, \quad t_1 \gg t_2. \tag{141}$$

Exponent λ within the Mazenko theory.

	λ			
d	$n=1$	$n=2$	$n=3$	$n=4$
1	0	0·301	0·378	0·414
2	0·711	0·829	0·883	0·912
3	1·327	1·382	1·413	1·432

This linear equation can be solved by spatial Fourier transform. Choosing an initial condition at $t_1 = \alpha t_2$, with $\alpha \gg 1$ to justify the use of equation (141) for all $t_1 \geqslant \alpha t_2$ gives

$$S(\mathbf{k}, t_1, t_2) = \left(\frac{t_1}{\alpha t_2}\right)^{\lambda/2} \exp\left[-k^2(t_1 - \alpha t_2)\right] S(\mathbf{k}, \alpha t_2, t_2). \tag{142}$$

Imposing the scaling form $S(\mathbf{k}, \alpha t_2, t_2) = t_2^{d/2} g(k^2 t_2)$, with $g(0) =$ constant, and Fourier transforming back to real space gives, for $t_1 \gg \alpha t_2$,

$$C(12) = \text{constant} \left(\frac{t_2}{t_1}\right)^{(d-\lambda)/2} \exp\left(-\frac{r^2}{4t_1}\right). \tag{143}$$

The constant cannot be determined from the linear equation alone; it is, of course independent of α.

Comparison of equation (143) with the general form (88) shows that $\bar{\lambda} = d - \lambda$, that is the parameter λ of the Mazenko theory is precisely the exponent λ associated with the response function $G(\mathbf{k}, t)$ (equation (94)), related to $\bar{\lambda}$ by equation (95). This connection was first pointed out by Liu and Mazenko [93]. The values of λ obtained (table) are in reasonable agreement with those extracted from simulations [17, 19, 68, 94]. For example, for the scalar theory in $d = 2$ simulations [17, 19, 93] give $\lambda \approx 0{\cdot}75$ (argued to be $\frac{3}{4}$ exactly in [19]), compared with 0·711 from the table.

To summarize, the virtues of the Mazenko approach are

(1) only the assumption that the field m is Gaussian is required,
(2) the scaling function has a non-trivial dependence on d (whereas, apart from the trivial dependence through the diffusion constant D, equations (122), (126) and (131) are independent of d) and
(3) the non-trivial behaviour of *different-time* correlation functions [20] emerges in a natural way [93].

In addition, the OJK result (126) and its generalization (131) are reproduced for $d \to \infty$, while the exact scaling function (108) of the $1 - d$ Glauber model is recovered from equation (139) in the limit $d \to 1$ [95]. In practice, however, for $d \geqslant 2$ the shape of the scaling function $f(x)$ differs very little from that of the OJK function given by equations (126) and (122), or its generalization (131) for vector fields [58]. All these functions are in good agreement with numerical simulations. The Mazenko function for $n = 1$, $d = 2$ is included in figure 12, while the BPT results for vector fields are compared with simulations in figures 14 and 15 later. The Mazenko approach can also be used, with some modifications, for conserved scalar [86] and vector [75] fields.

To conclude this section we note that the crucial Gaussian approximation, used in all these theories, has recently been critically discussed by Yeung *et al.* [97]. By explicit simulation they find that the distribution $P(m)$ for the field m at a single point is flatter than a Gaussian at small m. In section 6 we shall show that the joint distribution $P(m(1), m(2))$ can be calculated analytically when $|m(1)|$, $|m(2)|$ and r are all small compared with $L(t)$. The result is non-Gaussian but is consistent with the Gaussian form (123) in the limit $d \to \infty$. Below, we present evidence that the Gaussian approximations becomes exact for $d \to \infty$. Finally we note that very recent work by Mazenko [98] presents a first attempt to go beyond the Gaussian approximation.

5.2. *A systematic approach*

All the treatments discussed above suffer from the disadvantage that they invoke an uncontrolled approximation at some stage. Very recently, however, a new approach

has been developed [87] which recovers the OJK and BPT scaling functions in leading order but has the advantage that it can, in principle, be systematically improved.

5.2.1. *Scalar fields*

For simplicity of presentation, we shall begin with scalar fields. The TDGL equation for a non-conserved scalar field $\phi(\mathbf{x}, t)$ is given by equation (2). We recall that, according to the Allen–Cahn equation (18), the interface motion is determined solely by the local curvature. It follows that the detailed form of the potential $V(\phi)$ is not important, a fact that we can usefully exploit; the principal role of the double-well potential is to establish and maintain well-defined interfaces.

Following Mazenko [85] we define the function $\phi(m)$ by equation (132) with boundary conditions $\phi(\pm\infty) = \pm 1$. We have noted that $\phi(m)$ is just the equilibrium domain-wall profile function, with m playing the role of the distance from the wall. Therefore the spatial variation in m near a domain wall is completely smooth (in fact, linear). The additional condition $\phi(0) = 0$ locates the centre of the wall at $m = 0$. Figure 13 illustrates the difference between ϕ and m for a cut through the system. Note that, while ϕ saturates in the interior of domains, m is typically of order $L(t)$, the domain scale. Rewriting equation (2) in terms of m and using equation (132) to eliminate V' give

$$\partial_t m = \nabla^2 m - \frac{\phi''(m)}{\phi'(m)}(1 - |\nabla m|^2). \tag{144}$$

For general potentials $V(\phi)$, equation (144) is a complicated nonlinear equation, not obviously simpler than the original TDGL equation (2). For reasons discussed in section 2.3, however, we expect the scaling function $f(x)$ to be *independent* both of the detailed form of the potential and of the particular choice of the distribution of initial conditions. Physically, the motion of the interfaces is determined by their *curvature*. The potential $V(\phi)$ determines the domain wall *profile*, which is irrelevant to the large-scale structure.

Similarly, the initial conditions determine the early-time locations of the walls, which should again be irrelevant for late-stage scaling properties. For example, in the Mazenko approximate theory, both the potential and the initial conditions drop out from the equation of the scaling function $f(x)$.

The key step in the present approach is to exploit the notion that the scaling function should be independent of the potential (or, equivalently, independent of the wall profile) by choosing a particular $V(\phi)$ such that equation (144) takes a much simpler form (equation (148)). Specifically we choose the domain-wall profile function $\phi(m)$ to satisfy

$$\phi''(m) = -m\phi'(m) \tag{145}$$

This is equivalent, via equation (132), to a particular choice of potential, as discussed below. First we observe that equation (145) can be integrated, with boundary conditions $\phi(\pm\infty) = \pm 1$ and $\phi(0) = 0$ to give the wall profile function

$$\phi(m) = \left(\frac{2}{\pi}\right)^{1/2} \int_0^m \mathrm{d}x \exp\left(-\frac{x^2}{2}\right) = \mathrm{erf}\left(\frac{m}{2^{1/2}}\right), \tag{146}$$

where $\mathrm{erf}(x)$ is the error function. Also equation (132) can be integrated once, with the

zero of potential defined by $V(\pm 1) = 0$, to give

$$V(\phi) = \tfrac{1}{2}(\phi')^2 = \frac{1}{\pi}\exp(-m^2) = \frac{1}{\pi}\exp\{-2[\mathrm{erf}^{-1}(\phi)]^2\}, \tag{147}$$

where $\mathrm{erf}^{-1}(x)$ is the inverse function of $\mathrm{erf}(x)$. In particular, $V(\phi) \approx 1/\pi - \phi^2/2$ for $\phi^2 \ll 1$, while $V(\phi) \approx \frac{1}{4}(1-\phi^2)^2|\ln(1-\phi^2)|$ for $(1-\phi^2) \ll 1$.†

With the choice (145), equation (146) reduces to the much simpler equation

$$\partial_t m = \nabla^2 m + (1 - |\nabla m|^2)m. \tag{148}$$

This equation, although still non-linear, represents a significant simplification of the original TDGL equation. It is clear, however, on the basis of the physical arguments discussed above, that it retains all the ingredients necessary to describe the universal scaling properties.

We now proceed to show that the usual OJK result is recovered by simply replacing $|\nabla m|^2$ by its average (over the ensemble of initial conditions) in equation (148), and choosing a Gaussian distribution for the initial conditions. In order to make this replacement in a controlled way, however, and to facilitate the eventual computation of corrections to the leading order results, we systematize the treatment by attaching to the field m an internal 'colour' index α which runs from 1 to N, and generalize equation (148) to

$$\partial_t m_\alpha = \nabla^2 m_\alpha + \left(1 - N^{-1}\sum_{\beta=1}^{N} |\nabla m_\beta|^2\right)m_\alpha. \tag{149}$$

Equation (148) is the case $N = 1$. The OJK result is obtained, however, by taking the limit $N \to \infty$, when $N^{-1}\Sigma_{\beta=1}^{N}|\nabla m_\beta|^2$ may be replaced by its average. In this limit, equation (148) becomes (where m now stands for one of the m_α)

$$\partial_t m = \nabla^2 m + a(t)m, \tag{150}$$

$$a(t) = 1 - \langle|\nabla m|^2\rangle, \tag{151}$$

a self-consistent *linear* equation for $m(\mathbf{x}, t)$.

It is interesting that the replacement of $|\nabla_m|^2$ by its average in equation (148) is also justified in the limit $d \to \infty$, because $|\nabla m|^2 = \Sigma_{i=1}^{d}(\partial m/\partial x_i)^2$. If m is a Gaussian random field (and the self-consistency of this assumption follows from equation (150); see below) then the different derivatives $\partial m/\partial x_i$ at a given point x are independent random variables, and the central limit theorem gives, for $d \to \infty$, $|\nabla m|^2 \to d\langle(\partial m/\partial x_i)^2\rangle = \langle|\nabla m|^2\rangle$, with fluctuation of relative order $1/d^{1/2}$. While this approach is not so simple to systematize as that adopted above, it seems clear that the leading order results become exact for large d.

As discussed above, we shall take the initial conditions for m to be Gaussian, with mean zero and correlator (in Fourier space)

$$\langle m_{\mathbf{k}}(0) m_{-\mathbf{k}'}(0)\rangle = \Delta\delta_{\mathbf{k},\mathbf{k}'}, \tag{152}$$

representing short-range spatial correlations at $t = 0$. Then m is a Gaussian field at all

† Equation (147) only fixes $V(\phi)$ for $\phi^2 \leqslant 1$. Note that, for $T = 0$, $\phi^2(\mathbf{x}, 0) \leqslant 1$ everywhere implies that $\phi^2(\mathbf{x}, t) \leqslant 1$ everywhere; so $\phi(\mathbf{x}, t)$ does not depend on the form of $V(\phi)$ for $\phi^2 > 1$. Of course, for stability against thermal fluctuations the points $\phi = \pm 1$ must be global minima of $V(\phi)$.

times. The solution of equation (150) is

$$m_{\mathbf{k}}(t) = m_{\mathbf{k}}(0)\exp[-k^2t + b(t)], \tag{153}$$

$$b(t) = \int_0^t \mathrm{d}t'\, a(t'). \tag{154}$$

Inserting this into equation (151) yields

$$a(t) \equiv \frac{\mathrm{d}b}{\mathrm{d}t} = 1 - \Delta \sum_{\mathbf{k}} k^2 \exp(-2k^2t + 2b). \tag{155}$$

After evaluating the sum, one obtains, for large t (where the $\mathrm{d}b/\mathrm{d}t$ term can be neglected), $\exp(2b) \approx (4t/\Delta d)\,(8\pi t)^{d/2}$, and hence $a(t) \approx (d+2)/4t$. This form for $a(t)$ in equation (150), arising completely naturally in this scheme, reproduces exactly the Oono–Puri [89] modification of the OJK theory, designed to keep the wall–width finite as $t \to \infty$, which was discussed in section 5.1.2.

The explicit result for $m_{\mathbf{k}}(t)$, valid for large t, is

$$m_{\mathbf{k}}(t) = m_{\mathbf{k}}(0)\left(\frac{4t}{\Delta d}\right)^{1/2} (8\pi t)^{d/4} \exp(-k^2t), \tag{156}$$

from which the equal-time two-point correlation functions in Fourier and real space follow immediately:

$$\langle m_{\mathbf{k}}(t) m_{-\mathbf{k}}(t)\rangle = \frac{4t}{d}(8\pi t)^{d/2}\exp(-2k^2t), \tag{157}$$

$$\langle m(1)m(2)\rangle = \frac{4t}{d}\exp\left(-\frac{r^2}{8t}\right), \tag{158}$$

where 1 and 2 are the usual shorthand for space–time points $(\mathbf{r}_1, t)$ and $(\mathbf{r}_2, t)$, and $r = |\mathbf{r}_1 - \mathbf{r}_2|$.

We turn now to the evaluation of the correction function of the original fields ϕ. Since, from equation (158), m is typically of order $t^{1/2}$ at late times it follows from equation (146) that the field ϕ is saturated (i.e. $\phi = \pm 1$) almost everywhere at late times. As a consequence, the relation (146) between ϕ and m may, as usual, be simplified to $\phi = \mathrm{sgn}(m)$ as far as the late-time scaling behaviour is concerned. Thus $C(12) = \langle \mathrm{sgn}(m(1))\,\mathrm{sgn}(m(2))\rangle$. The calculation of this average for a Gaussian field m proceeds just as in the OJK calculation. The OJK result, given by equations (126) and (122), (with $D = 1$) is recovered. The present approach, however, makes possible a systematic treatment in powers of $1/N$. The work involved in calculating the next term is comparable to that required to obtain the $O(1/n)$ correction to the $n = \infty$ result for the $O(n)$ model [20, 69].

5.2.2. *Vector fields*

For vector fields, the TDGL equation is given by equation (57), where $V(\vec{\phi})$ is the usual 'Mexican hat' potential with ground-state manifold $\vec{\phi}^2 = 1$. This time we introduce a *vector* field $\vec{m}(\mathbf{x}, t)$, related to $\vec{\phi}$ by the vector analogue of equation (132), namely [57, 58]

$$\nabla_m^2 \vec{\phi} = \frac{\partial V}{\partial \vec{\phi}}, \tag{159}$$

where ∇_m^2 means $\Sigma_{a=1}^n \partial^2/\partial m_a^2$ for an n-component field. We look for a radially symmetrical solution of equation (159), $\vec{\phi}(\vec{m}) = \hat{\mathbf{m}} g(\rho)$, with boundary conditions

$g(0) = 0$, $g(\infty) = 1$, where $\rho = |\vec{m}|$ and $\hat{\mathbf{m}} = \vec{m}/\rho$. Then the function $g(\rho)$ is the defect profile function for a topological defect in the n-component field, with ρ representing the distance from the defect core [57, 58]. In terms of $\vec{m}$, the TDGL equation for a vector field reads

$$\sum_b \frac{\partial \phi_a}{\partial m_b}\frac{\partial m_b}{\partial t} = \sum_b \frac{\partial \phi_a}{\partial m_b}\nabla^2 m_b + \sum_{bc}\frac{\partial^2 \phi_a}{\partial m_b\,\partial m_c}\nabla m_b \cdot \nabla m_c - \nabla_m^2 \phi_a. \tag{160}$$

Just as in the scalar theory, we can attach an additional 'colour' index α ($= 1, \ldots, N$) to the vector field $\vec{m}$, such that the theory in the limit $N \to \infty$ is equivalent to replacing $\nabla m_b \cdot \nabla m_c$ by its mean, $\langle |\nabla m_b|^2 \rangle \delta_{bc}$ in equation (160). Noting also that $\langle |\nabla m_b|^2 \rangle$ is independent of b from global isotropy, equation (160) simplifies in this limit to

$$\sum_b \frac{\partial \phi_a}{\partial m_b}\frac{\partial m_b}{\partial t} = \sum_b \frac{\partial \phi_a}{\partial m_b}\nabla^2 m_b - \nabla_m^2 \phi_a (1 - \langle |\nabla m_1|^2 \rangle), \tag{161}$$

where m_1 is any component of $\vec{m}$. Finally, this equation can be reduced to the linear form (150), with m replaced by $\vec{m}$, through the choice $\nabla_m^2 \phi_a = -\Sigma_b (\partial \phi_a/\partial m_b) m_b$ or, more compactly, $\nabla_m^2 \vec{\phi} = -(\vec{m} \cdot \nabla_m)\vec{\phi}$, to determine the function $\vec{\phi}(\vec{m})$. Substituting the radially symmetric form $\vec{\phi} = \hat{\mathbf{m}} g(\rho)$ gives the equation

$$g'' + \left(\frac{n-1}{\rho} + \rho\right) g' - \frac{n-1}{\rho^2} g = 0, \tag{162}$$

a generalization of equation (145), for the profile function $g(\rho)$, with boundary conditions $g(0) = 0$, $g(\infty) = 1$. The solution is linear in ρ for $\rho \to 0$, while $g(\rho) \approx 1 - (n-1)/2\rho^2$ for $\rho \to \infty$. The potential $V(\vec{\phi})$ corresponding to this profile function can be deduced from equation (159), although we have been unable to derive a closed-form expression for it. Note that we are making here the natural assumption that scaling functions are independent of the details of the potential for vectors fields, as well as for scalar fields.

For the vector theory, equation (150) and (151) hold separately for each component of the field. Taking Gaussian initial conditions, with correlator (120), yields $a(t) \approx (d+2)/4t$ again, giving equation (158) for each component. The final step, the evaluation of the two point function $C(12) = \langle \vec{\phi}(1) \cdot \vec{\phi}(2) \rangle$, proceeds exactly as in the KYG treatment of section 5.1.2: since $|\vec{m}|$ scales as $t^{1/2}$ we can replace the function $\vec{\phi}(\vec{m})$ by $\hat{\mathbf{m}}$ at late times. Then $C(12) = \langle \hat{\mathbf{m}}(1) \cdot \hat{\mathbf{m}}(2) \rangle$ in the scaling regime. The required Gaussian average over the fields $\vec{m}(1)$ and $\vec{m}(2)$ yields the BPT scaling function (131). Again, it can be systematically improved by expanding in $1/N$.

5.2.3. *The Porod tail*

It is easy to show [55–58] that equation (131) contains the singular term of order r^n (with an additional logarithm for even n) that generates the Porod tail (70) in the structure factor. This feature was effectively built into the theory through the mapping $\vec{\phi}(\vec{m})$. Specifically, the singular part of equation (131) for $\gamma \to 1$ is [99]

$$C_{\text{sing}} = \frac{n\gamma}{2\pi}\left[B\left(\frac{n+2}{2}, \frac{1}{2}\right)\right]^2 \frac{\Gamma((n+2)/2)\Gamma(-n/2)}{\Gamma^2(1/2)}(1-\gamma^2)^{n/2}. \tag{163}$$

Using $\gamma = \exp(-r^2/8t) = 1 - r^2/8t + \ldots$ for $r \ll t^{1/2}$ and simplifying the beta and gamma functions give

$$C_{\text{sing}} = \frac{1}{\pi}\frac{\Gamma^2((n+1)/2)\Gamma(-n/2)}{\Gamma(n/2)}\frac{r^n}{(4t)^{n/2}}. \tag{164}$$

It will be interesting to compare this result with the exact short-distance singularity derived in section 6.

In figures 14 and 15, we compare the BPT scaling function with numerical simulation results [100, 101], both for the pair correlation function $C(\mathbf{r}, t)$ and the structure factor $S(\mathbf{k}, t)$. Since the defect density ρ scales as L^{-n}, a natural choice for the scaling length L is $\rho^{-1/n}$. Note that ρ can be measured independently in the simulation; so using $r\rho^{1/n}$ as scaling variable provides a direct zero-parameter test of the scaling hypothesis itself. For the scalar systems, the scaling variable $r\langle 1-\phi^2\rangle$ was employed [101]; because $1-\phi^2$ is non-zero only near domain walls, $\langle 1-\phi^2\rangle$ is equal to ρ, up to a time-independent constant.

The resulting scaling plots (figure 14) provide very good evidence for scaling except for $d=2=n$ where clear scaling violations are apparent; the data drift to the right with increasing time, that is they are 'undercollapsed'. In this case we can apparently make the data scale, however, by plotting against $r/L(t)$ with $L(t)$ chosen independently at each time t to provide the best data collapse. The collapse is then as good as for any of the other systems.

The theoretical curves in figure 14 are the BPT function (131), which reduces to the OJK scaling function for $n=1$. In making the fits, γ was replaced by $\exp[-\alpha r^2/L(t)^2]$ with the scale factor $\alpha(n, d)$ adjusted to give the best fit by eye.

The structure factor plots of figure 15, on a log–log scale, confirm the existence of the Porod tail (70) in the data. On the logarithmic scale, the poor scaling of the $d=2=n$ data against $r\rho^{1/2}$ is reflected in a slight spreading of the data at small k in the corresponding structure factor plot. We do not show the structure factor plots for $n=1$; the existence of the Porod tail for scalar systems is implicit in the linear short-distance regime in the real-space plots.

It should be noted that the real-space correlation function (131) is *independent of the space dimensionality d*. The d dependence of the structure factor enters only through the process of Fourier transformation. Within the BPT theory, therefore, the Porod tail is obtained for *any n* and d. The same feature is present in the structure factor computed using the Mazenko method [57, 58]. In section 6, however, we shall show that the Porod tail is a direct consequence of the presence of stable topological defects in the system and, furthermore, that the *amplitude* of the tail can be evaluated exactly in terms of density of defect core. Since stable defects are only possible for $n \leqslant d$, the Porod tail obtained from the BPT function (131) for $n > d$ is an artefact of the approximations invoked. This scenario is consistent with our claim that the BPT function actually represents an exact solution in the limit $d \to \infty$. In this limit, of course, the condition $n \leqslant d$ is always satisfied!

5.2.4. *External fields; thermal noise; quenched disorder*

Remarkably, the systematic approach can be readily extended to treat the situation where a general (space- and/or time-dependent) external field is present and/or the initial conditions contain a bias. This also allows the effects of thermal fluctuations to be incorporated to a limited extent. For simplicity we shall treat only scalar fields.

Consider the following equation of motion:

$$\frac{\partial \phi}{\partial t} = \nabla^2 \phi - V_0'(\phi) + h(\mathbf{x}, t) V_1'(\phi). \tag{165}$$

Here $V_0(\phi)$ is the usual symmetrical double-well potential sketched in figure 3, while $V_1(\phi)$ has the sigmoid sketched in figure 16(*a*). The full potential

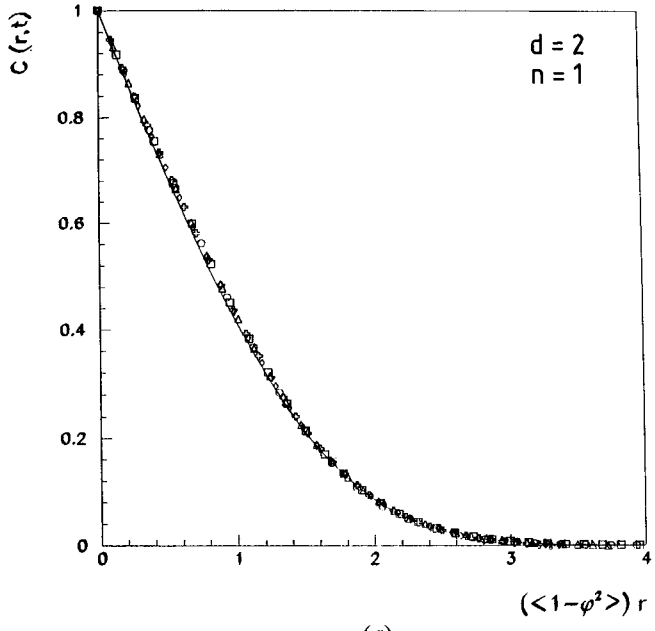
C (r,t)
d = 2
n = 1
1
0.8
0.6
0.4
0.2
0
0
1
2
3
4
(<1−φ²>) r

(*a*)

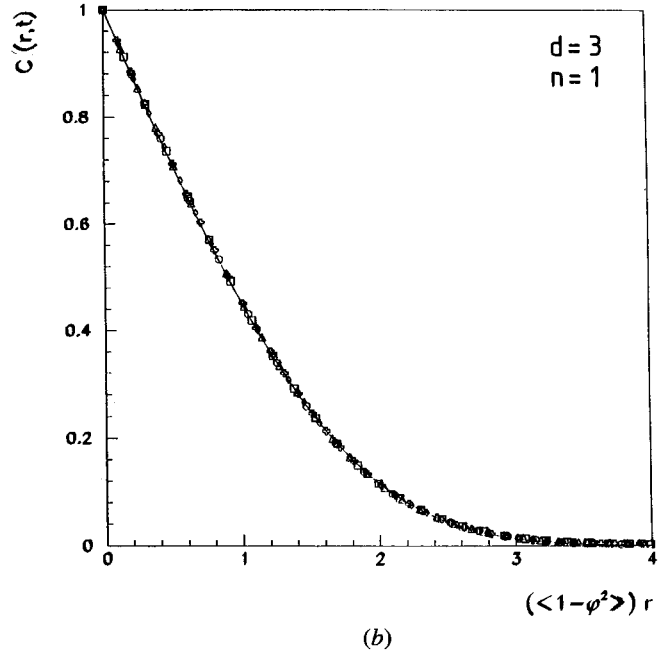
C (r,t)
d = 3
n = 1
1
0.8
0.6
0.4
0.2
0
0
1
2
3
4
(<1−φ²>) r

(*b*)

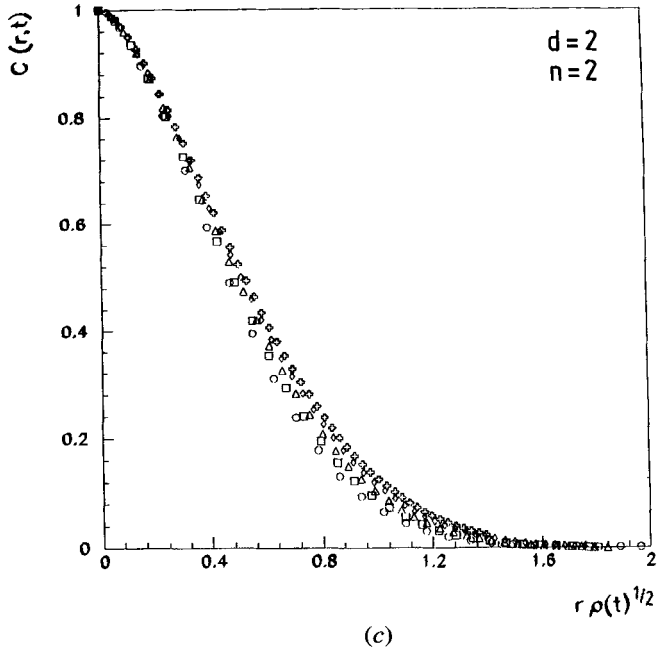
C (r,t)
d = 2
n = 2
0
0.2
0.4
0.6
0.8
1
0
0.4
0.8
1.2
1.6
2
r ρ(t)^1/2

(*c*)

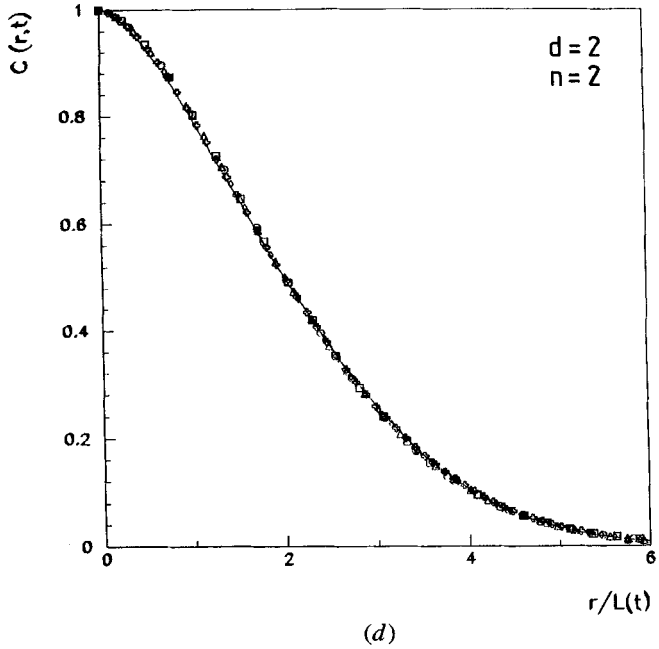
C (r,t)
d = 2
n = 2
0
0.2
0.4
0.6
0.8
1
0
2
4
6
r/L(t)

(*d*)

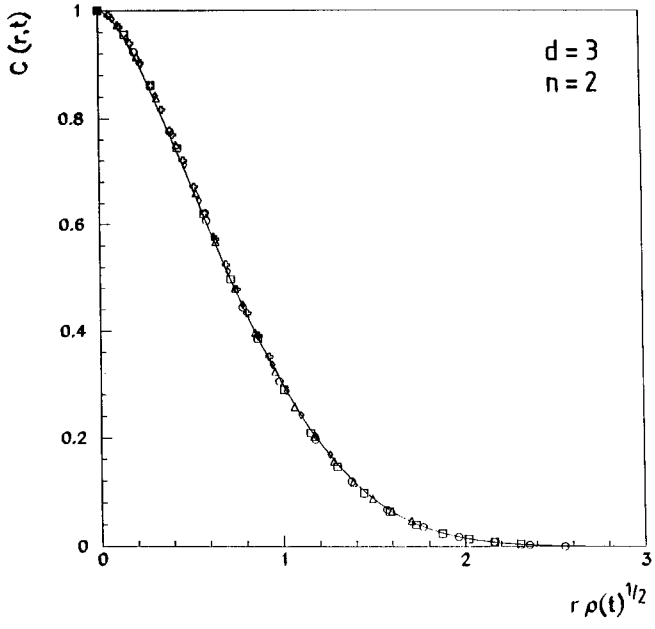

(*e*)

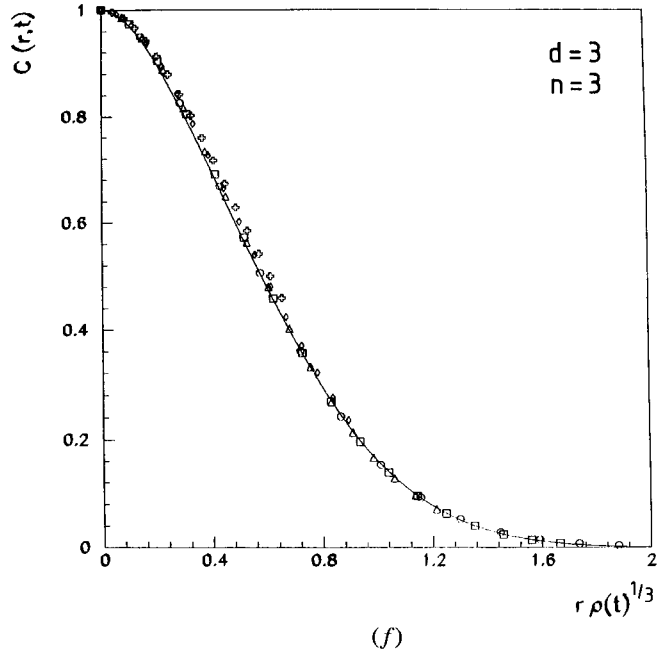

(*f*)

Figure 14. Scaling plots for the pair correlation function of non-conserved systems with an O(n)-symmetric vector order parameter, plotted against $r\rho^{1/n}$ where ρ is the defect density (proportional to $\langle 1 - \phi^2 \rangle$ for $n = 1$). The data are taken from [100]. In (d), the length scale $L(t)$ was chosen independently at each time to give the best collapse. The solid curves are 'best fits by eye' of the BPT prediction [55, 56].

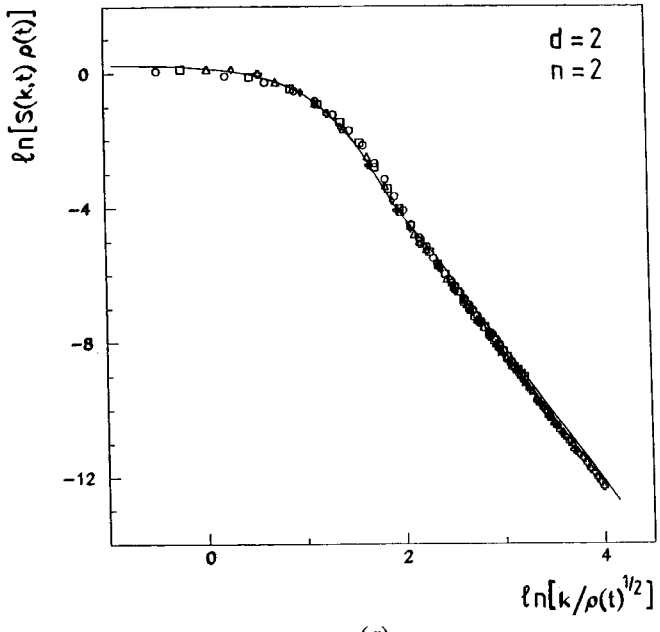
d = 2
n = 2
ℓn[S(k,t) ρ(t)]
0
-4
-8
-12
0
2
4
ℓn[k/ρ(t)^1/2]

(*a*)

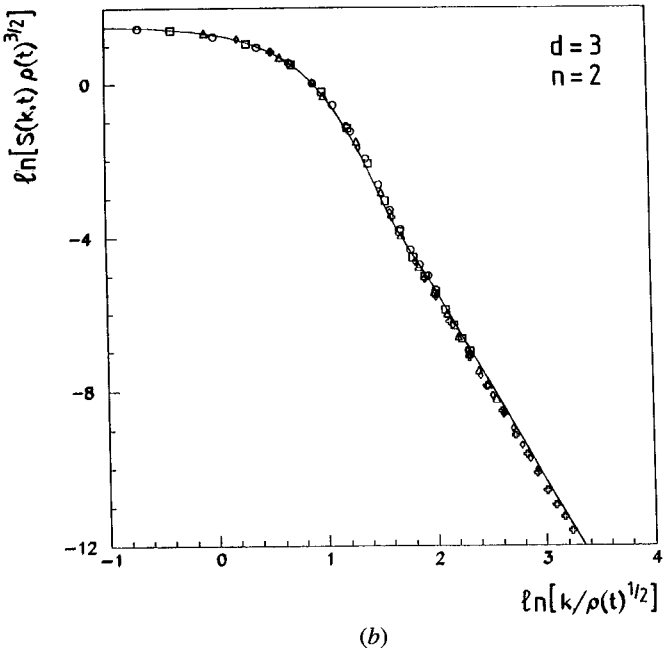
d = 3
n = 2
ℓn[S(k,t) ρ(t)^3/2]
0
-4
-8
-12
-1
0
1
2
3
4
ℓn[k/ρ(t)^1/2]

(*b*)

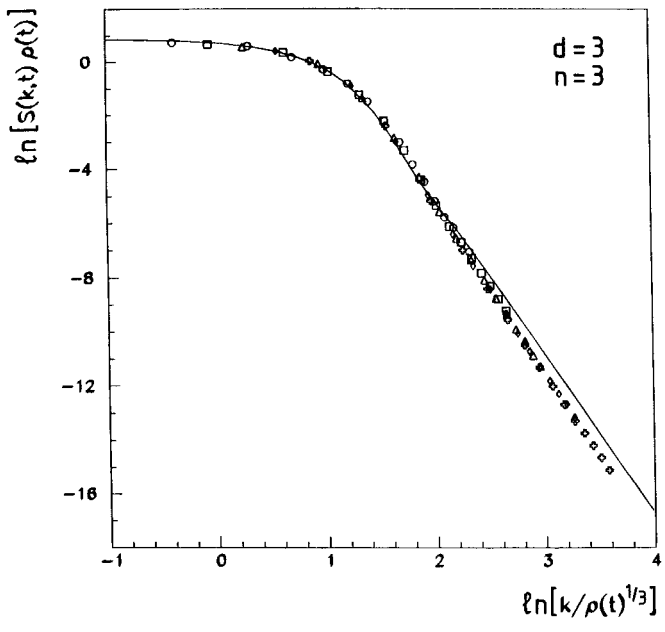

(*c*)

Figure 15. The log–log scaling plots of the structure factor for non-conserved systems with an O(n)-symmetrical vector order parameter. The data are taken from [100]. The solid curves are the Fourier transforms of the corresponding curves in figure 14. The data exhibit the expected $k^{-(d+n)}$ tails for large $kL(t)$.

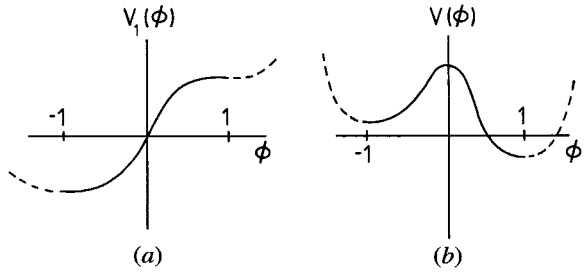

(*a*) (*b*)

Figure 16. Schematic forms of (*a*) the potential $V_1(\phi)$ and (*b*) the total potential $V(\phi)$ used to incorporate external fields into the systematic approach (section 5.2.4). The broken lines indicate parts of the potential that are irrelevant to the dynamics described by equation (170).

$V(\phi; \mathbf{x}, t) = V_0(\phi) - h(\mathbf{x}, t)V_1(\phi)$ has (for given $\mathbf{x}$ and t) the asymmetric double-well form shown in figure 16 (*b*), with the right-hand minimum lower for $h > 0$.

As in our treatment of the case $h = 0$, we can exploit the insensitivity of the domain growth to specific details of the potential to choose especially convenient forms for V_0 and V_1. This rests on the physical truth that the motion of an interface depends only on the local curvature K and the local field. To see this, consider again equation (17) for the interface motion, this time for a general potential $V(\phi)$. Multiplying through by $(\partial\phi/\partial g)_t$, integrating over g through the interface and using (11) give the local velocity

of the interface as

$$v = -K + \frac{\Delta V}{\sigma}, \tag{166}$$

instead of equation (18), where ΔV is the potential difference across the interface. The essential point is that the interface motion depends on the external field only through ΔV. This gives us a great deal of flexibility in the choice of $V_1(\phi)$, since all that matters is the potential difference between the minima of $V(\phi)$. For example, we can choose the minima to remain at $\phi = \pm 1$, as in figure 16(*b*).

With these insights, we now change variables to the auxiliary field m, with $\phi = \phi(m)$. Then equation (165) becomes

$$\phi' \frac{\partial m}{\partial t} = \phi' \nabla^2 m + \phi'' |\nabla m|^2 - V_0'(\phi) + h(\mathbf{x}, t) V_1'(\phi), \tag{167}$$

where $\phi' \equiv \mathrm{d}\phi/\mathrm{d}m$, etc. Simplifications analogous to those that led to equation (148) are achieved through the choices

$$V_0'(\phi) = \phi'' = -m\phi', \tag{168}$$

$$V_1'(\phi) = \phi', \tag{169}$$

which give immediately

$$\partial_t m = \nabla^2 m + (1 - |\nabla m|^2) m + h(\mathbf{x}, t), \tag{170}$$

a simple extension of equation (148).

The right-hand side of equation (168) gives (with the appropriate boundary conditions) the usual error function profile (146), while the left-hand side leads to the previous form (147) for $V_0(\phi)$. Integrating equation (169) gives, with the boundary condition $V_1(0) = 0$, the result

$$V_1(\phi) = \frac{2}{\pi} \int_0^m \mathrm{d}t \exp(-t^2) = \frac{1}{\pi^{1/2}} \operatorname{erf}(m) = \frac{1}{\pi^{1/2}} \operatorname{erf}[2^{1/2} \operatorname{erf}^{-1}(\phi)]. \tag{171}$$

Again, this only defines $V_1(\phi)$ for $-1 \leqslant \phi \leqslant 1$, but this is the only region we require for the $T = 0$ dynamics.

The difference $V_1(1) - V_1(-1)$ is $2/\pi^{1/2}$; so the difference between the minima of the full potential, $V = V_0 - hV_1$, is $-2h/\pi^{1/2}$, corresponding to an effective magnetic field $h_{\mathrm{eff}} = h/\pi^{1/2}$ as far as the interface dynamics are concerned.

5.2.4.1. *External fields/initial bias.* As a simple application of equation (170), consider the case $h(\mathbf{x}, t) = h$, representing a uniform time-independent magnetic field. In order to solve the equation, we take the same limit ($d \to \infty$, or number N of 'colours' large) as in section 5.2, enabling the replacement of $|\nabla m|^2$ by its mean. Additionally, we allow for a bias $\langle m(0) \rangle = m_0(0)$ in the (Gaussian) initial conditions, while the other Fourier components ($\mathbf{k} \neq \mathbf{0}$) of m still satisfy equation (152). Then the equations for the $\mathbf{k} \neq \mathbf{0}$ components of m, and the self-consistency condition, are unchanged by the field; $a(t) = 1 - |\nabla m|^2$ and $b(t) = \int_0^t \mathrm{d}t'\, a(t')$ are the same as for $h = 0$. The equation for the $\mathbf{k} = \mathbf{0}$ component is $\mathrm{d}m_0/\mathrm{d}t + a(t) m_0 = h$, with solution

$$m_0(t) = m_0(0) \exp[b(t)] + h \int_0^t \mathrm{d}t' \exp[b(t) - b(t')]. \tag{172}$$

Inserting the result $\exp b \approx (4t/\Delta d)^{1/2} (8\pi t)^{d/4}$, valid for large t, from section 5.2 gives,

for large t,

$$m_0(t) = m_0(0)\left(\frac{4t}{\Delta d}\right)^{1/2}(8\pi t)^{d/4} + h\int_{t_0}^{t} \mathrm{d}t' \left(\frac{t}{t'}\right)^{(d+2)/4}, \tag{173}$$

where $t_0 \sim (\Delta d)^{2/(d+2)}$ is a short-time cut-off (to allow for the breakdown, at short times, of the form used for $b(t)$).

Exploiting the Gaussian property of m (which now has a non-zero mean given by equation (173)), we can calculate the expectation value of the original field ϕ:

$$\langle\phi\rangle = \langle \mathrm{sgn}\,(m)\rangle = \mathrm{erf}\left(\frac{\langle m\rangle}{(2\langle m^2\rangle_c)^{1/2}}\right), \tag{174}$$

where $\langle m^2\rangle_c \equiv \langle m^2\rangle - \langle m\rangle^2$ is the second cumulant of m. It is given by the same expression, equation (158) with $1 \equiv 2$, as for $h = 0$: $\langle m^2\rangle_c = 4t/d$. So,

$$\langle\phi\rangle = \mathrm{erf}\left(\frac{m_0(0)}{(2\Delta)^{1/2}}(8\pi t)^{d/4} + h\left(\frac{d}{8t}\right)^{1/2}\int_{t_0}^{t} \mathrm{d}t' \left(\frac{t}{t'}\right)^{(d+2)/4}\right). \tag{175}$$

The time dependence of the mean order parameter $\langle\phi\rangle$ depends on d. Consider the argument of the error function. The initial bias $m_0(0)$ gives a contribution of order $t^{d/4}$ for any d, but the contribution from the external field h scales as $t^{1/2}$ for $d < 2$ (when times t' of order t dominate the integral in equation (175)), as $t^{1/2}\ln(t/t_0)$ for $d = 2$, and as $t^{d/4}$ for $d > 2$ (when the integral is dominated by times near the lower cut off). Thus for large t, the external field dominates over the initial bias for $d \leqslant 2$, whereas for $d > 2$ both terms are of the same order. For an arbitrary time-dependent field $h(t)$, the final term in the argument of the error function is simply $(d/8t)^{1/2}\int_{t_0}^{t} \mathrm{d}t'\, h(t')(t/t')^{(d+2)/4}$. This shows that the field becomes less important at late times and, for $d > 2$, a constant field has all its effect at early times or order t_0. For $d \leqslant 2$, a constant field continues to have an effect at late times.

One can make exact statements [102] about the 'initial growth' regime, where $\langle\phi\rangle \ll 1$. The main modification is that $t^{d/4}$ ($= L^{d/2}$) is replaced by L^{λ}, where λ is the exponent in the scaling form (94) for the response to the initial condition. This result is essentially obvious from the definition (91) of the response function. The cross-over (in d) between the two regimes no longer occurs at $d = 2$, but at the dimension where $\lambda = 1$ [102]. The virtue of equation (175) is that it gives the complete time dependence, from the initial regime to final saturation ($\langle\phi\rangle = 1$).

5.2.4.2. *Thermal fluctuations.* Thermal fluctuations can be included, to some extent, within the present formalism by choosing $h(\mathbf{x}, t)$ to be a Gaussian white noise, with mean zero and correlator $\langle h(\mathbf{x}, t)h(\mathbf{x}', t')\rangle = 2D\delta(\mathbf{x} - \mathbf{x}')\delta(t - t')$. The original equation of motion (165) may be recast using equations (168) and (169) as $\partial\phi/\partial t = \nabla^2\phi - V_0'(\phi) + [2V_0(\phi)]^{1/2}h(\mathbf{x}, t)$. Recall that $V_0(\phi)$ vanishes in the bulk phases: $V_0(\pm 1) = 0$. The noise in the ϕ equation therefore also vanishes in the bulk phases, differing from zero only in the interfaces. Consequently, this noise will be effective in thermally roughening the interfaces, but will be incapable of nucleating bubbles of stable phase from a metastable state, or thermally exciting reversed regions within a domain.

5.2.4.3. *Quenched disorder.* Quenched random fields are generated by a time independent, spatially random field $h(\mathbf{x})$. Again, in the original ϕ variable the field is multiplied by $[2V_0(\phi)]^{1/2}$, and so is active only at the interfaces. Since driving forces

due to the field act only at the interfaces, this way of including a random field is perfectly adequate. Unfortunately, however, our leading order approximation of replacing $|\nabla m|^2$ by its average misses the important interface pinning effects induced by the disorder; so this term has to be kept in full. A detailed discussion of quenched disorder, using RG concepts, is given in section 8.3.2.

5.3. *Higher-order correlation functions*

Until now we have focused exclusively on the pair correlation function $C(\mathbf{r}, t)$ and its Fourier transform, the structure factor $S(\mathbf{k}, t)$. These primarily probe the spatial correlations in the *sign*, or *direction* (for vector fields), of the order parameter. However, one can also study the spatial correlations in the *amplitude* of the order parameter [53]. This is worthwhile for two reasons. In certain systems, such as superconductors and superfluids, the (complex scalar) order parameter ψ does not directly couple to experimental probes. Rather, such probes couple to $|\psi|^2$, and any scattering experiment, for example, measures the Fourier transform of $\langle|\psi(1)|^2|\psi(2)|^2\rangle$. The second reason to study these correlation functions is that the simultaneous calculation of two different correlation functions provides an exacting test of theory. This is because plotting one correlation function against another provides an 'absolute' (i.e. free of adjustable parameters) prediction [101]. Tested this way, the predictions of the Gaussian theories of the OJK and BPT (or Mazenko) type are not quite as impressive as they at first seem.

In this section we shall be concerned specifically with the normalized correlation function

$$C_4(12) = \frac{\langle[1-\vec{\phi}(1)^2][1-\vec{\phi}(2)^2]\rangle}{\langle 1-\vec{\phi}(1)^2\rangle\langle 1-\vec{\phi}(2)^2\rangle}, \tag{176}$$

where the 1 in the parentheses represents the saturated (i.e. equilibrium) value of $\vec{\phi}^2$. The function $C_4(12)$ can be evaluated using any of the Gaussian field methods discussed above [53]. For definiteness, we adopt the 'systematic approach' of section 5.2.. The details of the calculation are qualitatively different for scalar and vector fields.

5.3.1. *Scalar fields*

In terms of the Gaussian auxiliary field m the numerator in equation (176) is given by

$$C_4^N = \int \mathrm{d}m(1) \int \mathrm{d}m(2)\, P(m(1), m(2))[1-\phi(m(1))^2][1-\phi(m(2))^2], \tag{177}$$

where P is the probability distribution (123). Since $1-\phi^2(m)$ approaches zero exponentially for scalar fields, the integrals are dominated by values of $m(1)$ and $m(2)$ close to zero (i.e. within an interfacial width of zero). The variation in P with $m(1)$ and $m(2)$, on the other hand, is set by the length scales r and $L(t)$, which are both large in the scaling limit. Defining the interfacial width ξ by $\xi = \int \mathrm{d}m\,[1-\phi(m)^2]$ gives, in the scaling limit,

$$C_4^N = \xi^2 P(0,0) = \frac{\xi^2}{[2\pi(1-\gamma^2)]^{1/2}}, \tag{178}$$

while the normalized correlator C_4 is

$$C_4 = (1-\gamma^2)^{-1/2}. \tag{179}$$

Here we recall that $\gamma \equiv \gamma(12)$ is the normalized correlator (122) of the field m. In particular, $\gamma(0) = 1$ and $\gamma(\infty) = 0$. Using $\gamma = 1 - \text{constant}\ r^2/t$ for $r \ll t^{1/2}$, we see that

$C_4 \sim L/r$ for $r \ll L \sim t^{1/2}$. This result will be derived using elementary arguments in section 6.4. Note that the $1/r$ dependence at small r implies a power-law tail $S_4(\mathbf{k}) \sim Lk^{-(d-1)}$, in the Fourier transform of C_4.

By eliminating γ between C_4 and the pair correlation function $C = (2/\pi)\sin^{-1}\gamma$ (see equation (126)), we obtain the 'absolute' relation

$$\frac{1}{C_4} = \cos\left(\frac{\pi C}{2}\right) \tag{180}$$

between the two correlation functions, with no adjustable parameters. We emphasize that equation (180) is a prediction of all Gaussian theories, which differ only in the relation between γ and the scaling variable $x \equiv r/t^{1/2}$. Thus a test of equation (180) is a test of the Gaussian assumption itself.

In figure 17 we show $1/C_4$ plotted against C, where C_4 and C were measured simultaneously in 'cell dynamics' simulations [103] in $d = 2$ and $d = 3$ [100]. Also shown is the prediction (180). It is clear that the agreement is much poorer than that obtained by fitting C alone (see figure 14). The agreement is significantly better, however, for $d = 3$ than for $d = 2$, consistent with our claim in section 5.2 that the Gaussian assumption becomes exact for $d \to \infty$.

5.3.2. *Vector fields*

The first step is a simple generalization of equation (177) to vector fields:

$$C_4^N = \int \mathrm{d}\vec{m}(1) \int \mathrm{d}\vec{m}(2)\, P(\vec{m}(1), \vec{m}(2))[1 - \vec{\phi}(\vec{m}(1))^2][1 - \vec{\phi}(\vec{m}(2))^2], \tag{181}$$

where P is a product of separate factors (123) for each component (since $\vec{m}$ is assumed to be Gaussian). The subsequent analysis is different from the scalar case, however, because for vector fields $\vec{\phi}(\vec{m})^2$ approaches its saturated value of unity for $|\vec{m}| \to \infty$ only as a power law. To see this we recall that the function $\vec{\phi}(\vec{m})$ is defined as the equilibrium profile function for a radially symmetric topological defect. The amplitude equation satisfies equation (58) with $f \to |\vec{\phi}|$ and $r \to |\vec{m}|$. From equation (59) we obtain directly

$$1 - \vec{\phi}(\vec{m})^2 \to \frac{\xi^2}{|\vec{m}|^2}, \quad |\vec{m}| \to \infty, \tag{182}$$

where $\xi^2 = 2(n-1)/V''(1)$. We shall use this to define the core size ξ for topological defects in vector fields.

Inserting equation (182) in equation (181), we see that for $n > 2$ the factors $1 - \vec{\phi}(\vec{m})^2$ do not, in contrast with scalar fields, converge the integral at small $|\vec{m}|$ (i.e. at $|\vec{m}| \sim \xi$). Instead, the integrals are converged in this case by the probability distribution P, which sets a typical scale $L(t)$ for $|\vec{m}|$. This justifies the use of the asymptotic form (182) in the scaling limit:

$$C_4^N = \xi^4 \int \frac{\mathrm{d}\vec{m}(1)}{|\vec{m}(1)|^2} \int \frac{\mathrm{d}\vec{m}(2)}{|\vec{m}(2)|^2} P(\vec{m}(1), \vec{m}(2)). \tag{183}$$

It is now a straightforward matter to evaluate the $\vec{m}$ integrals [53]. Dividing by the large-distance limit (corresponding to $\gamma = 0$) gives the normalized correlator (176) as

$$C_4 = F\left(1, 1; \frac{n}{2}; \gamma^2\right), \tag{184}$$

where F is again the hypergeometric function ${}_2F_1$.

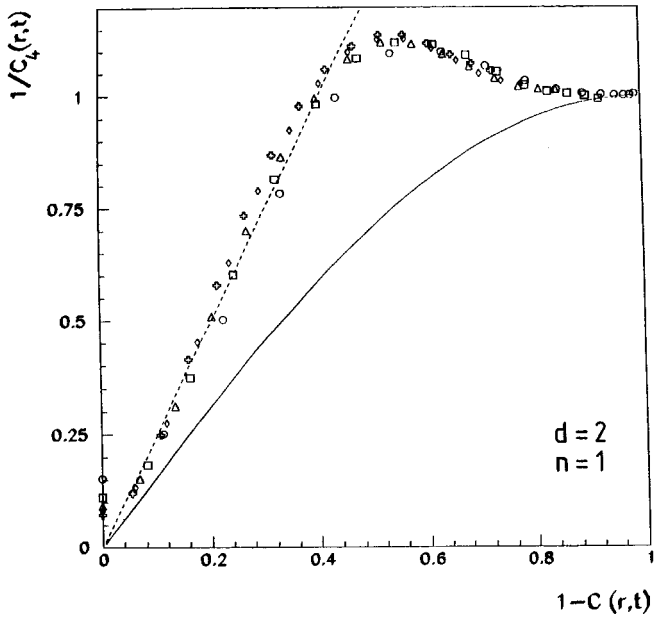

(*a*)

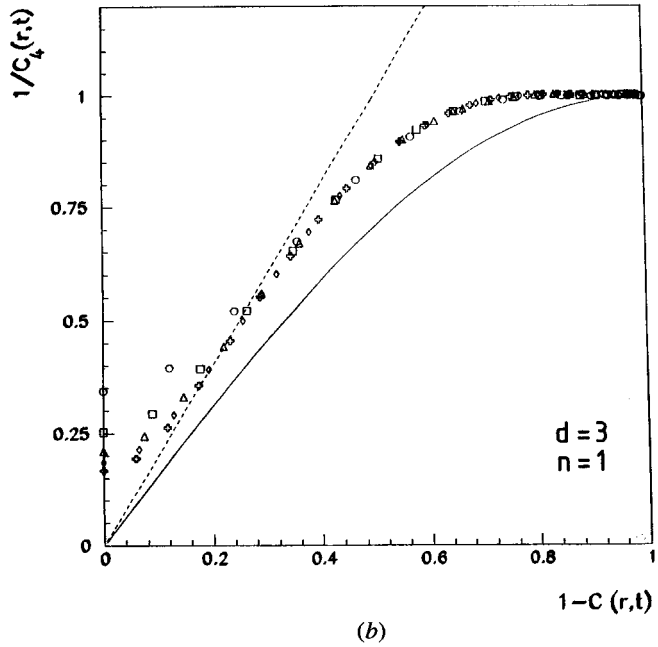

(*b*)

Figure 17. An 'absolute test' for theories of non-conserved dynamics based on an assumed Gaussian auxiliary field. Here C and C_4 are the pair correlation functions for the order parameter and its square, the latter normalized by its large-distance limit (equation (176)). The data are for a scalar order parameter in dimension (*a*) $d = 2$ and (*b*) $d = 3$. The solid curve (independent of d) is the prediction of Gaussian theories based on the OJK or Mazenko approaches. The broken lines give the predicted short-distance behaviour (see [100] and section 6).

For $\gamma \to 1$, C_4 has a short-distance singularity proportional to $(1-\gamma^2)^{(n-4)/2} \sim (L/r)^{4-n}$ (with logarithmic corrections for even n). It follows that the Fourier transform has the power-law tail $S_4 \sim L^{4-n}k^{-(d+n-4)}$ [53], for $n > 2$.

For the special case $n = 2$, one has to be more careful, as the integral (183) is formally logarithmically divergent at small $|\vec{m}(1)|, |\vec{m}(2)|$, and has to be cut off at $|\vec{m}| \sim \xi$. A careful analysis [53] shows that C_4^N exhibits logarithmic scaling violations in this case. However, in the scaling limit $r \to \infty$, $L(t) \to \infty$ with $r/L(t)$ fixed, the extra logarithm cancels in the *normalized* correlator C_4, and equation (184) is recovered, but with logarithmic corrections to scaling [53, 100].

Equation (184) simplifies for physical (i.e. integer) values of n, giving $(1-\gamma^2)^{-1}$ for $n = 2$ and $[\sin^{-1}(\gamma)]/\gamma(1-\gamma^2)^{1/2}$ for $n = 3$. As for the scalar theory, one can eliminate γ between equations (184) and (131) to obtain a parameter-free relation between C_4 and C that may be used as an absolute test of the Gaussian assumption. Figure 18 shows data for $1/C_4$ plotted against $1 - C$, from cell-dynamics simulations [100], and the corresponding predictions of the Gaussian theory. It can be seen that the Gaussian theory is again rather poor but, as for the scalar theory, it improves with increasing d, once more in accord with our argument that it becomes exact for large d.

5.3.3. *Defect–defect correlations*

As a final example, we consider the correlation functions of the defect density itself. In terms of the auxiliary field $\vec{m}$, the defect density is $\rho(\mathbf{x}) = \delta(m(\mathbf{x}))J$, where J is the Jacobian between the field $\vec{m}$ and the spatial coordinate $\mathbf{x}$, for example $J = |\nabla m|$ for scalar fields. A significant simplification is achieved by choosing Mazenko's definition of $\vec{m}$, near defects, as a coordinate normal to the defect. Then $J = 1$ holds identically at defects, giving simply $\rho = \delta(\vec{m})$. Making *now* the Gaussian approximation for m, the one-point distribution function is

$$P(\vec{m}) = (2\pi S_0)^{-n/2} \exp\left(-\frac{\vec{m}^2}{2S_0}\right), \tag{185}$$

where $S_0 = \langle m^2 \rangle$ is mean-square value of *one component* of $\vec{m}$. Equation (158) gives $S_0 = 4t/d$. The mean defect density is therefore

$$\rho_{\text{def}}^{\text{Gauss1}} = \langle \delta(m) \rangle = P(0) = \left(\frac{d}{8\pi t}\right)^{n/2}. \tag{186}$$

The superscript 'Gauss1' indicates that this is *one* way to calculate ρ_{def} within the Gaussian approximation. An alternative approach, pursued by Liu and Mazenko [104], is to retain the Jacobian explicitly. This gives a different result, because $J = 1$ at defects is true for the *exact* $\vec{m}$, but not for the Gaussian approximation. With the Jacobian retained, the calculation has not been completed for general d and n.

With $J = 1$, the pair correlation function is also trivially evaluated:

$$\langle \rho(1)\rho(2) \rangle = P(0,0) = \left(\frac{d}{8\pi t}\right)^{n} (1-\gamma^2)^{-n/2}, \tag{187}$$

where we used equation (123) for $P(0,0)$. In the short-distance limit $r \ll t^{1/2}$, this becomes

$$\langle \rho(1)\rho(2) \rangle \to \frac{\rho_{\text{def}}}{r^n} \left(\frac{d}{2\pi}\right)^{n/2}, \quad r \ll L(t). \tag{188}$$

Again, the short-distance behaviour can be evaluated exactly (see section 6.4), and the r^{-n} short-distance behaviour recovered from simple geometrical arguments, which

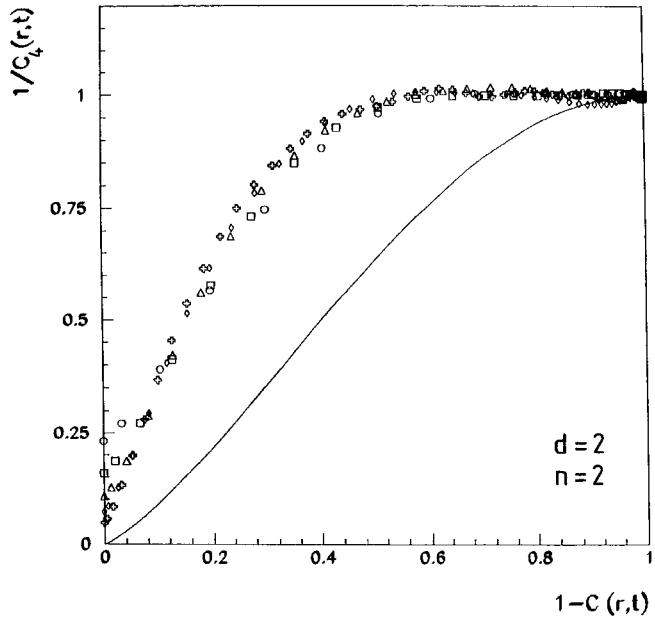
1/C4(r,t)
1
0.75
0.5
0.25
0
0
0.2
0.4
0.6
0.8
1
1−C (r,t)
d = 2
n = 2

(*a*)

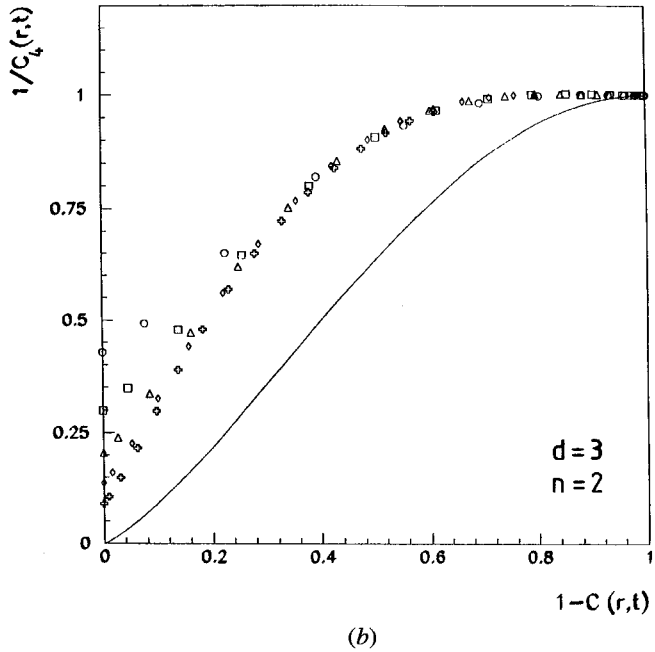
1/C4(r,t)
1
0.75
0.5
0.25
0
0
0.2
0.4
0.6
0.8
1
1−C (r,t)
d = 3
n = 2

(*b*)

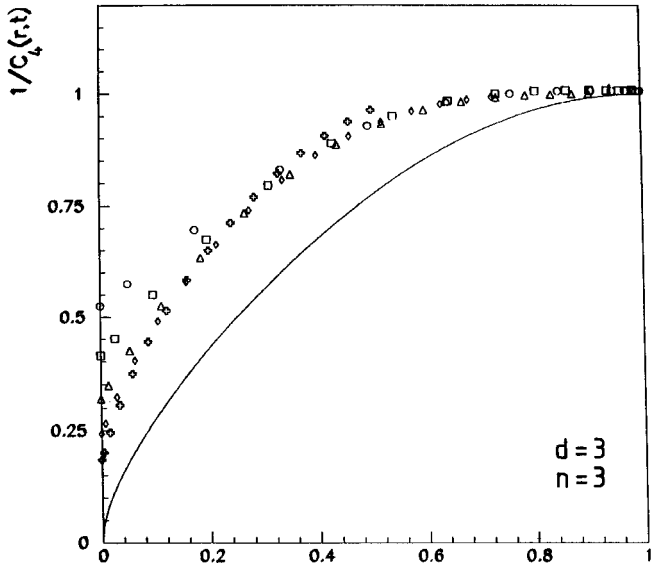

(*c*)

Figure 18. Same as figure 17, but for vector fields: (*a*) $d = 2 = n$, (*b*) $d = 3, n = 2$; (*c*) $d = 3 = n$. The solid curves are the predictions of the Gaussian theories. The data are taken from [100].

exclude, however, point defects (i.e. $n = d$). This failure to capture the correct short-distance behaviour for point defects is another weakness of the Gaussian approximation.

5.4. *Nematic liquid crystals*

We have not succeeded in applying the systematic approach to the equation of motion (74) for nematics. Application of the KYG method (see section 5.1.2), however, is relatively straightforward [64]. For orientation purposes, we first recall the use of the KYG method for vector fields [55]. Recall that, in the scaling regime, the relation between the order parameter field $\vec{\phi}$ and the auxiliary field $\vec{m}$ can be simplified to $\vec{\phi} = \hat{\mathbf{m}}$, a unit vector, and that $\vec{m}$ may be taken to satisfy the diffusion equation $\partial_t \vec{m} = \nabla^2 \vec{m}$. As was stressed in section 5.1.2, this approach is somewhat *ad hoc* and is not even guaranteed to yield the correct time dependence for $L(t)$. In practice, however, it gives good results for scaling functions since it builds in, through the zeros of $\vec{m}$, the correct topological defects. Therefore we adopt this as a reasonable first attempt. It turns out that, for nematics, we do in fact recover the correct growth $L \sim t^{1/2}$, as shown in section 7.

The first step is to introduce the (traceless symmetric) *tensor* auxiliary field m, satisfying the diffusion equation. The only tricky part is to determine the mapping $Q(m)$, between the auxiliary field and the order parameter, analogous to $\phi(m) = \mathrm{sgn}(m)$ for scalar fields and $\vec{\phi}(\vec{m}) = \hat{\mathbf{m}}$ for vector fields. The key observation is that these latter results simply represent the mapping from an initial value of m to the nearest minimum of the potential or, equivalently, they describe the attractors of the dynamics (74) for a spatially uniform initial state. It is easy to show [64] that, for a nematic, an equivalent

procedure is the following. The director **n** at a given space–time point 1 is obtained as the eigenvector with largest eigenvalue of the tensor $m(1)$ obtained by evolving the diffusion equation $\partial_t m = \nabla^2 m$ forward from a random initial condition. The physical tensor $Q(1)$ then has elements $Q_{ab}(1) = S[n_a(1)n_b(1) - \delta_{ab}/3]$, where S is an arbitrary amplitude that has the value $\frac{3}{2}$ for the particular coefficients in the equation of motion (74). The pair correlation function is then obtained as

$$C(12) = \tfrac{2}{3}\langle \mathrm{Tr}\,[Q(1)Q(2)]\rangle, \tag{189}$$

where the factor $\frac{2}{3}$ normalizes (for $S = \frac{3}{2}$) the correlation function to unity when points 1 and 2 are the same. The average in equation (189) is over the (Gaussian) joint probability distribution for $m(1)$ and $m(2)$, which can be deduced from the diffusion equation for m and the assumed Gaussian initial conditions.

The results for the pair correlation function and scaled structure factor are shown in figure 19, together with the simulation data of Blundell and Bray [65], and the experimental structure factor data of Wong *et al.* [61]. The inset in figure 19 (*a*) shows that the real-space scaling function $f(x)$ has the short-distance behaviour $f(x) = 1 + ax^2 \ln x - bx^2 + \ldots$. This is the same short-distance form as the O(2) model and leads to the same k^{-5} tail in the structure factor, reflecting the presence of line defects (disclinations). The fit to the simulation data (with the length scale $L(t)$ adjusted at each time) is good. Remarkably, the BPT function (131) for $n = 2$ fits just as well, and indeed the simulation data for the two systems are essentially indistinguishable. This provides a dramatic illustration of the central role played by the topological defects; the nematic might naively be regarded as more like an $n = 3$ than an $n = 2$ system.

The theoretical curve in figure 19 (*b*) represents the O(2) theory, as this was simpler to obtain, by numerical Fourier transform of the analytical result for the real-space scaling function, than the Fourier transform of the nematic correlation function, which had to be generated numerically [64]. Again the agreement is quite good. The data of Wong *et al.* can be shifted by an arbitrary amount, both horizontally and vertically, but we were unable to collapse it precisely on to the analytical result or simulation data. In addition, experimental data have not yet reached the asymptotic k^{-5} regime expected on the basis of the string defects present. A line of slope -5 is included as a guide to the eye.

5.5. *Conserved fields*

We have seen that the OJK scaling function (126) and its generalization (131) to vector fields provide a very good description of the pair correlation function for *non-conserved* fields, subject to the caveat that the scale length $L(t)$ is fitted when comparing with data. Furthermore, we have argued that the Gaussian approximation for the auxiliary field $\vec{m}$ is exact in certain limits and provides a starting point for a systematic treatment.

For conserved fields, the theory is less well developed. The most naive approach, for example, does not even give the correct growth law $L(t) \sim t^{1/3}$ (for scalar fields). One can still attempt to make progress by introducing an auxiliary field m but, in contrast to non-conserved fields, there is no evidence for any simple limit in which the theory for m becomes tractable.

To put the difficulties into context, we start with scalar fields, and recall that the chemical potential μ satisfies the Laplace equation (25), with boundary conditions (28) imposed at the interfaces. The interfaces act as sources of the field μ. To see this we

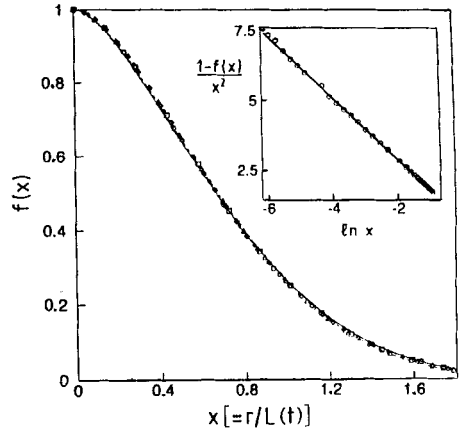

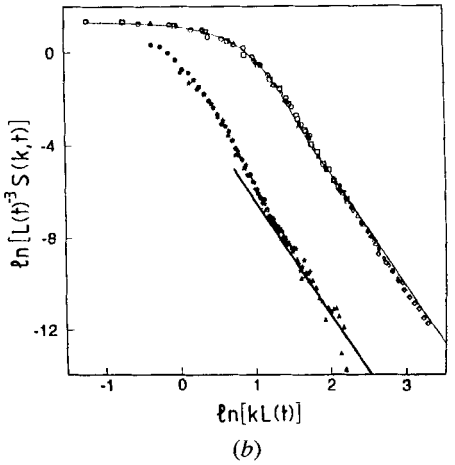

Figure 19. (*a*) Real-space pair correlation function for a nematic liquid crystal within the equal-constant approximation, calculated using the KYG approach as described in the text. The scaling variable x is $r/(8t)^{1/2}$. The data are the Monte Carlo simulations from [65], with $L(t)$ fixed from the best fit to the theory. The inset shows the short-distance behaviour of the theory, showing a leading $x^2 \ln x$ singularity. (*b*) The log–log plot for the scaled structure factor of a nematic liquid crystal. The solid curve shows the O(2) theory, and the points the simulation data from [65], with $L(t)$ chosen as in (*a*). Experimental data from [61] are shown on the left, arbitrarily positioned; they can be moved left or right and up or down. The straight line is a guide to the eye, with a slope of -5.

integrate $\nabla^2\mu$ over a volume element dV enclosing an interface surface element dS. Using equation (29) gives a source density $-2v(\mathbf{r})\delta(m(\mathbf{r}))|\nabla m(\mathbf{r})|$, where v is the interface velocity (measured in the direction of increasing ϕ) and $m(\mathbf{r})$ is an auxiliary field whose zeros define the interfaces (so that $\delta(m(\mathbf{r}))|\nabla m(\mathbf{r})|$ gives the volume density of interfacial area). Our usual choice for the field m, defined by equation (132), gives $|\nabla m| = 1$ at interfaces. This gives the Poisson equation

$$\nabla^2\mu = -2v(\mathbf{r})\delta(m(\mathbf{r})), \tag{190}$$

with solution (for $d = 3$)

$$\mu(\mathbf{r}) = \frac{1}{2\pi} \int \frac{\mathrm{d}\mathbf{r}'}{|\mathbf{r} - \mathbf{r}'|} v(\mathbf{r}') \delta(m(\mathbf{r}')). \tag{191}$$

The Gibbs–Thomson boundary condition gives $\mu = -\sigma K/2$ at an interface, where $K = \nabla \cdot \mathbf{n} = \nabla^2 m$ is the interface curvature. Using equation (117) (with $|\nabla m| = 1$) for the interface velocity in equation (191), and the Gibbs–Thomson boundary condition for μ, gives

$$\begin{aligned} \frac{\sigma}{2} \nabla^2 m &= \frac{1}{2\pi} \int \frac{\mathrm{d}\mathbf{r}'}{|\mathbf{r} - \mathbf{r}'|} \frac{\partial m(\mathbf{r}')}{\partial t} \delta(m(\mathbf{r}')) \\ &= \frac{1}{4\pi} \int \frac{\mathrm{d}\mathbf{r}'}{|\mathbf{r} - \mathbf{r}'|} \frac{\partial}{\partial t} \{\operatorname{sgn}[m(\mathbf{r}')]\} \end{aligned} \tag{192}$$

at interfaces. The same result could be obtained directly from the Cahn–Hilliard equation $\partial_t \phi = \nabla^2 \mu$ by operating on both sides by the inverse Laplacian and setting $\mu = -\sigma K/2 = -(\sigma/2) \nabla^2 m$ on the interfaces.

For *non-conserved fields*, the extension of the interface equation away from the interfaces (as in, for example, the OJK theory) is a mathematical convenience which does not change the underlying physics of interfaces moving under their local curvature. For conserved fields, however, the interface dynamics are non-local and the extension of equation (192) away from interfaces in non-trivial. Any extension should satisfy the following criteria.

(*a*) The equation reduces to equation (192) at interfaces.
(*b*) The chemical potential satisfies $\nabla^2 \mu = 0$ *except* at interfaces.
(*c*) $\nabla \mu$ is discontinuous at interfaces, the normal component of the discontinuity generating the interface velocity as in equation (29).
(*d*) The conservation of the order parameter should be preserved.

Unfortunately, it is very difficult to construct an approximate theory that satisfies all these criteria, and I am not aware of any successful attempts. In addition, a good theory would ideally incorporate two further features.

(*e*) The structure factor should vanish as k^4 for $k \to 0$ (see section 5.5.2).
(*f*) The short-distance expansion of the real-space scaling function should contain (after the leading 1) only odd powers of r, the so-called Tomita [96], sum rule deriving from the smoothness of the interfaces.

A number of approximate theories have been proposed which satisfy a subset of these requirements. The theories of Ohta and Nozaki [105], Tomita [106] and Yeung *et al.* [97] all involve a Gaussian approximation for the correlator of the auxiliary field m. The correct $t^{1/3}$ growth is obtained, and the scaling functions describe the real-space simulation data [43] very well out to reasonable values of the scaling variable but violate the conservation law. A recent attempt by Kramer and Mazenko [107] and Mazenko [108] corresponds to an off-interface extension of equation (192) in which the left-hand side replaced by $-\mu = (\sigma/2)(\nabla^2 m + u\phi/L)$, with u a constant. The real-space scaling function is obtained by multiplying through by ϕ at a different space point, and averaging both sides with the usual Gaussian assumption for m. The resulting scaling function has the desired k^4 small-k form in Fourier space, although this behaviour does not have the same origin as in the derivation of this form in section 5.5.2. The real-space fit is not as good as earlier theories. In addition, the chemical potential (rather than its gradient) is discontinuous at interfaces.

Yeung *et al.* [97] have critically analysed approximation schemes based on a Gaussian assumption for m. Using data of Shinozaki and Oono [43] for the pair correlation function $C(\mathbf{r}, t)$ in $d = 3$ to infer a value for the normalized correlator of m, namely $\gamma = \sin(\pi C/2)$ (see equation (126)), they found that the Fourier transform γ_k would have to be negative at small k to fit the data. However, this is impossible since $\gamma_k \geqslant 0$ by definition. Yeung *et al.* concluded that no Gaussian theory could adequately describe the data, at least for scalar fields in $d = 3$. Nevertheless, we conclude this subsection by considering the approach of Mazenko for conserved fields, which is explicitly built on a Gaussian assumption for m. This is especially interesting for vector fields, since it allows us to make contact with the large-n calculation of section 4.3. The reader may recall that the exact solution of Coniglio and Zannetti [16] for conserved fields with $n = \infty$ exhibits a novel multiscaling behaviour. A natural question is whether this behaviour survives at finite n. Employing the Mazenko approach, we find multiscaling behaviour for n strictly infinite, but conventional scaling for any finite n [75].

5.5.1. *The Mazenko method for conserved vector fields*

A naive application of the Mazenko technique to the Cahn–Hilliard equation (3) and its generalization to vector fields, yields, in complete analogy to equation (138),

$$\frac{1}{2}\frac{\partial C}{\partial t} = -\nabla^2\left(\nabla^2 C + a(t)\gamma\frac{\mathrm{d}C}{\mathrm{d}\gamma}\right), \tag{193}$$

with $a(t)$ still defined by equation (137). The only difference between equation (138) and (193) is the extra $-\nabla^2$ on the right-hand side. The form (193) is obtained for any n, with the function $C(\gamma)$ given by equation (131).

If we seek a scaling solution of equation (193), of the form $C(\mathbf{r}, t) = f(r/L(t))$, it is immediately clear that consistency requires $a(t) \sim 1/L(t)^2$ and $L(t) \sim t^{1/4}$. We shall show in section 7 that this is the correct growth law for $n > 2$, while there is a logarithmic correction $L(t) \sim (t \ln t)^{1/4}$, for $n = 2$ (and $d > 2$). For $n = 1$, however, equation (193) fails to give the correct $t^{1/3}$ growth. The reason is clear. Taking ϕ to be a sigmoid function of a Gaussian field from the outset overlooks the vital role of the bulk diffusion field in transferring material between interfaces. Recognizing this fact, Mazenko [86] writes ϕ as a superposition of 'ordering' and 'diffusing' components, $\phi = \psi(m) + \tilde{\phi}$, with m a Gaussian field. It is then possible to construct a consistent theory with $t^{1/3}$ growth [86], although the results do not agree well with simulations [109].

Here we shall concentrate on vector fields with $n > 2$, for which equation (193) does give the correct $t^{1/4}$ growth. For general n this equation can be solved numerically for the scaling function $f(x)$ [110]. Somewhat surprisingly, the solution for $d = 3$, $n = 2$, is very close to the simulation data of Siegert and Rao [73], despite the (logarithmically) wrong growth law. For large n, however, we can make analytical progress and contribute to the debate on the possibility of multiscaling for finite n.

For large n equation (193) is simplified as follows. Expanding equation (131) to first order in $1/n$ gives $C = \gamma - \gamma(1 - \gamma^2)/2n + O(n^{-2})$, and so $\gamma\, \mathrm{d}C/\mathrm{d}\gamma = C + C^3/n + O(n^{-2})$. Putting this in equation (193) gives

$$\frac{1}{2}\frac{\partial C}{\partial t} = -\nabla^4 C - a(t)\nabla^2\left(C + \frac{C^3}{n}\right), \tag{194}$$

correct to $O(1/n)$. The solution of this equation is very different for n strictly infinite than for n large but finite.

For $n = \infty$, the C^3/n term can be dropped and the resulting linear equation solved by Fourier transformation to give

$$S(\mathbf{k}, t) = S(\mathbf{k}, 0) \exp[-2k^4 t + 2k^2 b(t)] \tag{195}$$

for the structure factor, where $b(t) = \int_0^t dt'\, a(t')$. This result is *identical* with the exact result obtained by Coniglio and Zannetti [16] in the same limit (compare for example, equation (97)) and leads to same multiscaling form (103).

For n finite, we try scaling forms consistent with the expected $t^{1/4}$ growth, namely $S(\mathbf{k}, t) = t^{d/4} g(kt^{1/4})$, $a(t) = q_m^2/t^{1/2}$, and $C(\mathbf{r}, t) = f(r/t^{1/4})$, where $f(x)$ is the Fourier transform of $g(q)$ and q_m is a constant. Using these in equation (194) gives

$$\frac{dg}{dq} = -\left(\frac{d}{q} + 8q^3 - 8q_m^2 q\right) g + qB(q), \tag{196}$$

$$B(q) = \frac{8q_m^2}{n} (f^3)_{\mathbf{q}}, \tag{197}$$

where $(f^3)_{\mathbf{q}}$ indicates the Fourier transform of $f(x)^3$. Note that $g(0) = 0$ must hold for a conserved order parameter; otherwise $S(\mathbf{k}, 0)$ would grow as $L(t)^d$, violating the conservation law. Integrating equation (196) with initial condition $g(0) = 0$ gives

$$g(q) = q^{-d} \exp(-2q^4 + 4q_m^2 q^2) \int_0^q dq'\, q'^{d+1} B(q') \exp(2q'^4 - 4q_m^2 q'^2). \tag{198}$$

The constant q_m is fixed by the condition $f(0) = 1$, that is $\Sigma_{\mathbf{q}} g(q) = 1$. For very large n we find *a posteriori* that q_m is large. Then $g(q)$ is strongly peaked near $q = q_m$, justifying a steepest-descent evaluation of the sum over $\mathbf{q}$. For q near q_m the integral in equation (198) is dominated by q' values of order q_m^{-1}, giving [75]

$$g(q) \approx 2^{-(d+3)} \Gamma\left(1 + \frac{d}{2}\right) B(0) q_m^{-(d+2)} q^{-d} \exp(-2q^4 + 4q_m^2 q^2) \tag{199}$$

for q near q_m. Using this form in $\Sigma_{\mathbf{q}} g(q) = 1$ and evaluating the sum by steepest descents gives

$$1 = 2^{-(d+5)} (2\pi)^{1/2} K_d \Gamma\left(1 + \frac{d}{2}\right) q_m^{-(d+4)} \exp(2q_m^4)\, B(0), \tag{200}$$

where $K_d = 2/(4\pi)^{d/2}\Gamma(d/2)$. Using this to eliminate $B(0)$ from equation (198) gives the desired scaling solution, valid for $q_m^{-1} \ll q \lesssim q_m$,

$$g(q) = \frac{4}{K_d (2\pi)^{1/2}} q_m^2 q^{-d} \exp[-2(q^2 - q_m^2)^2]. \tag{201}$$

In the limit $q_m \to \infty$, the width of the peak at $q = q_m$ vanishes as q_m^{-1}; so in this limit we can write

$$g(q) \to K_d^{-1} q_m^{1-d} \delta(q - q_m), \quad q_m \to \infty. \tag{202}$$

The final step is to use equation (197) with $q = 0$ to obtain a second relation (in addition to equation (200)) between $B(0)$ and q_m. From equation (197), $B(0) = (8q_m^2/n) \int d^d x\, f(x)^3$. Using equation (202) for $g(q)$ gives $f(x) = A(q_m x)$, where $A(y) = \text{constant}\, J_\nu(y)/y^\nu$, with $\nu = (d-2)/2$, and hence

$$B(0) = \frac{8q_m^2}{n} \int d^d x A(q_m x)^3 = \text{constant} \frac{q_m^{2-d}}{n}. \tag{203}$$

Putting this in equation (200) gives $1 = \text{constant}\, q_m^{-2(d+1)} \exp(2q_m^4)/n$, giving $q_m \approx [(\ln n)/2]^{1/4}$ for large n. This in turn implies a characteristic length scale $L(t) \sim (t/\ln n)^{1/4}$.

To summarize, we have shown that, within the Mazenko approximation, scaling solutions are obtained for any finite n. Only for n strictly infinite is the multiscaling form (103) of Coniglio and Zannetti recovered. Note that the amplitude of the $t^{1/4}$ growth depends in a singular way on n (as $(\ln n)^{-1/4}$) for $n \to \infty$, that is our result is non-perturbative in $1/n$ and could not be obtained by expanding around the large-n solution. The scaling solution is obtained when the limit $t \to \infty$ is taken at fixed n.

5.5.2. *The small-*k *behaviour of the structure factor*

One slightly unsatisfactory aspect of the above treatment is that it does not recover the correct small-q behaviour (indeed, the same shortcoming afflicts the scalar version of the calculation [86]). For $q \to 0$, equation (198) gives $g(q) \to B(0)q^2/(d+2)$. There are compelling arguments, however, for a q^4 behaviour at small q [18, 111–114], strongly supported by numerical simulations [43], as well as experiment [115], for a scalar order parameter. Here we discuss both scalar and vector fields. We begin by deriving an inequality for the small-q behaviour, using an approach based on that of Yeung [111].

We recall that the equation of motion for conserved fields takes the form $\partial_t \phi = \nabla^2 \mu$, where μ is the chemical potential. Multiplying through by ϕ at a different space point, averaging and Fourier transforming give

$$\frac{1}{2}\frac{\partial S(\mathbf{k})}{\partial t} = -k^2 \langle \mu_{\mathbf{k}} \phi_{-\mathbf{k}} \rangle \leqslant \mathbf{k}^2 [S(\mathbf{k})]^{1/2} \langle \mu_{\mathbf{k}} \mu_{-\mathbf{k}} \rangle^{1/2}, \tag{204}$$

where the final line follows the Cauchy–Schwartz inequality. Now we impose scaling: $S(\mathbf{k}) = L^d g(kL)$. Since $\mu \sim 1/L$ for scalar fields, the analogous scaling form is $\langle \mu_{\mathbf{k}} \mu_{-\mathbf{k}} \rangle = L^{d-2} g_\mu(kL)$. Putting these into equation (204) and using $L \sim t^{1/3}$ for scalar fields give

$$dg(q) + qg'(q) \leqslant \text{constant}\, q^2 [g(q) g_\mu(q)]^{1/2}. \tag{205}$$

For $q \to 0$ one expects $g(q) \sim q^\delta$ and $g_\mu(q) \to$ constant, because μ is not a conserved field. Then equation (205) gives the inequality $\delta \geqslant 4$. An approximate treatment which gives the expected q^4 small-q behaviour has been proposed by Kramer and Mazenko [107].

For vector fields, it is shown in sections 7 and 8 that $L(t) \sim t^{1/4}$ provided that $n > 2$ (see section 7 for discussion of $n = 2$). This suggests that the (vector) chemical potential scales as $\vec{\mu} \sim 1/L^2$ for $n > 2$, which gives equation (205) again and $\delta \geqslant 4$ as before.

It is easy to show, using an argument of Furukawa [18, 112], that the lower bound for δ implied by Yeung's argument is realized, that is $\delta = 4$. Integrating the equation of motion $\partial_t \phi_{\mathbf{k}} = -k^2 \mu_{\mathbf{k}}$ gives $\phi_{\mathbf{k}}(t) = \phi_{\mathbf{k}}(0) - k^2 \int_0^t dt_1\, \mu_{\mathbf{k}}(t_1)$. This yields

$$S(\mathbf{k}, t) = -S(\mathbf{k}, 0) + 2\langle \phi_{\mathbf{k}}(t) \phi_{-\mathbf{k}}(0) \rangle + k^4 \int_0^t dt_1 \int_0^t dt_2\, \langle \mu_{\mathbf{k}}(t_1) \mu_{-\mathbf{k}}(t_2) \rangle. \tag{206}$$

It is clear that the first two terms on the right must be negligible in the scaling regime; otherwise Yeung's inequality would be violated! It is simple, however, to show this explicitly. In the scaling limit ($k \to 0$, $L \to \infty$ with kL fixed), $S(\mathbf{k}, t)$ increases as L^d. Therefore the time-independent first term on the right of equation (206) is certainly negligible. Now consider the second term. The autocorrelation

function $A(t) \equiv \langle \phi(\mathbf{x}, t)\phi(\mathbf{x}, 0)\rangle$ decreases as $A(t) \sim L(t)^{-\bar{\lambda}}$. This implies that $\langle \phi_{\mathbf{k}}(t)\phi_{-\mathbf{k}}(0)\rangle = L^{d-\bar{\lambda}}a(kL)$, where $a(q)$ is a scaling function. Since this term grows less rapidly than L^d, it also is a negligible contribution to $S(\mathbf{k}, t)$ for large L. It follows that the structure-factor scaling function $g(q)$ is obtained entirely from the final term in equation (206). It vanishes as q^4 because μ is not a conserved field; so $\langle \mu_{\mathbf{k}}\mu_{-\mathbf{k}}\rangle$ is non-zero at $k = 0$, as discussed above. Furukawa has gone slightly further and shown explicitly that this final term is indeed of order L^d. Inserting the two-time scaling form (for scalar fields) $\langle \mu_{\mathbf{k}}(t_1)\mu_{-\mathbf{k}}(t_2)\rangle = L_1^{d-2}g_\mu(kL_1, L_2/L_1)$ (a natural generalization of the equal-time scaling form given above), using $L \sim t^{1/3}$, and evaluating the double time integral by power counting, gives $S(\mathbf{k}, t) \sim k^4 t^{2+(d-2)/3} \sim k^4 L^{d+4}$ as required.

Finally we note that Tomita [113] has given a rather general argument for the k^4 behaviour based on the isotropy of the scaling functions.

5.6. *Binary liquids*

The equation of motion appropriate to binary liquids, equation (51), was derived in section 2.7 for the case where the inertial terms in the Navier–Stokes equation can be neglected. Equation (51) leads to an asymptotic linear growth $L(t) \sim t$. Here we shall discuss how one might attempt to calculate an approximate scaling function for pair correlations in this regime.

In the regime where $L(t) \sim t$, the 'advective' term in equation (51) dominates the 'diffusive' term $\lambda \nabla^2 \mu$ on the right-hand side; so we shall discard the latter. In the spirit of the 'systematic approach' of section 5.2, we introduce an auxiliary field m defined by equation (132), with the additional choice (145), corresponding to a convenient choice of the potential $V(\phi)$. Then the chemical potential μ can be expressed as

$$\begin{aligned} \mu \equiv \frac{\delta F}{\delta \phi} &= V'(\phi) - \nabla^2 \phi \\ &= -\phi'(m)[\nabla^2 m + (1 - |\nabla m|^2)m]. \end{aligned} \tag{207}$$

Expressing the equation of motion (51) in terms of m, and using equation (207) for μ gives

$$\begin{aligned} \frac{\partial m(\mathbf{r})}{\partial t} = \int d\mathbf{r}' \, [\nabla m(\mathbf{r}) \cdot T(\mathbf{r} - \mathbf{r}') \cdot \nabla' m(\mathbf{r}')][\phi'(m(\mathbf{r}'))]^2 \{\nabla'^2 m(\mathbf{r}') \\ + [1 - |\nabla' m(\mathbf{r}')|^2] m(\mathbf{r}')\}. \end{aligned} \tag{208}$$

Now we recall that $[\phi'(m)]^2$ acts very much like a delta function on the interfaces. The result (compare equation (11)) $\sigma = \int dm \, (d\phi/dm)^2$ for the surface tension leads to the identification $(d\phi/dm)^2 = \sigma\delta(m)$. Using this in equation (208) gives

$$\frac{\partial m(\mathbf{r})}{\partial t} = \sigma \int d\mathbf{r}' \, [\nabla m(\mathbf{r}) \cdot T(\mathbf{r} - \mathbf{r}') \cdot \nabla' m(\mathbf{r}')]\delta(m(\mathbf{r}')) \nabla'^2 m(\mathbf{r}'). \tag{209}$$

With the identification $\phi(\mathbf{r}) = \operatorname{sgn}[m(\mathbf{r})]$ this equation can be rewritten as an equation for ϕ, by multiplying both sides by $\delta(m(\mathbf{r}))$:

$$\frac{\partial \phi(\mathbf{r})}{\partial t} = \frac{\sigma}{2} \int d\mathbf{r}' \, [\nabla \phi(\mathbf{r}) \cdot T(\mathbf{r} - \mathbf{r}') \cdot \nabla' \phi(\mathbf{r}')] \nabla'^2 m(\mathbf{r}'). \tag{210}$$

This equation could serve as a convenient starting point for approximate treatments of the pair correlation function $C(\mathbf{r}, t)$. Note, however, that equation (210) is

fundamentally nonlinear, and approximate scaling functions that capture the correct physics are difficult to construct. The correct growth law is, nevertheless, built into equation (210); simple power counting (remembering that m scales as $L(t)$) gives immediately $L(t) \sim \sigma t/\eta$, as required.

In the above discussion, the field m was taken to have zero mean, corresponding to a critical quench. An off-critical quench can be handled in similar fashion by allowing m to have a non-zero mean [116]. An outstanding challenge is to devise an approximate treatment which includes the 'switching off' of the linear growth at small volume fractions, when the minority phase is no longer continuous, and to properly incorporate thermal fluctuations in this regime (see the discussion in section 2.7).

6. Short-distance singularities and Porod tails

In the previous section, various approximate treatments of correlation functions were discussed. In this section we show that exact statements can be made about the short-distance behaviour or, more precisely, the short-distance singularities, of these functions. In particular, the qualitative arguments of section 3.3 can be made precise [54], and the *amplitude* of the $k^{-(d+n)}$ Porod tail obtained in terms of the density $\rho_{\rm def}$ of defect core which scales as L^{-n}. The basic result is a generalization of equation (68), in which the leading singular contribution to $C(\mathbf{r}, t)$ is a term of order $|\mathbf{r}|^n$ for n odd (or n real, in a continuation of the theory to real n), and $|\mathbf{r}|^n \ln|\mathbf{r}|$ for n even. This in turn implies a power law tail $k^{-(d+n)}$ in $S(\mathbf{k}, t)$.

We first illustrate the method for the case of point defects ($n = d$). The extension to the general case $n \leqslant d$ is relatively straightforward. Next we discuss the short-distance singularities of some higher-order correlation functions, namely the function C_4 defined by equation (176), and the defect–defect correlation function. We also calculate the Porod tails in the corresponding structure factors. Finally, we compute for scalar fields the joint probability distribution $P(m(1), m(2))$ of the auxiliary field m of section 5, in the limit where $|m(1)|$, $|m(2)|$ and the distance $r = |\mathbf{r}_1 - \mathbf{r}_2|$ are all small compared with $L(t)$. We find that the distribution is *not* Gaussian, except perhaps for $d = \infty$.

6.1. *Point defects* (n = d)

Consider the field $\vec{\phi}$ at points $\mathbf{x}$ and $\mathbf{x} + \mathbf{r}$ in the presence of a point defect at the origin. We consider the case where $|\mathbf{x}|$, $|\mathbf{x} + \mathbf{r}|$ and $|\mathbf{r}|$ are all small compared with a typical interdefect distance L, but large compared with the defect core size ξ. Then the field at the points $\mathbf{x}$ and $\mathbf{x} + \mathbf{r}$ is saturated in length (i.e. of unit length) and not significantly distorted by the presence of other defects. Moreover, the field can be taken, up to a global rotation, to be directed radially outwards from the origin, as illustrated in figure 10. Thus

$$\vec{\phi}(\mathbf{x}) \cdot \vec{\phi}(\mathbf{x} + \mathbf{r}) = \frac{\mathbf{x} \cdot (\mathbf{x} + \mathbf{r})}{|\mathbf{x}|\,|\mathbf{x} + \mathbf{r}|}. \tag{211}$$

With $\mathbf{r}$ held fixed we average equation (211) over all possible relative positions of the point defect, that is over all values of $\mathbf{x}$ within a volume of order L^n around the pair of points, with the appropriate probability density $\rho_{\rm def}$. Focusing on the *singular* part of the correlation function we obtain

$$C_{\rm sing}(\mathbf{r}, t) = \rho_{\rm def} \int^{L} \mathrm{d}^n x \left(\frac{\mathbf{x} \cdot (\mathbf{x} + \mathbf{r})}{|\mathbf{x}|\,|\mathbf{x} + \mathbf{r}|} - \text{analytic terms} \right). \tag{212}$$

The analytic terms in equation (212) serve to converge the $\mathbf{x}$ integral at large $|\mathbf{x}|$, and

allow us to extend the integral over all space. We include as many terms in the expansion of (211) in powers of $\mathbf{r}$ as are necessary to ensure the convergence of the integral. When n is even, there is a residual logarithmic singularity. This case can be retrieved from the general n result by taking a suitable limit (see below).

At this point, two comments are in order. Firstly, by taking the field to be directed radially outwards from the origin, we seem to be limiting ourselves to defects and excluding antidefects. The antidefect of a point defect, however, can be generated (up to arbitrary rotations), by 'inverting' ($\phi_i \to -\phi_i$) an odd number of Cartesian components of the vector $\vec{\phi}$. Reference to figure 10 (*a*) shows immediately that, for $n = 2 = d$ for example, the antivortex can be generated from the vortex by this construction. Clearly, however, the scalar product $\vec{\phi}(1)\cdot\vec{\phi}(2)$ required for the evaluation of C_{sing} is invariant under this operation. Secondly, we seemed to need the assumption that the field near a given defect is not significantly distorted by the presence of other defects. This is not strictly necessary. Any distortion generated by the other defects provides an analytic background field that does not affect the contribution of the given defect to the singular part of C. (I am grateful to M. Zapotocky for a useful discussion of this point.)

The integral (212) (extended over all space) is evaluated in [54]. The result is

$$C_{\text{sing}} = n\pi^{n/2-1}B\left(\frac{n+1}{2}, \frac{n+1}{2}\right)\Gamma\left(-\frac{n}{2}\right)\rho_{\text{def}}|\mathbf{r}|^n, \tag{213}$$

where $\Gamma(x)$ is the gamma function, and $B(x, y) = \Gamma(x)\Gamma(y)/\Gamma(x+y)$ is the beta function. Note that the dependence on $|\mathbf{r}|$ can be extracted simply by a change in variable in equation (212).

The pole in the $\Gamma(-n/2)$ factor for even values of n signals a contribution of the form $|\mathbf{r}|^n \ln(|\mathbf{r}|/L)$ to C_{sing} for those cases. We shall discuss these cases explicitly when we have the result for general $n \leqslant d$.

6.2. *The general case* ($n \leqslant d$)

For $n < d$ the defects are spatially extended, but the analysis is only slightly more complicated. The defect defines a surface, or subspace, of dimension $d-n$ in the d-dimensional space. On the length scales of interest (small compared with $L(t)$), the defect is effectively 'flat' (walls) or 'straight' (lines), etc., and the vector $\vec{\phi}$ can be taken to lie in the n-dimensional subspace orthogonal to the defect (the 'orthogonal subspace'). The vector $\mathbf{r}$ can be resolved into components $\mathbf{r}_\perp$ and $\mathbf{r}_\parallel$ lying in this subspace and in the $(d-n)$-dimensional subspace of the defect respectively. Now consider the points $\mathbf{x}$ and $\mathbf{x}+\mathbf{r}$, where $\mathbf{x}$ lies in the orthogonal subspace, with the origin of $\mathbf{x}$ lying on the defect (see figure 20 for the case $d = 3, n = 2$). Then equation (211) has the same form, but with $\mathbf{r}$ replaced by $\mathbf{r}_\perp$ on the right-hand side. Proceeding as for point defects, the integration over the n-dimensional vector $\mathbf{x}$, with $\mathbf{r}$ fixed, gives

$$C_{\text{sing}} = n\pi^{n/2-1}B\left(\frac{n+1}{2}, \frac{n+1}{2}\right)\Gamma\left(-\frac{n}{2}\right)\rho_{\text{def}}|\mathbf{r}_\perp|^n, \tag{214}$$

where ρ_{def} is, as usual, the density of defect core.

The final step is to take the isotropic average of equation (214) over the orientations of $\mathbf{r}$, that is to compute $\langle|\mathbf{r}_\perp|^n\rangle$ where the angular brackets indicate an isotropic average. For generality, and because we shall need it later, we compute $\langle|\mathbf{r}_\perp|^\alpha\rangle$ for general α. To do this we set up generalized polar coordinates with the first $d-n$ polar axes in the

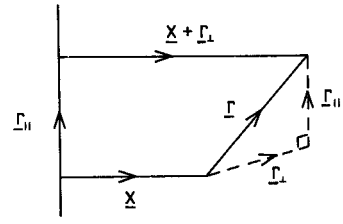

Figure 20. Coordinate system employed for the calculation of the amplitude of the Porod tail for $d = 3$, $n = 2$.

subspace of the defect. Then

$$|\mathbf{r}_\perp| = r \prod_{i=1}^{d-n} |\sin\theta_i|,$$

$$\langle |\mathbf{r}_\perp|^\alpha \rangle = r^\alpha \prod_{i=1}^{d-n} \left(\int_0^{\pi/2} \mathrm{d}\theta_i (\sin\theta_i)^{\alpha+d-1-i} \right) \Big/ \left(\int_0^{\pi/2} \mathrm{d}\theta_i (\sin\theta_i)^{d-1-i} \right)$$

$$= r^\alpha \frac{\Gamma(d/2)\Gamma((\alpha+n)/2)}{\Gamma(n/2)\Gamma((\alpha+d)/2)}. \tag{215}$$

Using equation (215) with $\alpha = n$ to perform the isotropic average of equation (214) gives the final result for the singular part of the correlation function, valid for all $n \leqslant d$:

$$C_{\mathrm{sing}} = \pi^{n/2-1} \frac{\Gamma(-n/2)\Gamma(d/2)\Gamma^2((n+1)/2)}{\Gamma((d+n)/2)\Gamma(n/2)} \rho_{\mathrm{def}} |\mathbf{r}|^n, \tag{216}$$

which reduces to equation (213) for $n = d$.

We remarked in the previous section that for even n the leading singularity is of the form $r^n \ln r$. The precise result can be extracted by setting $n = 2m + \epsilon$, with m an integer, letting ϵ go to zero, and picking up the term of order unity. The leading pole contribution, proportional to $\epsilon^{-1}(r^2)^m$, is analytical in $|\mathbf{r}|$ and therefore does not contribute to C_{sing}. The O(1) term (in the expansion in powers of ϵ) generates the logarithmic correction from the expansion of $|\mathbf{r}|^{2m+\epsilon}$. This gives, for even n,

$$C_{\mathrm{sing}} = -\left(\frac{4}{n}\right) \pi^{n/2-1} (-1)^{n/2} \frac{\Gamma(d/2)\Gamma^2((n+1)/2)}{\Gamma((d+n)/2)\Gamma^2(n/2)} \rho_{\mathrm{def}} r^n \ln r. \tag{217}$$

It turns out that the Fourier transform $S(\mathbf{k}, t)$ of $C_{\mathrm{sing}}(\mathbf{r}, t)$ has the same form for even, odd and real n; so we shall not need to consider the even-n case separately.

We can now compare the exact result (216) with the equivalent result (164) obtained within the Gaussian theory for non-conserved fields. Equating these provides another way of estimating the defect density within the Gaussian theory, namely

$$\rho_{\mathrm{def}}^{\mathrm{Gauss2}} = \frac{1}{(4\pi t)^{n/2}} \frac{\Gamma((d+n)/2)}{\Gamma(d/2)}. \tag{218}$$

Comparing this with equation (186), we see that the two estimates differ for general d, but agree for $d \to \infty$. This is another indication that the Gaussian approximation becomes exact in this limit.

6.3. *The structure factor tail*

It remains to Fourier transform equation (216) to obtain the tail of the structure factor. Although the Fourier transform of equation (216) by itself does not technically

exist (because the required integral does not converge), the following method gives the large-momentum tail correctly, as may be checked by back-transforming the result. Of course, the Fourier transform of the complete correlation function $C(\mathbf{r}, t)$ does exist, since $C(\mathbf{r}, t)$ vanishes at infinity.

Simple power counting on equation (216) gives immediately the power-law tail $S(\mathbf{k}, t) \sim k^{-(d+n)}$. To derive the *amplitude* we employ the integral representation

$$\Gamma\left(-\frac{n}{2}\right)|\mathbf{r}|^n = \int_0^\infty \mathrm{d}u\, u^{-n/2-1}[\exp(-ur^2) - \text{analytic terms}], \tag{219}$$

where analytic terms indicates, once more, as many terms in the expansion of $\exp(-ur^2)$ as are necessary to converge the integral. These terms will not contribute to the tail of the Fourier transform and can be dropped once the transform has been taken. The Fourier transform of equation (219) is therefore

$$\int_0^\infty \mathrm{d}u\, u^{-n/2-1} \int \mathrm{d}^d r \exp(-ur^2 - \mathrm{i}\mathbf{k}\cdot\mathbf{r}) = \pi^{d/2} \int_0^\infty \mathrm{d}u\, u^{-(d+n)/2-1} \exp\left(-\frac{k^2}{4u}\right)$$
$$= \pi^{d/2}\Gamma\left(\frac{d+n}{2}\right)\left(\frac{2}{k}\right)^{d+n}. \tag{220}$$

Inserting the remaining factors from equation (216) gives the final result

$$S(\mathbf{k}, t) = \frac{1}{\pi}(4\pi)^{(d+n)/2} \frac{\Gamma^2((n+1)/2)\Gamma(d/2)}{\Gamma(n/2)} \frac{\rho_{\mathrm{def}}}{k^{d+n}}. \tag{221}$$

We note that this expression is smooth as n passes through the even integers. The generality of the result should be noted; it is independent of any details of the dynamics, for example whether the order parameter is conserved or non-conserved, and holds independently of whether the scaling hypothesis is valid. We note that, as well as providing an exact result against which to test approximate theories, equation (221) can also be used to *determine* the defect density experimentally from scattering data.

Measurements of the tail amplitude in numerical simulations are in good agreement with equation (221) for both scalar [54] and vector [100] fields. As an example, we show in figure 21 the results for the cases $n = d = 2$, $n = d = 3$, and $n = 2$, $d = 3$ [100]. It is interesting that in all cases the asymptotic behaviour is approached *from above*. For a scalar order parameter ($n = 1$), the leading correction to equation (221) has been calculated by Tomita [96]. It is a term of order $k^{-(d+3)}$, associated with the curvature of the interfaces and obtained from a short-distance expansion of the form $C(\mathbf{r}) = 1 - ar + br^3 - \ldots$. The absence of an r^2 term leads to the Tomita [96] sum rule for the structure factor, $\int_0^\infty \mathrm{d}k\,[k^{d+1}S(k) - A] = 0$, where A is the amplitude of the Porod tail.

The discussion has so far been restricted to the cases $n \leqslant d$, where singular topological defects exist. What can be said about the structure factor tail for $n > d$? The case $n = d + 1$ may be complicated by the presence of topological textures [117]. For $n > d + 1$, preliminary numerical studies for nonconserved dynamics [118] suggest that the structure-factor scaling function $g(y)$ has a stretched-exponential tail, $g(y) \sim \exp(-y^\delta)$, with $\delta \approx 1$ for $d = 1, n = 3$, and $\delta \approx \frac{1}{2}$ for $d = 2, n = 4$. Similar studies by Toyoki were analysed in terms of a power-law tail $g(y) \sim y^{-\chi}$, with $\chi > d + n$, but are also consistent with stretched exponential decay [119]. In contrast with $n \leqslant d$, the tail behaviour for $n > d$ may be different for conserved and non-conserved dynamics. Recent results for conserved dynamics [74] suggest a stretched-exponential form but with $\delta \approx 1{\cdot}7$ for both $d = 2, n = 4$ and $d = 1, n = 3$, while $\delta \approx 2{\cdot}7$ for $d = 1, n = 2$.

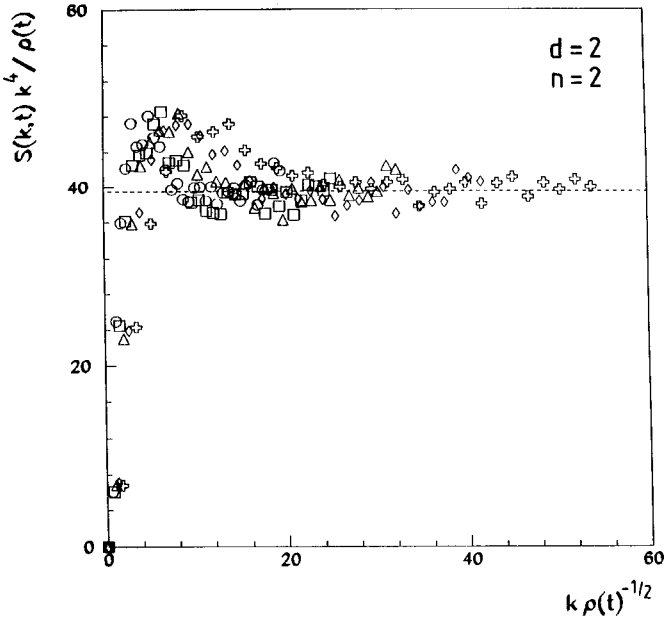
d = 2
n = 2
S(k,t) k^4 / ρ(t)
k ρ(t)^-1/2
0
20
40
60

(*a*)

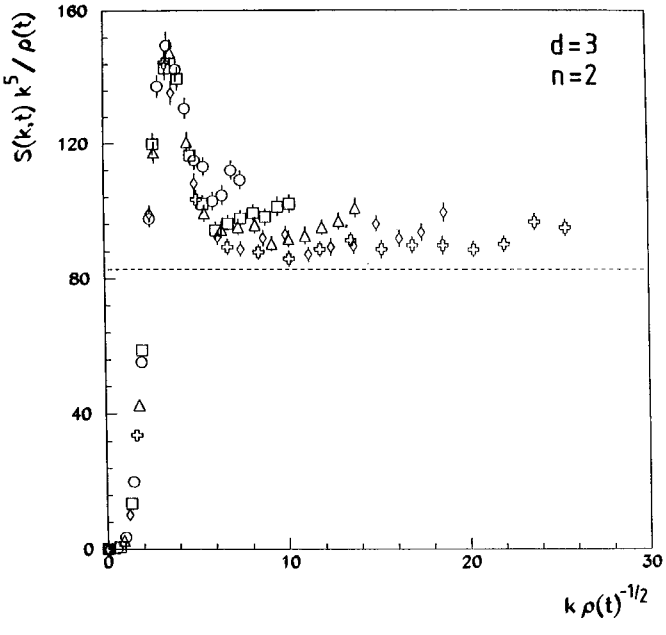
d = 3
n = 2
S(k,t) k^5 / ρ(t)
k ρ(t)^-1/2
0
40
80
120
160
10
20
30

(*b*)

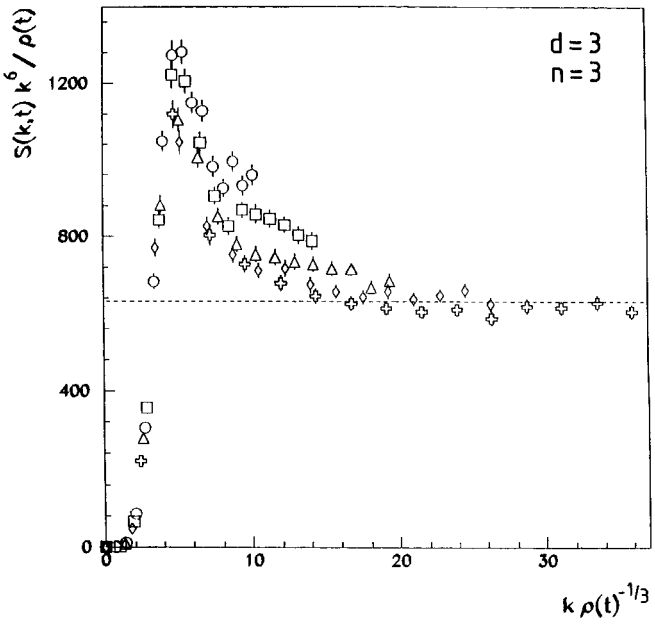

(*c*)

Figure 21. Simulation data from figure 15 replotted to reveal the amplitude $A(n, d)$ of the Porod tail, defined by $S(\mathbf{k}, t) \to A(n, d)\rho_{\text{def}}/k^{d+n}$ for $kL(t) \gg 1$. The horizontal broken lines are the prediction of equation (221) for the asymptotic limit.

6.4. *Higher-order correlation functions*

We consider first the correlation function C_4, defined by equation (176), of the square of the order parameter. We concentrate here on the numerator C_4^N, defined by

$$C_4^N = \langle [1 - \vec{\phi}(1)^2][1 - \vec{\phi}(2)^2] \rangle. \tag{222}$$

For $n \leqslant d$, the presence of topological defects leads to a singular short-distance behaviour that can be evaluated in direct analogy to that of the usual pair correlation function C. As in the approximate calculation of C_4, using Gaussian auxiliary field methods, in section 5.3, we have to distinguish between scalar and vector fields.

6.4.1. *Scalar fields*

For scalar fields, $1 - \phi^2$ is sharply peaked near domain walls. It is convenient to introduce the auxiliary field m defined as in the Mazenko approximate theory, but *not* assumed to be Gaussian! We recall that the function $\phi(m)$ represent the equilibrium domain wall profile, with m the coordinate normal to the wall. Since ϕ^2 saturates to unity within a width of order ξ of the wall, we can use, for the calculation of scaling functions,

$$1 - \phi^2(m) = \xi\delta(m), \tag{223}$$

where we have used our usual definition of the wall width $\xi = \int_{-\infty}^{\infty} dm\,[1 - \phi^2(m)]$.

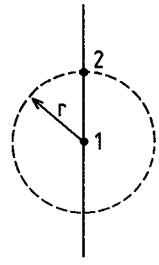

Figure 22. Relative positions of points 1 and 2 for the small-r limit of $C_4(12)$.

Putting equation (223) in equation (222) gives

$$C_4^N(1,2) = \xi^2\langle\delta(m(1))\delta(m(2))\rangle \tag{224}$$

$$= \xi^2 P(1,2) \tag{225}$$

$$= \xi^2 P(1|2)P(2). \tag{226}$$

Here we have used the fact that the wall area density (area per unit volume) $\delta(m)|\nabla m|$ can be simplified to $\delta(m)$ since $|\nabla m| = 1$ at interfaces from the definition of m as a coordinate normal to the interface. In equation (225), therefore, $P(1,2)$ indicates the joint probability density to find both 1 and 2 in an interface. In the final equality, $P(1|2)$ is the probability density to find 1 in an interface given that 2 is in an interface. Clearly $P(2) = \rho$, the average wall density. For $r \ll L(t)$, $P(1|2)$ is dominated by cases where 1 and 2 lie in the *same* wall, which can be regarded as flat on this scale, as illustrated in figure 22. For general d, $P(1|2) = S_{d-1}/S_d r$, where $S_d = 2\pi^{d/2}/\Gamma(d/2)$ is the surface area of a d-dimensional sphere of unit radius. Assembling everything in equation (226) gives

$$C_4^N \to \xi^2\rho\frac{S_{d-1}}{S_d r}, \quad \xi \ll r \ll L(t). \tag{227}$$

This result breaks down when r becomes comparable with ξ, since it is no longer adequate to neglect the thickness of the walls. The small-r behaviour (227) implies the power-law tail $S_4(\mathbf{k}, t) \sim k^{-(d-1)}$ for the corresponding structure factor, valid when $k\xi \ll 1 \ll kL(t)$.

To obtain the normalized correlation function C_4, we divide equation (227) by its large-r limit $\langle 1 - \phi^2\rangle^2$. However,

$$\langle 1 - \phi^2\rangle = \xi\langle\delta(m)\rangle = \xi\rho, \tag{228}$$

giving

$$C_4 \to \frac{S_{d-1}}{S_d\rho r}, \quad \xi \ll r \ll L(t), \tag{229}$$

from which the wall width ξ has dropped out. The exact result for the tail of the corresponding structure factor is obtained by Fourier transformation. Inserting the expression for S_d gives

$$S_4(\mathbf{k}, t) \to \frac{2}{\rho}(4\pi)^{(d-2)/2}\Gamma\left(\frac{d}{2}\right)k^{-(d-1)}, \quad k\xi \ll 1 \ll kL(t). \tag{230}$$

This could be measured by small-angle scattering in a situation where all the scattering was from the interfaces. The $d = 3$ result has been derived by Onuki, together with the leading correction, of relative order $1/(kL)^2$ [120].

A heuristic derivation of the $k^{-(d-1)}$ tail, based purely on scaling, proceeds as follows [53]. Since $\langle 1-\phi^2\rangle \sim \rho \sim 1/L$, C_4^N has the scaling form $C_4^N = L^{-2} f(r/L)$, giving $S_4^N = L^{d-2} g(kL)$ but, for $kL \gg 1$, the scattering intensity should scale as the defect density, that is as $1/L$. This requires $g(y) \sim y^{-(d-1)}$ for $y \gg 1$. This argument can be generalized to vector fields, as we shall see.

It is interesting that equation (229) can be combined with equation (216) (with $n = 1$) to obtain an exact relation, valid at short distances, between the two correlation functions [100]. For $n = 1$, equation (216) implies the short-distance behaviour

$$C(\mathbf{r},t) = 1 - \frac{2}{\pi^{1/2}} \frac{\Gamma(d/2)}{\Gamma((d+1)/2)} \rho r. \tag{231}$$

Eliminating ρr between equations (229) and (231) yields

$$C_4^{-1} = \frac{\pi}{2} \frac{\Gamma((d-1)/2)\Gamma((d+1)/2)}{\Gamma^2(d/2)} (1-C), \tag{232}$$

valid at short distances (i.e. $\xi \ll r \ll L(t)$). Let us compare this exact result with equation (180), obtained using Gaussian auxiliary field methods. For short distances, when C is close to unity, equation (180) becomes $C_4^{-1} = (\pi/2)(1-C)$. This has the same form as equation (232), but with a different coefficient of $1-C$. However, the exact coefficient approaches the 'Gaussian' value of $\pi/2$ in the limit $d \to \infty$, consistent with our argument that the auxiliary field m is indeed Gaussian in this limit.

6.4.2. *Vector fields*

For vector fields, $\vec{\phi}^2$ saturates to unity only as an inverse power of the distance from a defect, and the representation (223) is no longer appropriate. Instead, equation (59) (see also equations (182)) implies that

$$1 - \vec{\phi}^2 \to \frac{\xi^2}{r^2} \tag{233}$$

when the distance r from the core satisfies $\xi \ll r \ll L(t)$. The calculation of the singular part of C_4^N, due to the presence of defects, then follows that of the usual pair correlation function C:

$$C_{4\,\mathrm{sing}}^N = \xi^4 \rho_{\mathrm{def}} \int \mathrm{d}^n x \left\langle \frac{1}{|\mathbf{x}|^2 |\mathbf{x} + \mathbf{r}_\perp|^2} \right\rangle, \tag{234}$$

where $\mathbf{r}_\perp$ is the usual component of $\mathbf{r}$ in the plane perpendicular to the defect, and the angular brackets indicate an isotropic average over the orientations of $\mathbf{r}$. Evaluating the $\mathbf{x}$ integral first gives

$$C_{4\,\mathrm{sing}}^N = \xi^4 \rho_{\mathrm{def}} \pi^{n/2} \frac{\Gamma(2-n/2)\Gamma^2(n/2-1)}{\Gamma(n-2)} \langle |\mathbf{r}_\perp|^{n-4} \rangle. \tag{235}$$

Using equation (215), with $\alpha = n-4$, gives (after some algebra)

$$C_{4\,\mathrm{sing}}^N = -\xi^4 \rho_{\mathrm{def}} \pi^{n/2} \frac{\Gamma(n/2-1)\Gamma(1-n/2)\Gamma(d/2)}{\Gamma((d+n-4)/2)} r^{n-4}. \tag{236}$$

This result gives the *singular* part of C_4^N for all $n > 2$. The poles in the numerator at even-n signal additional factors of $\ln r$ (actually $\ln(r/L)$), as in the calculation of C. The amplitude of the logarithm can be extracted by setting $n = 2m + \epsilon$, with m an integer, letting ϵ go to zero and picking up the term of order unity. This gives, for even

n greater than 2,

$$C^N_{4\,\mathrm{sing}} = -4\xi^4\rho_{\mathrm{def}}(-\pi)^{n/2}\frac{\Gamma(d/2)}{(n-2)\Gamma((d+n-4)/2)}r^{n-4}\ln r. \tag{237}$$

This singular short-distance behaviour implies, as usual, a power-law tail in Fourier space, $S_4(\mathbf{k},t)\sim k^{-(d+n-4)}$ for $n>2$, in agreement with the prediction of the Gaussian theories (section 5.3 and [53]). Again, there is a heuristic argument for this [53]). The result $\langle(1-\vec{\phi}^2)\rangle\sim 1/L^2$ for $n>2$ suggests the scaling from $C^N_4 = L^{-4}f(r/L)$, with Fourier transform $L^{d-4}g(kL)$. Extracting the expected proportionality to $\rho_{\mathrm{def}}\sim L^{-n}$ for $kL\gg 1$ generates the required $k^{-(d+n-4)}$ tail.

The case $n=2$ is more complicated, owing to an additional pole in equation (236). The same technique, however, can be used. We put $n=2+\epsilon$ in equation (236), let ϵ go to zero and pick up the term of order unity. The result is

$$C^N_{4\,\mathrm{sing}} = \xi^4\rho_{\mathrm{def}}\pi(d-2)\frac{\ln^2 r}{r^2}, \quad d>n=2. \tag{238}$$

For $d=2$, we must set $d=2$ in equation (236) before taking ϵ to zero. This gives

$$C^N_{4\,\mathrm{sing}} = 2\pi\xi^4\rho_{\mathrm{def}}\frac{\ln r}{r^2}, \quad d=n=2. \tag{239}$$

The corresponding structure factor (the Fourier transform of $C^N_{4\,\mathrm{sing}}$ has a large-momentum tail of the form $[\xi^4\rho_{\mathrm{def}}\ln^2(k\xi)]/k^{d-2}$. These results have been discussed in more detail in [100]. In particular, it is shown that the result for $d=n=2$ is inconsistent with a conventional scaling form.

6.4.3. *Defect–defect correlations*

The short-distance behaviour of the defect–defect correlation functions, introduced in section 5.3.3, may also be determined exactly, at least for extended defects. The argument is a simple extension of that used to calculate C_4 for scalar fields. From the first part of equation (187), the correlator $\langle\rho(1)\rho(2)\rangle$ is just the joint probability density $P(0,0)$ for points 1 and 2 both lying on a defect. Clearly $P(0,0)=\rho_{\mathrm{def}}P(2|1)$, in the usual notation but, for $r\ll L$, $P(2|1)$ is dominated by cases where 1 and 2 are in the *same* defect (*provided* that the defects are spatially extended, i.e. $n<d$). An obvious generalization of equation (227) gives

$$\begin{aligned}\langle\rho(1)\rho(2)\rangle &= \rho_{\mathrm{def}}\frac{S_{d-n}}{S_d r^n}\\ &= \frac{\rho_{\mathrm{def}}}{\pi^{n/2}r^n}\frac{\Gamma(d/2)}{\Gamma((d-n)/2)}.\end{aligned} \tag{240}$$

This result differs from equation (188), obtained using the Gaussian approximation, but approaches it in the limit $d\to\infty$, as we have by now come to expect. In the exact result (240), the amplitude of the r^{-n} divergence vanishes for point defects ($n=d$), an important physical feature that is missing from the Gaussian approximation (188).

6.5. *The probability distribution* P(m(*1*), m(*2*))

To conclude this section on short-distance behaviour, we compute the exact form of $P(m(1),m(2))$ for scalar fields, valid for $|m(1)|$, $|m(2)|$ and r all much smaller than $L(t)$, and show explicitly that it is not Gaussian. Technically, the regime in which we are working corresponds to taking the limit $L(t)\to\infty$ with $|m(1)|$, $|m(2)|$ and r fixed but arbitrary. This situation is illustrated in figure 23, where the domain wall can be regarded

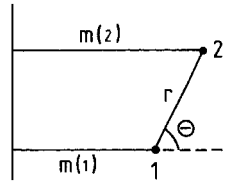

Figure 23. Calculation of the short-distance limit of $P(m(1), m(2))$.

as flat in the limit of interest. The identity $P(m(1), m(2)) = P(m(1))P(m(2)|m(1))$, where $P(x|y)$ indicates a conditional probability, gives

$$P(m(1), m(2)) = \rho\langle\delta(m(2) - m(1) - r\cos\theta)\rangle, \tag{241}$$

where the angular brackets indicate an isotropic average over θ, and we have used $P(m(1)) = \rho$, the wall density, for $|m(1)| \ll L$. Carrying out the angular average (with weight proportional to $\sin^{d-2}\theta$) gives

$$P(m(1), m(2)) = \left[B\left(\frac{1}{2}, \frac{d-1}{2}\right)\right]^{-1} \frac{\rho}{r}\left(1 - \frac{(m(2) - m(1))^2}{r^2}\right)^{(d-3)/2}, \tag{242}$$

for $|m(1) - m(2)| \leqslant r$, and $P = 0$ otherwise. Clearly $P(m(1), m(2))$ is not Gaussian for general d. However, it approaches a Gaussian for large d, as we now show.

It is clear from equation (242) that, in the limit $d \to \infty$, $P(m(1), m(2))$ vanishes except when $|m(1) - m(2)|/r$ is of order $1/d^{1/2}$. Therefore we define

$$\Delta = \frac{d^{1/2}[m(1) - m(2)]}{r}. \tag{243}$$

Now the large-d limit can be taken at fixed Δ. Taking d large in the beta function too gives

$$P(m(1), m(2)) \to \left(\frac{d}{2\pi}\right)^{1/2} \frac{\rho}{r} \exp\left(-\frac{\Delta^2}{2}\right), \quad d \to \infty. \tag{244}$$

Let us compare this result with that of the systematic approach, which we argued is exact for large d, by evaluating equation (123) in the same limit. Equation (158) gives $S_0 = 4t/d$ and $\gamma = \exp(-r^2/8t)$. Inserting these in equation (123) and taking the limit $t \to \infty$, with $r, m(1)$ and $m(2)$ held fixed, give

$$P(m(1), m(2)) = \frac{d}{4\pi r t^{1/2}} \exp\left(-\frac{\Delta^2}{2}\right). \tag{245}$$

Equations (244) and (245) agree if $\rho = (d/8\pi t)^{1/2}$, which is just equation (186). We conclude that the exact result (242) is consistent with the Gaussian approximation in the limit $d \to \infty$, but not for any finite d.

7. Growth laws

The exact short-distance singularities derived in the previous section, together with the scaling hypothesis, provide a basis for deriving exact growth laws for all phase-ordering systems with purely dissipative dynamics.

Although the growth laws for both non-conserved and conserved scalar systems, and conserved fields in general, have been derived by a number of methods, there has up until now been no simple general technique for obtaining $L(t)$. In particular, the

growth laws for non-conserved vector fields have, until recently, been somewhat problematic. Here we describe a very general approach, recently developed by BR [79], to obtain $L(t)$ consistently by comparing the global rate of energy change with the energy dissipation from the local evolution of the order parameter. This method allows the explicit derivation of growth laws for O(n) models, but the results can also be applied to other systems with similar defect structures.

The BR approach is based on the dissipation of energy that occurs as the system relaxes towards its ground state. The energy dissipation is evaluated by considering the motion of topological defects, when they exist. The defect contribution either dominates the dissipation or gives a contribution that scales with time in the same way as the total dissipation. The global rate of energy change, computed from the time derivative of the total energy, is equated to the energy dissipation from the local evolution of the order parameter. For systems with a single characteristic scale $L(t)$, this approach self-consistently determines the time-dependence of $L(t)$.

7.1. *A useful identity*

We begin by writing down the equation of motion for the Fourier components $\phi_{\mathbf{k}}$:

$$\partial_t \vec{\phi}_{\mathbf{k}} = -k^{\mu} \frac{\partial F}{\partial \vec{\phi}_{-\mathbf{k}}}. \tag{246}$$

The conventional non-conserved (model A) and conserved (model B) cases are $\mu = 0$ and $\mu = 2$ respectively. (Elsewhere in this article, the symbol μ has been used for the chemical potential; the meaning should be clear from the context.)

Integrating the rate of energy dissipation from each Fourier mode, and then using the equation of motion (246), we find

$$\begin{aligned} \frac{\mathrm{d}\epsilon}{\mathrm{d}t} &= \int_{\mathbf{k}} \left\langle \frac{\partial F}{\partial \vec{\phi}_{\mathbf{k}}} \cdot \partial_t \vec{\phi}_{\mathbf{k}} \right\rangle \\ &= -\int_{\mathbf{k}} k^{-\mu} \langle \partial_t \vec{\phi}_{\mathbf{k}} \cdot \partial_t \vec{\phi}_{-\mathbf{k}} \rangle, \end{aligned} \tag{247}$$

where $\epsilon = \langle F \rangle / V$ is the mean energy density, and $\int_{\mathbf{k}}$ is the momentum integral $\int \mathrm{d}^d k/(2\pi)^d$. We shall relate the scaling behaviour of both sides of equation (247) to that of appropriate integrals over the structure factor $S(\mathbf{k}, t)$ and its two-time generalization. Either the integrals converge and the dependence on the scale $L(t)$ can be extracted using the scaling form (7) (or its two-time generalization (8)), or the integrals diverge in the ultraviolet and have to be cut off at $k_{\max} \sim 1/\xi$, corresponding to a dominant contribution from the core scale. It is just this small-scale structure that is responsible for the generalized Porod law (70) for the structure factor, and the time dependence of any integrals controlled by the core scale can be extracted from a knowledge of the defect structure.

7.1.1. *The energy integral*

To see how this works, we first calculate the scaling behaviour of the energy density ϵ which is captured by that of the gradient term in equation (1):

$$\begin{aligned} \epsilon &\sim \langle |\nabla \vec{\phi}|^2 \rangle \\ &= \int_{\mathbf{k}} k^2 L^d g(kL), \end{aligned} \tag{248}$$

where we have used the scaling form (7) for the structure factor. For $n > 2$ the integral is ultraviolet convergent, and a change in variables yields $\epsilon \sim L^{-2}$. For $n \leqslant 2$, when the integral is ultraviolet divergent, we use the Porod law (70) and impose an ultraviolet cut-off at $k \sim 1/\xi$, to obtain [56]

$$\epsilon \sim \begin{cases} L^{-n}\xi^{n-2}, & n < 2, \\ L^{-2}\ln\left(\dfrac{L}{\xi}\right), & n = 2, \\ L^{-2}, & n > 2. \end{cases} \tag{249}$$

We see that the energy is dominated by the defect core density $\rho_{\text{def}} \sim L^{-n}$ for $n < 2$, by the defect field at all length scales between ξ and L for $n = 2$, and by variations in the order parameter at scale $L(t)$ for $n > 2$.

7.1.2. *The dissipation integral*

We now attempt to evaluate the right-hand side of equation (247) in a similar way. Using the scaling hypothesis for the two-time function,

$$\langle \vec{\phi}_{\mathbf{k}}(t) \cdot \vec{\phi}_{-\mathbf{k}}(t') \rangle = k^{-d} g(kL(t), kL(t')), \tag{250}$$

which is the spatial Fourier transform of equation (8), we find that

$$\begin{aligned} \langle \partial_t \vec{\phi}_{\mathbf{k}} \cdot \partial_t \vec{\phi}_{-\mathbf{k}} \rangle &= \frac{\partial^2}{\partial t\, \partial t'}\bigg|_{t=t'} \langle \vec{\phi}_{\mathbf{k}}(t) \cdot \vec{\phi}_{-\mathbf{k}}(t') \rangle \\ &= \dot{L}^2 L^{d-2} h(kL), \end{aligned} \tag{251}$$

where $\dot{L} \equiv \mathrm{d}L/\mathrm{d}t$.

When the momentum integral on the right of equation (247) is ultraviolet convergent we obtain, using equation (251), $\mathrm{d}\epsilon/\mathrm{d}t \sim -\dot{L}^2 L^{\mu-2}$. If, however, the integral is ultraviolet divergent, it will be dominated by the behaviour of the integrand near the upper limit; so we need to know the form of the scaling function h in equation (251) for $kL \gg 1$. It turns out that, in general, the large-kL form is quite complicated, with many different cases to consider [27]. However, we need only the result for those cases where the dissipation integral requires an ultraviolet cut-off; otherwise simple power counting is sufficient. For those cases, one additional assumption, which can be verified *a posteriori*, yields a simple and rather general result (equation (259) below).

7.2. *Evaluating the dissipation integral*

7.2.1. *An illustrative example*

To see what difficulties arise, and how to circumvent them, it is instructive to consider a scalar field. We want to calculate $\langle \partial_t \phi_{\mathbf{k}}\, \partial_t \phi_{-\mathbf{k}} \rangle$ in the limit $kL \gg 1$. It is clear that $\partial_t \phi$ is appreciably different from zero only near interfaces. Since $\mathrm{d}\phi/\mathrm{d}t = 0$ in a frame comoving with the interface, we have, near an interface, $\partial_t \phi = -\mathbf{v} \cdot \nabla \phi$, where $\mathbf{v}$ is the interface velocity. In real space, therefore,

$$\langle \partial_t \phi(1) \partial_t \phi(2) \rangle = \langle [\mathbf{v}(1) \cdot \nabla \phi(1)][\mathbf{v}(2) \cdot \nabla \phi(2)] \rangle \tag{252}$$

The large-kL behaviour in Fourier space is obtained from the short-distance ($r \ll L$) behaviour in real space. For $r \ll L$, the points 1 and 2 must be close to the *same* interface. For a typical interface, with radius of curvature of order $1/L$, the speed v is slowly varying along the interface. Furthermore, the interface may be regarded as 'flat' for the

calculation of the short-distance correlation, just as in the derivation of the Porod law. It follows that the averages over the interface velocity and position can be carried out independently, giving

$$\langle \partial_t \phi(1) \partial_t \phi(2) \rangle = \frac{1}{d} \langle v^2 \rangle \langle \nabla \phi(1) \cdot \nabla \phi(2) \rangle. \tag{253}$$

Fourier transforming this result gives

$$\langle \partial_t \phi_{\mathbf{k}} \partial_t \phi_{-\mathbf{k}} \rangle \begin{cases} = \dfrac{\langle v^2 \rangle}{d} k^2 S(\mathbf{k}, t), & kL \gg 1 \\ \sim \dfrac{\langle v^2 \rangle}{L k^{d-1}}, & kL \gg 1, \end{cases} \tag{254}$$

where the Porod result (69) was used in the final line. We shall see that equation (254) requires a careful interpretation.

The next step is to evaluate $\langle v^2 \rangle$. Since the characteristic interface velocity is $\dot{L}$, we expect $\langle v^2 \rangle \sim \dot{L}^2$. This assumes, however, that the average is dominated by 'typical' values. This, as we shall see, is the key question. Consider a small spherical domain of radius r in a non-conserved system. The interface velocity (see equation (16)) is $v \sim 1/r$. For a conserved system, equation (31) gives $v \sim 1/r^2$. Thus the relation $v(r) \sim 1/r^{z-1}$ where $z = 2$ and 3 for non-conserved and conserved systems respectively (and the growth law is $L \sim t^{1/z}$) covers both cases. The fact that v diverges at small r raises the possibility that $\langle v^2 \rangle$ is dominated by small domains. The domain-size distribution function $n(r)$ has the scaling form $n(r) = L^{-(d+1)} f(r/L)$ (in order that $\int \mathrm{d}r\, n(r) \sim L^{-d}$, consistent with scaling). The important small-x behaviour of the function $f(x)$ can be determined as follows. Consider a small time interval Δt. The domains that will have disappeared after this time interval are those with radius smaller than $r_{\Delta t} \sim (\Delta t)^{1/z}$. The number of such domains is of order $L^{-(d+1)} \int_0^{r_{\Delta t}} \mathrm{d}r\, f(r/L)$. The requirement that this be linear in Δt forces $f(x) \sim x^{z-1}$ for $x \to 0$. Using $v \sim r^{-(z-1)}$ we can estimate the contribution to $\langle v^2 \rangle$ from short scales:

$$\begin{aligned} \langle v^2 \rangle &\sim \left(\int_\xi^L \mathrm{d}r\, r^{d-1} n(r) v^2(r) \right) \Big/ \left(\int_\xi^L \mathrm{d}r\, r^{d-1} n(r) \right) \\ &\sim \left(\int_\xi^L \mathrm{d}r\, r^{d-z} \right) \Big/ \int_\xi^L \mathrm{d}r\, r^{d+z-2}. \end{aligned} \tag{255}$$

The integral in the denominator converges at short scales, giving a result of order L^{d+z-1}. For non-conserved fields ($z = 2$), the numerator converges for all $d > 1$, giving L^{d-1} for the numerator, and $\langle v^2 \rangle \sim 1/L^2$. Since $\dot{L} \sim 1/L$ for this case, we have $\langle v^2 \rangle \sim \dot{L}^2$ as expected. For conserved fields ($z = 3$), however, the numerator only converges at short scales for $d > 2$. For those cases, one again finds $\langle v^2 \rangle \sim \dot{L}^2$. For $d = 2$, however, the numerator is of order $\ln(L/\xi)$. This gives $\langle v^2 \rangle \sim L^{-4} \ln(L/\xi)$, that is there are contributions from all scales, and $\langle v^2 \rangle \sim \dot{L}^2$ no longer holds. Putting this into equation (254) gives

$$\langle \partial_t \phi_{\mathbf{k}} \partial_t \phi_{-\mathbf{k}} \rangle \overset{?}{\sim} \frac{\ln(L/\xi)}{L^5 k}, \quad kL \gg 1, \quad (d = 2, \text{ conserved}). \tag{256}$$

We shall now show that this result is wrong!

The factor $1/L$ in equation (254) represents the total interfacial area density; equation (254) implies that interfaces contribute additively to $\langle \partial_t \phi_{\mathbf{k}} \partial_t \phi_{-\mathbf{k}} \rangle$. In the derivation of equation (254), however, we explicitly assumed that only interfaces of typical curvature, of order $1/L$, contribute. For a piece of interface of local curvature $1/R$, the condition that the interface be regarded as locally flat on the scale $1/k$ requires that $kR \gg 1$ and not simply that $kL \gg 1$. For fixed $k \gg 1/L$, sharply curved interfaces, with $R \lesssim 1/k$, *do not contribute to the Porod tail.* This means that, as far as the computation of the large-kL behaviour is concerned, there is an *effective short-distance cut-off* at $1/k$; only interfaces with radius of curvature $R \gg 1/k$ should be included. For the calculation of the usual Porod tail in $\langle \phi_{\mathbf{k}} \phi_{-\mathbf{k}} \rangle$ this makes no difference, because interfaces with $R \lesssim 1/k$ make a negligible contribution to the total interfacial area as $kL \to \infty$. For the calculation of $\langle \partial_t \phi_{\mathbf{k}} \partial_t \phi_{-\mathbf{k}} \rangle$, however, it can make a big difference, because of the extra factor of v^2 inside the average. This means that, in evaluating $\langle v^2 \rangle$, $1/k$ rather than ξ is the appropriate short-distance cut-off. Applying this to conserved scalar fields in $d = 2$ gives $\langle v^2 \rangle \sim L^{-4} \ln(kL)$, and

$$\langle \partial_t \phi_{\mathbf{k}} \partial_t \phi_{-\mathbf{k}} \rangle \overset{?}{\sim} \frac{\ln(kL)}{L^5 k}, \quad kL \gg 1, \quad (d = 2, \text{ conserved}), \tag{257}$$

instead of equation (256).

The final step is to insert equation (257) into the dissipation integral (247), with $d = 2 = \mu$. One immediately sees that the integral is ultraviolet convergent; the L dependence can be extracted trivially by a change of variable, $\mathrm{d}\epsilon/\mathrm{d}t \sim -1/L^4$. So we did not actually need the asymptotic form of $\langle \partial_t \phi_{\mathbf{k}} \partial_t \phi_{-\mathbf{k}} \rangle$ after all (except to show that the dissipation integral is ultraviolet convergent)! Note that the final result $\mathrm{d}\epsilon/\mathrm{d}t \sim -1/L^4$ is consistent with $\epsilon \sim 1/L$ (equation (249) with $n = 1$) and the result $\dot{L} \sim 1/L^2$ for conserved (i.e. $\mu = 2$) scalar fields.

There is, however, one last complication. Equation (257) is still not quite correct! This is because the expression $v(r) \sim 1/r^2$ for the velocity of a small drop (i.e. with $r \ll L$) breaks down for $d = 2$ owing to the singular nature of the Green function for the Laplacian. For this case one finds instead [27] $v(r) \sim 1/r^2 \ln(L/r)$. Using this gives finally $\langle \partial_t \phi_{\mathbf{k}} \partial_t \phi_{-\mathbf{k}} \rangle \sim \{\ln[\ln(kL)]\}/L^5 k$ for $kL \gg 1$, instead of equation (257). This does not alter, of course, the conclusion that the dissipation integral is ultraviolet convergent and can therefore be evaluated simply by a change of variable.

7.2.2. *The way forward*

We have gone through this one case in some detail, because we can extract from it a general principle that avoids treating every case separately (although this can be done [27]). The central point, given extra emphasis by the discussion above, is that we only need to know the asymptotics of $\langle \partial_t \vec{\phi}_{\mathbf{k}} \cdot \partial_t \vec{\phi}_{-\mathbf{k}} \rangle$ in those cases where the dissipation integral is ultraviolet divergent. The main result (with exceptions that can be enumerated) is that in all such cases the 'naive' estimates, obtained by using $\langle v^2 \rangle \sim \dot{L}^2$, are correct.

To make further progress we introduce the additional assumption, which can be checked *a posteriori*, that the dissipation is dominated by the motion of defect structures of 'characteristic scale' $L(t)$. By the 'characteristic scale' we mean the typical radius of curvature for extended defects ($n \leq d$), or the typical defect separation for point defects ($n = d$). That is, we are assuming that the dissipation is dominated by the motion of typical defect structures, and not by the disappearance of small domain bubbles and small vortex loops, or by the annihilation of defect–antidefect pairs. If the latter were

true, the dissipation would be dominated by structure at the core scale, and the arguments given below would fail. We recall that, for the case $d = 2 = \mu$ discussed above, the final **k** integral for the dissipation was convergent, implying that the dominant k-values are of order $1/L$, and the worries about the possible importance of small-scale structure were ultimately groundless. If the final **k** integral *were* ultraviolet divergent, *and* the large-kL limit of $\langle \partial_t \vec{\phi}_{\mathbf{k}} \cdot \partial_t \vec{\phi}_{-\mathbf{k}} \rangle$ had important contributions from short scales, then the dissipation *would* be dominated by structure at the core scale, violating our assumption. Therefore, when our assumption holds, *either* $\langle \partial_t \vec{\phi}_{\mathbf{k}} \cdot \partial_t \vec{\phi}_{-\mathbf{k}} \rangle$ is dominated by defect structures of scale L, *or* the final integral is ultraviolet convergent, or both.

For the required cases where the final integral is ultraviolet divergent, the large-$kL(t)$ limit of equation (251) can be extracted from the physical or geometrical arguments used to obtain the generalized Porod law (70). According to our assumption, we can treat the defects as locally flat (or well separated, for point defects) for $kL \gg 1$. From equation (251), we are interested in the behaviour of the two-time structure factor $S(\mathbf{k}, t, t') \equiv \langle \vec{\phi}_{\mathbf{k}}(t) \cdot \vec{\phi}_{-\mathbf{k}}(t') \rangle$, in the limit that the two times are close together. In the limit $kL \gg 1$, this will be proportional to the total density L^{-n} of defect core. Introducing $L = [L(t) + L(t')]/2$ and $\Delta = [L(t) - L(t')]/2$, we obtain

$$\langle \vec{\phi}_{\mathbf{k}}(t) \cdot \vec{\phi}_{-\mathbf{k}}(t') \rangle \to \frac{1}{L^n k^{d+n}} a(k\Delta), \quad kL \gg 1, \tag{258}$$

where consistency with the Porod law for $t = t'$ requires $a(0) =$ constant. Using this in equation (251) gives

$$\langle \partial_t \vec{\phi}_{\mathbf{k}} \cdot \partial_t \vec{\phi}_{-\mathbf{k}} \rangle \sim \frac{\dot{L}^2}{L^n k^{d+n-2}}, \quad kL \gg 1. \tag{259}$$

This reduces to equation (254) for $n = 1$ (with $\langle v^2 \rangle \sim \dot{L}^2$). It should be stressed that we are *not* claiming that equation (259) is a general result, only that it is valid when we need it, i.e. when the dissipation integral (247) requires an ultraviolet cut-off. There are three possibilities:

(*a*) The integral is ultraviolet convergent, its dependence on $L(t)$ can be extracted by a change in variable, and the large-kL behaviour of $\langle \partial_t \vec{\phi}_{\mathbf{k}} \cdot \partial_t \vec{\phi}_{-\mathbf{k}} \rangle$ is not required.

(*b*) The integral is ultraviolet divergent, but the dissipation is still dominated by structures of scale $L(t)$. Then we can use equation (259).

(*c*) The dissipation has significant contributions from structures with local curvature (or spacing) of order the core scale. Then one cannot treat the contributions from different defect core elements as independent, equation (259) no longer holds, and the present approach is not useful.

For the moment we shall proceed on the assumption that (*a*) and (*b*) obtain. We shall show that these possibilities cover nearly all cases. Examples of when (*c*) holds will also be given. These include the physically interesting case $d = n = 2$.

7.3. *Results*

Putting equation (259) into the dissipation integral (247) shows that the integral is ultraviolet convergent for $kL \gg 1$ when $n + \mu > 2$. Otherwise the integral is dominated

by k near the upper cut-off $1/\xi$. This gives

$$\int_{\mathbf{k}} k^{-\mu}\langle \partial_t \vec{\phi}_{\mathbf{k}} \cdot \partial_t \vec{\phi}_{-\mathbf{k}} \rangle \sim \begin{cases} \dot{L}^2 L^{-n} \xi^{n+\mu-2}, & n+\mu<2, \\ \dot{L}^2 L^{-n} \ln\left(\dfrac{L}{\xi}\right), & n+\mu=2, \\ \dot{L}^2 L^{\mu-2}, & n+\mu>2. \end{cases} \tag{260}$$

The final step is to equate the dissipation rate (260) to the time derivative of the energy density (249), as required by equation (247), and to solve for $L(t)$. The results are summarized in figure 24, as a function of n and μ, for systems with purely short-range interactions. The two straight lines separating regimes of different behaviour are the lines $n=2$ and $n+\mu=2$ at which the energy and dissipation integrals change their form. Note that conservation of the order parameter (which applies in a global sense for any $\mu>0$) is irrelevant to the growth law for $\mu<2-n$. where n is treated here as a continuous variable. At the marginal values, logarithmic factors are introduced. The growth laws obtained are independent of the spatial dimension d of the system.

For non-conserved fields ($\mu=0$), we find that $L\sim t^{1/2}$ for all systems (with $d>n$ or $n>2$). Leading corrections in the $n=2$ case are interesting; the $\ln L$ factors in equations (249) and (260) will in general have different effective cut-offs, of the order of the core size ξ. This leads to a logarithmic correction to scaling, $L\sim t^{1/2}(1+\mathrm{O}(1/\ln t))$, and may account for the smaller exponent (about 0·45) seen in simulations of O(2) systems [100, 121, 122]. Note that, for non-conserved scalar fields, the energy (249) and the dissipation (260) have the *same* dependence on the core size ξ (i.e. both contain a factor ξ^{-1}); so this dependence cancels from $L(t)$. The fact that the correct $t^{1/2}$ growth is obtained from naive power counting on the linear terms in the equation of motion should therefore be regarded as fortuitous. For example, with long-range interactions, this cancellation or errors no longer occurs, and naive power counting gives an incorrect result for nonconserved scalar fields [79, 123].

For conserved fields ($\mu>0$), our results agree with an earlier RG analysis [10, 11], with additional logarithmic factors for the marginal cases $n=2$ and $n+\mu=2$. Note that the conservation law is only relevant for $n+\mu\geqslant 2$. Therefore, for vector fields ($n\geqslant 2$), any $\mu>0$ is sufficient to change the growth law while, for scalar fields ($n=1$), the conservation law is irrelevant for $\mu<1$, in agreement with the RG analysis [11] and earlier work of Onuki [124].

Siegert and Rao [73] have performed extensive simulations for $n=2$, $d=3$ and $\mu=2$. In their original paper they fitted $L(t)$ to a simple power and obtained a growth exponent slightly larger than $\frac{1}{4}$. Recently, however, Siegert [125] has shown that a very much better fit is obtained when the predicted logarithmic correction is included.

7.3.1. *Exceptional cases* ($n=d\leqslant 2$)

In what cases is our key assumption, that dissipation is dominated by the motion of defect structures of characteristic scale, L, correct? Certainly, for any $n>2$, the energy density (249) itself (and hence dissipation) is dominated by variations at scale $L(t)$. Therefore we limit the discussion to the case $n\leqslant 2$.

For $n\leqslant 2$, the energy density is proportional to the defect core volume (with an extra factor $\ln(L/\xi)$ for $n=2$; see equation (249)), but we shall show that, in general, dissipation is still dominated by defect structures with length scales of order L. To see this, we investigate the contribution to the energy dissipation from small-scale

structures (e.g. small domains, vortex loops or defect–antidefect pairs):

$$\frac{\mathrm{d}\epsilon}{\mathrm{d}t} = \partial_t \int_\xi^\infty \mathrm{d}l\, n(l,t)\epsilon(l)$$
$$= -\int_\xi^\infty \mathrm{d}l\, \partial_l j(l,t)\epsilon(l)$$
$$= j(\xi)\epsilon(\xi) + \int_\xi^\infty \mathrm{d}l\, j(l)\frac{\partial \epsilon}{\partial l}, \tag{261}$$

where $n(l,t)$ is the number density of defect features of scale l, $\epsilon(l) \sim l^{d-n}$ is the energy of a defect feature (with an extra $\ln(l/\xi)$ factor for $n=2$), and $j(l,t)$ is the number flux of defect features. We have used the continuity equation, $\partial_t n + \partial_l j = 0$ to obtain the second line of equation (261), and the t dependence has been suppressed in the final line. The total number N, of defect features scales as $N \sim L^{-d}$, and so N does not change significantly over times smaller than $\dot{L}/L$. Since defects vanish only on the core scale, we have $\dot{N} = j(\xi)$. It follows that $j(l)$ has a finite non-zero short-distance limit of order $\dot{N} \sim -\dot{L}/L^{d+1}$. We can use this to examine the convergence (at short-distance) of the final integral in equation (261).

For $d > n$, the integral in equation (261) is well behaved at small l, because $\epsilon(l) \sim l^{d-n}$ ($\epsilon(l) \sim l^{d-n}\ln(l/\xi)$ for $n=2$), and the integral dominates the $j(\xi)\epsilon(\xi)$ term. The integral can be estimated by setting $j(l) \approx j(\xi)$ and introducing a large-distance cut-off at $l \sim L$. This gives $\mathrm{d}\epsilon/\mathrm{d}\tau \sim j(\xi)L^{d-n} \sim -\dot{L}/L^{n+1}$ ($\times \ln(L/\xi)$ for $n=2$). This is just what one gets from differentiating equation (249) (for the cases $n \leqslant 2$ considered here), verifying the consistency of the calculation.

For $d = n$ and $n < 2$, however, $\epsilon(l) \sim$ constant, since the (point) defects interact only weakly through the tails of the defect profile. (The one physical example is the $d=1$ scalar system.) The leading contribution to the energy of a defect pair is just the core energy of the individual defects, and dissipation is dominated by the $j(\xi)\epsilon(\xi)$ term in equation (261), which describes the annihilation of defect pairs. Since the dissipation occurs at separations $l \sim \xi \ll L$, the derivation of equation (259) no longer holds. Since the energy of a defect pair depends only weakly on the separation for $l \gg L$, the system will be disordered, with an equilibrium density of defects at any non-zero temperature. At $T=0$, we expect slow growth that depends on the details of the potential $V(\phi)$ [126]. These cases, including the $d=1$ scalar system, are at their lower critical dimension and are beyond the scope of the simplified approach presented here (see [126] for a fuller discussion).

The two-dimensional planar system ($n = d = 2$) is a special case. The logarithm in the energy of a vortex pair, $\epsilon \sim \ln(l/\xi)$, leads to a logarithmically divergent integral in equation (261), i.e. vortex pairs with separations between ξ and L contribute significantly to the energy dissipation. In this case equation (259), which depends on the fact that the $kL \gg 1$ limit is a single-defect property, is again questionable. As a result the present method cannot address this case. Indeed, the contributions to the dissipation from all length scales suggest a possible breakdown of scaling.

7.3.2. *Systems without defects*

Since systems without topological defects ($n > d+1$) will have convergent momentum integrals for $kL \gg 1$, we obtain $L \sim t^{1/(2+\mu)}$ for these cases. We can also apply this result to systems with topological textures ($n = d+1$), even though the appropriate Porod law is not known. Since defects with $n > d$ must be spatially extended and without

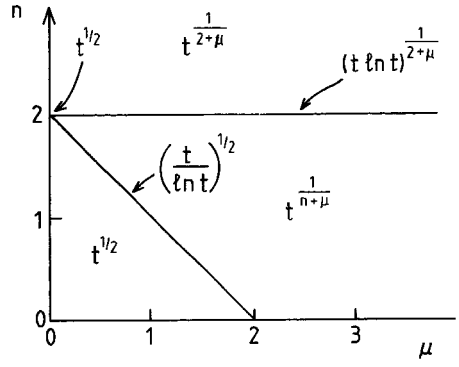

Figure 24. Time dependence of the characteristic scale $L(t)$ for systems with purely dissipative dynamics. Exceptional cases are discussed in the text.

a core, they will have a smaller large-k tail to their structure factor $S(\mathbf{k}, t)$ than any defects with cores. So, for $n > 2$, when the energy dissipation clearly occurs at length scales of order $L(t)$ (see equation (249)) and the momentum integrals for defects with cores converge, our results should apply ([27] contains a fuller discussion of this point). Consequently the results in figure 24 will apply for *any* system, apart from those systems explicitly excluded above.

Of course, all this is subject to the caveat that the two-time structure factor exhibits the scaling form (251), on which the whole of this section is built. One explicit counter-example is the $d = 1, n = 2$, system discussed in section 4.5, for which equation (251) explicitly fails. As a result, the growth law characterizing equal-time correlations is *not* $L \sim t^{1/2}$, as suggested by figure 24, but $L \sim t^{1/4}$. Indeed one can use the two-time result (113) to calculate $\langle \partial_t \vec{\phi}_{\mathbf{k}} \cdot \partial_t \vec{\phi}_{-\mathbf{k}} \rangle$ explicitly for this system [80] and show that it is consistent with $L \sim t^{1/4}$ growth.

7.3.3. *Other systems*

The strength of this approach is that it can be applied to systems with more complicated order parameters than n-component vectors, provided that they have purely dissipative dynamics. Then an equation of the form (247) can be written down. The details of the energy functional (1) are unimportant.† The important ingredients are the existence of an 'elastic energy', associated with spatial gradients of the order parameter, the conservation law (if any), characterized by μ, and the defect structure if any. The derivation is independent of the initial conditions, and so, for example, applies equally to critical and off-critical quenches *as long as the system scales at late times*. We simply choose a Porod law (70) to represent the dominant defect type, which is the one responsible for the asymptotic tails of the structure factor scaling function, namely that with the smallest n. When the energy density is dominated by defects, that is when the energy integral (248) is ultraviolet divergent, the relation (248) between the energy density and the structure factor, shows that the 'dominant' defects will also be those

† Of course, this means that the present approach will not address systems with a potential-dependent growth law, for example $d = n$ for $n < 2$. We also do not address quenches in which thermal noise is essential, such as systems with static disorder (see, however, section 8.3.2) or quenches to a $T > 0$ critical point.

which dominate the energy density. As examples, we consider nematic liquid crystals and Potts models.

In bulk nematic liquid crystals, the 'dominant' defects (in the above sense) are strings, giving a Porod tail (70) with $n = 2$, which with no conservation law implies that $L \sim t^{1/2}$, consistent with recent experiments [60, 61] and simulations [65].

The q-state Potts model has q equivalent equilibrium phases, which give rise to $q(q-1)/2$ different types of domain wall. These can be indexed $\alpha\beta$, where $\alpha, \beta = 1, \ldots q$, are the phases separated by the wall. Three domain walls of type $\alpha\beta$, $\alpha\gamma$ and $\beta\gamma$ can meet at a point ($d = 2$) or line ($d = 3$), which represents a new type of defect. It is clear, however, that the Porod tail and energy density are dominated by the walls, so that the Potts model behaves as an $n = 1$ system. As a result, $L(t) \sim t^{1/2}$ and $t^{1/3}$ for non-conserved and conserved order parameter respectively. Recent numerical results [127, 128] support these predictions, after initial suggestions that the growth was slower. The $t^{1/3}$ growth for conserved systems is also predicted by the RG approach of section 8.

It should be emphasized that the classification of nematic liquid crystals and Potts models as '$n = 2$-like' and '$n = 1$-like' respectively pertain only to the Porod tails and the growth laws. As far as scaling functions (e.g. for pair correlations) are concerned, these systems belong to their own universality classes. Similarly, for off-critical quenches of conserved systems, the growth law is independent of the volume fractions of the phases, but the scaling functions are not.

8. Renormalization group results

As with any other scaling phenomenon, it is tempting to try to apply RG concepts to the late stages of phase ordering. The basic idea is to associate the scaling behaviour with a fixed point of the equation of motion under a RG procedure consisting of a coarse-graining step combined with a simultaneous rescaling of length and time. Such a procedure, if successful, would indeed provide a first-principles derivation of the scaling behaviour itself, which has, up to now, been lacking (except for specific soluble models discussed in section 4).

Underlying such an idea is the schematic RG flow for the temperature, depicted in figure 4. The critical point T_C corresponds to a fixed point of the RG transformation. At temperatures above (below) T_C, coarse graining the system leads to a system which is more disordered (ordered), corresponding to a system at a higher (lower) temperature. This schematic flow is indicated by the arrows in figure 4. It follows from this that a quench from any $T > T_C$ to any $T < T_C$ should give the same asymptotic scaling behaviour. Any short-range correlations present at the initial temperature will become irrelevant when $L(t) \gg \xi_0$, where ξ_0 is the correlation length for the initial condition. A different universality class is obtained, however, when the initial condition contains sufficiently *long-range* (power-law) spatial correlations, for example following a quench from T_C. Such cases will be discussed below. It follows from the previous section that the initial conditions *cannot* affect the growth law (provided that they still yield scaling behaviour).

According to figure 4, asymptotic scaling is controlled by the zero-temperature (or *strong-coupling*) fixed point, justifying the neglect of thermal noise in the equations of motion. We shall see below how this works out in practice. A classification of systems according to the role of thermal noise has been given by Lai *et al.* [129]. In some systems, such as the Cahn–Hilliard systems considered in this section, thermal noise can simply be neglected. For kinetic Ising models (with conserved dynamics), where freezing occurs for T strictly zero, the temperature modifies the bare transport

coefficient λ, but in a scale-independent way that does not change the growth law. In systems with quenched disorder, however, there is a *scale-dependent* renormalization of the kinetic coefficients that leads to logarithmic growth with T-dependent amplitudes. This case will be discussed in detail in section 8.3.2.

The idea of using RG methods in this context is not new (for example [129, 130]), but in practical applications the RG framework has been exploited mostly in the numerical context via, for example, the Monte Carlo RG [131].

The difficulty with applying the RG to phase ordering is that, owing to the absence of a convenient small parameter, analogous to $\epsilon = 4 - d$ for critical phenomena, one cannot obtain explicit RG recursion relations. However, one can still make some progress. For conserved fields, a very simple and general result taken over from critical phenomena can be used to determine growth exponents exactly [10, 11], without the need to construct explicit RG recursion relations for the entire set of parameters specifying the equation of motion. Without such explicit recursion relations, of course, the very existence of a fixed point has to be taken on trust. This is tantamount to assuming the validity of the scaling hypothesis *ab initio*, and inferring the existence of an underlying RG fixed point. This is the approach that we shall adopt. It will take us surprisingly far.

8.1. *The renormalization group procedure*

8.1.1. *Equation of motion*

We start by recalling the Cahn–Hilliard equation (3) for a conserved order parameter, generalized to vector fields. Introducing the transport coefficient λ explicitly on the right-hand side (we have previously absorbed λ into the time scale) gives

$$\frac{\partial \vec{\phi}}{\partial t} = \lambda \nabla^2 \left(\frac{\delta F}{\delta \vec{\phi}} \right). \tag{262}$$

Next we Fourier transform, and divide through by λk^2. For generality, and anticipating future requirements, we shall write the equation in the form

$$\left(\frac{1}{\lambda k^{\mu}} + \frac{1}{\Gamma} \right) \frac{\partial \vec{\phi}_{\mathbf{k}}}{\partial t} = - \frac{\delta F}{\delta \vec{\phi}_{-\mathbf{k}}} + \vec{\xi}_{\mathbf{k}}(t). \tag{263}$$

Here we have replaced k^2 by the more general k^{μ}, as in section 7, and included on the left-hand side a term $(1/\Gamma)\partial \vec{\phi}_{\mathbf{k}}/\partial t$ appropriate to non-conserved dynamics, which is recovered in the limit $\lambda \to \infty$. For any finite λ, however, the order parameter is conserved by the dynamics (263). We include the extra term because it will in any case be generated (along with many other terms) after one step of the RG procedure.

A Gaussian white-noise term $\vec{\xi}_{\mathbf{k}}(t)$, representing thermal noise, has also been included in equation (263). We require that the canonical distribution be recovered in equilibrium, that is $P[\vec{\phi}] \propto \exp(-F[\vec{\phi}]/T)$. The usual fluctuation–dissipation relation fixes the noise correlator

$$\langle \xi^i_{\mathbf{k}}(t_1) \xi^j_{-\mathbf{k}}(t_2) \rangle = 2T\delta_{ij}\delta(t_1 - t_2) \left(\frac{1}{\lambda k^{\mu}} + \frac{1}{\Gamma} \right), \tag{264}$$

where $i, j = 1, \ldots, n$ indicate Cartesian components in the internal space. We have argued previously that thermal noise is irrelevant. The RG approach shows this explicitly.

8.1.2. *The coarse-graining step*

One RG step consists of the following four stages:

(*a*) The Fourier components $\vec{\phi}_{\mathbf{k}}(t)$ for the 'hard' modes with $\Lambda/b < k < \Lambda$ are eliminated by solving equation (263) for the time evolution of these modes, and substituting the solution into the equation of motion for the remaining 'soft' modes with $k < \Lambda/b$. Here $\Lambda \sim 1/\xi$ is an ultraviolet cut-off, and b is the RG rescaling factor.

(*b*) A scale change is made, via the change of variable $k = k'/b$, in order to reinstate the ultraviolet cut-off for the soft modes to its original value Λ. Additionally, time is rescaled via $t = b^z t'$. The requirement, imposed by the scaling hypothesis, that the domain morphology is invariant under this procedure, fixes z as the reciprocal of the growth exponent, that is $L(t) \sim t^{1/z}$. Finally, the field $\vec{\phi}_{\mathbf{k}}(t)$ for $k < \Lambda/b$ is rewritten as

$$\vec{\phi}_{\mathbf{k}}(t) = \vec{\phi}_{\mathbf{k}'/b}(b^z t') = b^{\zeta}\vec{\phi}'_{\mathbf{k}'}(t'). \tag{265}$$

The scaling form (7) for the structure factor becomes $S(\mathbf{k}, t) = t^{d/z} g(kt^{1/z})$. From the definition of S and equation (265),

$$S(\mathbf{k}, t) = b^{2\zeta}\langle\vec{\phi}'_{\mathbf{k}'}(t')\cdot\vec{\phi}'_{-\mathbf{k}'}(t')\rangle = b^{2\zeta}t'^{d/z}g(k't'^{1/z}) = b^{2\zeta-d}t^{d/z}g(kt^{1/z}), \tag{266}$$

from which we identify that $\zeta = d/2$.

(*c*) The new equation of motion for the soft modes is interpreted in terms of a rescaled transport coefficient λ' and free energy F'. In addition, terms not originally present in equation (263) will be generated, and must be included in subsequent RG steps. Similarly, one must allow for a more general structure for the thermal noise than equation (264). Finally, the distribution $P_0(\{\vec{\phi}_{\mathbf{k}}(0)\})$ of initial conditions will also be modified by the coarse graining.

(*d*) Scaling behaviour is associated with a fixed point in which both the equation of motion and P_0 are invariant under the RG procedure. In particular the fixed-point free energy is that appropriate to the strong-coupling fixed point, which is attractive for systems below T_C. Note also that the fixed distribution P_0 contains the scaling morphology.

8.1.3. *Renormalization group recursion relations*

Unfortunately, the above procedure cannot be carried out explicitly, owing to the absence of a small parameter and remains largely a '*gedanken* RG'. (Cardy [132] has however, developed a perturbative RG treatment for a system described by the TDGL equation with potential $V(\phi) = g\phi^4$.) Nevertheless, on the assumption that a fixed point exists (equivalent to assuming scaling), the recursion relations for the transport coefficient λ and the temperature T can be written down exactly. This is sufficient to determine z and to test the stability of the *non-conserved* fixed point against the conservation constraint. These results agree with those in section 7. In addition, however, we can also identify universality classes, clarify the role of the initial conditions in determining the large-scale structure and make strong predictions about the effects of quenched disorder. All of these are beyond the scope of the methods of section 7. In this sense, the two approaches are complementary.

The observation that enables further progress is that the $1/\lambda k^{\mu}$ term in the equation of motion (263) is *singular* at $k = 0$. Since no new large-distance singularities can be introduced by the elimination of small length-scale degrees of freedom, it follows that the coarse-graining step (*a*) of the RG does not contribute to the renormalization of $1/\lambda$

in equation (263). (By contrast it can, and does, contribute to the renormalization of $1/\Gamma$ [11], which is a non-singular term in equation (263).) As a result, $1/\lambda$ is changed only by the rescaling step (b). Exactly the same argument at the critical point [9, 133] leads to the identity $z = 4 - \eta$ between the dynamic critical exponent z and the static critical exponent η. It is important to recognize that the latter result is *non-perturbative* and is not restricted to the conventional Wilson–Fisher fixed point.

Since the strong-coupling fixed point is *attractive* (see figure 4), the free-energy functional scales *up* at this fixed point, $F[\{\vec{\phi}_{\mathbf{k}'/b}\}] = b^y F[\{\vec{\phi}_{\mathbf{k}'}\}]$, where the exponent y can be determined by elementary arguments. Using this and equation (265) in equation (263) gives the coarse-grained equation of motion

$$\left(b^{\zeta+\mu-z}\frac{1}{\lambda k'^{\mu}} + b^{\zeta-z}\frac{1}{\Gamma}(1+\ldots)+\ldots\right)\frac{\partial\vec{\phi}'_{\mathbf{k}'}}{\partial t'} + \ldots = -b^{y-\zeta}\frac{\delta F}{\delta\vec{\phi}'_{-\mathbf{k}'}} + \vec{\xi}_{\mathbf{k}'/b}(b^z t'), \quad (267)$$

where ... indicates terms generated by the coarse-graining step. Dividing through by $b^{y-\zeta}$, to restore the right-hand side to its previous form, gives

$$\left(b^{2\zeta+\mu-y-z}\frac{1}{\lambda k'^{\mu}} + b^{2\zeta-y-z}\frac{1}{\Gamma}(1+\ldots)+\ldots\right)\frac{\partial\vec{\phi}'_{\mathbf{k}'}}{\partial t'} + \ldots = -\frac{\delta F}{\delta\vec{\phi}'_{-\mathbf{k}'}} + \vec{\xi}'_{\mathbf{k}'}(t'), \quad (268)$$

where the new noise term is

$$\vec{\xi}'_{\mathbf{k}'}(t') = b^{\zeta-y}\vec{\xi}_{\mathbf{k}'/b}(b^z t'), \quad (269)$$

with correlator

$$\langle\xi'^i_{\mathbf{k}'}(t'_1)\xi'^j_{-\mathbf{k}'}(t'_2)\rangle = b^{2\zeta-2y-z}2T\delta_{ij}\delta(t'_1-t'_2)\left(b^{\mu}\frac{1}{\lambda k'^{\mu}} + \frac{1}{\Gamma}(1+\ldots)\right). \quad (270)$$

The absence of contributions to the $1/\lambda k'^{\mu}$ terms, either in the equation of motion or the noise correlator, from the coarse-graining step, means that the recursion relations for $1/\lambda$ and T can be written down exactly:

$$\left(\frac{1}{\lambda}\right)' = b^{2\zeta+\mu-y-z}\left(\frac{1}{\lambda}\right), \quad (271)$$

$$T' = b^{-y}T. \quad (272)$$

The T equation is just what one would expect. Since the free-energy functional scales *up* as b^y at the strong-coupling fixed point, rewriting the equation of motion, as in equation (268), in a form in which the free-energy functional is *unchanged* is equivalent to scaling temperature *down* by a factor b^{-y}. At the same time, the transport coefficient λ renormalizes as in equation (271). This last equation determines the growth exponent for all cases in which the conservation constraint is *relevant*, in a sense to be clarified below.

8.2. *Fixed points and exponents*

In the strong-coupling phase (i.e. for $T < T_C$), T flows to zero under repeated iteration of the RG procedure, implying that $y > 0$ in equation (272). If the dynamical fixed point controlling the late-stage scaling regime is described by a non-zero value of $1/\lambda$ (i.e. when the conservation law is *relevant*), then equation (271) implies that

$$z = 2\zeta + \mu - y = d + \mu - y, \quad (273)$$

where we inserted the value $\zeta = d/2$ at the last step. Equation (273) is exact, given the scaling assumption underlying the RG treatment.

It is interesting to consider the same argument at the critical fixed point. Then $T' = T = T_C$ implies that $y = 0$ and $z = 2\zeta + \mu$. The structure factor scaling relation reads, for this case, $S(\mathbf{k}, t) = L^{2-\eta} g(kL) = t^{(2-\eta)/z} g(kt^{1/z})$; so the analogue of equation (266) fixes $\zeta = (2-\eta)/2$, and $z = 2 + \mu - \eta$. For $\mu = 2$, this is the familiar result $z = 4 - \eta$ for model B [9, 133], which we stress is an exact non-perturbative result. Equation (273) is just the generalization of this result to the strong-coupling fixed point.

To determine y for the strong-coupling fixed point, we coarse-grain the system on the scale $L(t)$. On this scale the system looks completely disordered; so the excess energy per degree of freedom (i.e. per volume $L(t)^d$) is of the order of the local excess energy density at that scale, that is of order $L(t)^y$. The excess energy density on the original scale therefore decreases as $\epsilon \sim L(t)^{y-d}$. Comparing this with the result (249) for ϵ obtained in section 7 gives

$$y = \begin{cases} d - n, & n \leqslant 2, \\ d - 2, & n \geqslant 2. \end{cases} \tag{274}$$

Note, however, the extra logarithm in equation (249) for $n = 2$.

For the usual scalar ($n = 1$) and vector ($n \geqslant 2$) fields, equation (274) gives the usual results $y = d - 1$ and $y = d - 2$ respectively, familiar from statics; b^{d-1} is just the energy cost of a domain wall of linear dimension b, while b^{d-2} is the energy cost of imposing a slow twist of the vector field over a region of size b^d. The extra logarithm in equation (249) for $n = 2$ is due to the vortices, which dominate over slow 'spin-wave' variations for this case. As an amusing aside, we note that equation (274) gives the 'lower critical dimension' d_l, below which long-range order is not possible for $T > 0$, for the continuation of the theory to real n. Since the existence of an ordered phase requires $y > 0$, we have $d_l = n$ for $n \leqslant 2$ and $d_l = 2$ for $n \geqslant 2$. The result for $n < 2$ recovers the known results for $n = 1$ (the scalar theory) and $n = 0$ (the self-avoiding walk).

Inserting equation (274) into equation (273) gives the final result for z:

$$z = \begin{cases} n + \mu, & n \leqslant 2, \\ 2 + \mu, & n \geqslant 2. \end{cases} \tag{275}$$

These results agree with those derived in section 7, which are summarized in figure 24. For scalar model B ($n = 1$; $\mu = 2$) we recover the usual $t^{1/3}$ Lifshitz–Slyozov growth, while for vector model B with $n > 2$ we obtain $t^{1/4}$ growth. At the cross-over value $n = 2$, there is an extra logarithm that the RG method does not see (since it determines only the growth *exponent*), but which *is* captured by our previous approach (section 7).

Comparison of equation (273) with figure 24 shows that equation (273) is not valid below the line $n + \mu = 2$. How do we see this within the RG approach? Recall that to derive equation (273) we have to assume that $1/\lambda$ is *non-zero* at the fixed point, that is that the conservation constraint is *relevant*, in the RG sense. Consider now the fixed point of the *non-conserved* system, with $\lambda = \infty$ in the equation of motion (263). Let the corresponding value of z be z_{nc}. Now introduce the conservation law through an infinitesimal $1/\lambda$. The recursion relation (271) then gives

$$\left(\frac{1}{\lambda}\right)' = b^{z_c - z_{nc}} \left(\frac{1}{\lambda}\right), \tag{276}$$

where $z_c = 2\zeta + \mu - y$ is the value of z (equation (273)) at the conserved fixed point. Equation (276) shows immediately that $1/\lambda$ iterates to zero for $z_c < z_{nc}$, that is *the conservation law is irrelevant when* $z_c < z_{nc}$. Since $L(t) \sim t^{1/z}$, this means that the

conserved system cannot exhibit *faster* growth than the non-conserved system. This is intuitively reasonable; an additional constraint cannot speed up the dynamics. There is an interchange of stability of RG fixed points when $z_c = z_{nc}$, the fixed point with the larger z being stable. It follows that $z = \max(z_c, z_{nc})$, with z_c given by equation (273) in general and by equation (275) for the O(n) model. Since $z = 2$ for the non-conserved O(n) model (see 7), this interchange of stability accounts for the crossover line $n + \mu = 2$ in figure 24. (We note that the same reasoning implies a similar interchange of stability, and the result $z = \max(z_c, z_{nc})$, at the *critical* fixed point [134].)

The generality of equation (273) deserves emphasis. For any system with purely dissipative conserved dynamics, one only needs to insert the value of y, which can be determined from the energetics as in the derivation of equation (274) for the O(n) model. As an example, consider again the q-state Potts model. The energy density is dominated by domain walls, so the energy density scales as $\epsilon \sim 1/L \sim L^{y-d}$, giving $y = d - 1$ just as for the Ising model. Therefore, the usual Lifshitz–Slyozov $t^{1/3}$ growth is obtained for $\mu = 2$. Of course, we already obtained this result in section 7. Recent numerical studies [128] confirm this prediction.

As a second example we note that, in agreement with our findings in section 7, the growth law is independent of the nature of the initial conditions (which played no role in the derivation), provided that scaling is satisfied. A case of experimental interest is a conserved scalar field; the $t^{1/3}$ Lifshitz–Slyozov growth is obtained for all volume fractions of the two phases. By contrast, the scaling functions *can* depend on the form of the initial conditions. This should not be too surprising, since the fixed-point distribution for the initial conditions contains the scaling morphology. This will be discussed in detail in section 8.3.1.

8.3. *Universality classes*

The present RG approach cannot, unfortunately, determine z_{nc}, since it rests on the fact that $1/\lambda$ is non-zero at the fixed point, nor can it explicitly pick up the logarithms on the boundary lines $n = 2$ and $n + \mu = 2$ of figure 24. So does it have any advantages over the seemingly more powerful energy scaling approach of section 7? The answer is an unequivocal yes. The reason is that the RG identifies *universality classes* as well as exponents. As an example, consider a scalar $n = 1$ system with $\mu < 1$. The energy scaling method tells us that $L(t) \sim t^{1/2}$, as for non-conserved dynamics, but tells us nothing about correlation functions. The RG, by contrast, tells us that, when the conservation is irrelevant, not only the exponents but also all correlation scaling functions are the same as those of the non-conserved system, that is for $\mu < 1$ the scalar system is in the *non-conserved universality class.*

At first this result seems paradoxical; in the scaling form for the structure factor $S(\mathbf{k}, t) = L^d g(kL)$, the scaling function $g(x)$ has a non-zero value at $x = 0$ for non-conserved dynamics whereas, for conserved dynamics, $g(x)$ must vanish at $x = 0$. So how can a system with conserved dynamics be in the non-conserved universality class? To understand this, one needs to remember that the scaling limit is defined by $k \to 0$, $L \to \infty$, with kL fixed but arbitrary. Onuki has argued that, for $\mu < 1$, $S(\mathbf{k}, t) \sim k^{2\mu} L^{d+2}$ for $k \to 0$ [124]. If we imagine plotting $S(\mathbf{k}, t)$ in scaling form, that is $g(x) = L^{-d} S(\mathbf{k}, t)$ against $x = kL$, then Onuki's small-k form gives a $g(x)$ of order unity when $x \sim L^{1-1/\mu}$, which is vanishingly small as $L \to \infty$ for $\mu < 1$. In other words, on a scaling plot the region of kL where the non-conserved scaling function is inaccurate shrinks to zero as $L \to \infty$.

8.3.1. *The role of the initial conditions*

To what extent do the scaling functions depend on the probability distribution for the initial conditions? The RG answers this question [81]. New universality classes are obtained when sufficiently long-ranged (power-law) spatial correlations are present immediately after the quench. These could either arise 'physically', as in a quench from T_C, or be put in 'by hand' as initial conditions on the $T = 0$ dynamics.

Consider initial conditions with a Gaussian probability distribution of variance

$$\langle \phi^i_{\mathbf{k}}(0)\phi^j_{-\mathbf{k}}(0)\rangle = \Delta(k)\delta_{ij}, \tag{277}$$

We recall the definitions, introduced in section 4.2, of the *response to* and *correlation with* the initial condition:

$$G(\mathbf{k},t) = \left\langle \frac{\partial \phi^i_{\mathbf{k}}(t)}{\partial \phi^i_{\mathbf{k}}(0)} \right\rangle \tag{278}$$

$$C(\mathbf{k},t) = \langle \phi^i_{\mathbf{k}}(t)\phi^i_{-\mathbf{k}}(0)\rangle \tag{279}$$

respectively, where $C(\mathbf{k},t)$ is a shorthand for the two-time structure factor $S(\mathbf{k},t,0)$. The Gaussian property of $\{\phi^i_{\mathbf{k}}(0)\}$ means that these two functions are related by

$$C(\mathbf{k},t) = \Delta(k)G(\mathbf{k},t), \tag{280}$$

a trivial generalization of equation (93) that can be proved using integration by parts.

The RG treatment proceeds as in section 8.1.2. The only additional feature is that the scaling form (94) for $G(\mathbf{k},t)$ implies that the initial condition $\vec{\phi}_{\mathbf{k}}(0)$ acquires an anomalous scaling dimension related to the exponent λ. (The exponent λ should not be confused with the transport coefficient; the meaning should be clear from the context.) Therefore we write, analogous to equation (265) for the rescaling of the field at late times,

$$\vec{\phi}_{\mathbf{k}}(0) = \vec{\phi}_{\mathbf{k}'/b}(0) = b^{\chi}\vec{\phi}^i_{\mathbf{k}'}(0) \tag{281}$$

for the rescaling of the initial condition. This gives, analogous to equation (266),

$$G(\mathbf{k},t) = b^{\zeta-\chi}\left\langle \frac{\partial \phi^i_{\mathbf{k}'}(t')}{\partial \phi^i_{\mathbf{k}'}(0)} \right\rangle = b^{\zeta-\chi}t'^{\lambda/z}g_R(k't'^{1/z}) = b^{\zeta-\chi-\lambda}t^{\lambda/z}g_R(kt^{1/z}), \tag{282}$$

from which we identify $\chi = \zeta - \lambda$. The scaling of the equal time structure factor gives, as before, $\zeta = d/2$; so $\chi = d/2 - \lambda$.

Under the RG transformation, the correlator $\Delta(k)$ of the initial condition becomes $b^{2\chi}\langle \phi'^i_{\mathbf{k}'}(0)\phi'^i_{-\mathbf{k}'}(0)\rangle = \Delta(k'/b) + \ldots$, where ... indicates the contribution from the coarse-graining step of the RG. So the new correlator $\Delta'(k') = \langle \phi'^i_{\mathbf{k}'}(0)\phi'^i_{-\mathbf{k}'}(0)\rangle$ is given by

$$\Delta'(k') = b^{2\lambda-d}\left[\Delta\left(\frac{k'}{b}\right) + \ldots\right]. \tag{283}$$

Consider now the case where $\Delta(k)$ has a piece corresponding to long-range (power-law) correlations:

$$\Delta(k) = \Delta_{\mathrm{SR}} + \Delta_{\mathrm{LR}}k^{-\sigma}, \tag{284}$$

with $0 < \sigma < d$. Then the real-space correlations decay as $r^{-(d-\sigma)}$. From equation (283) we can deduce the recursion relations for the short- and long-range parts of the

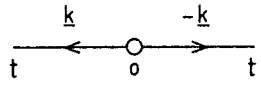

Figure 25. Long-range contribution to the structure factor, for long-range correlations in the initial conditions. The open circle represents the initial condition correlator, equation (277), while the external legs represent the response function (278).

correlator:

$$\Delta'_{\mathrm{SR}} = b^{2\lambda - d}(\Delta_{\mathrm{SR}} + \ldots), \tag{285}$$

$$\Delta'_{\mathrm{LR}} = b^{2\lambda - d + \sigma}\Delta_{\mathrm{LR}}. \tag{286}$$

Note that the long-range part Δ_{LR}, being the coefficient of a singular (as $k \to 0$) term, picks up no contributions from coarse graining; equation (286) is exact.

At the fixed point, both the equation of motion and the initial condition distribution must be invariant under the RG transformation. It follows from equation (286) that the long-range correlations are irrelevant at the 'short-range fixed point' (i.e. Δ_{LR} iterates to zero) if $\sigma < \sigma_{\mathrm{c}}$, where

$$\sigma_{\mathrm{c}} = d - 2\lambda_{\mathrm{SR}}, \tag{287}$$

and λ_{SR} is the value of λ for purely short-range correlations. When $\sigma > \sigma_{\mathrm{c}}$, the invariance of Δ_{LR} at the 'long-range fixed point' fixes $\lambda = \lambda_{\mathrm{LR}} = (d - \sigma)/2$, an exact result. Thus there is an exchange of stability of fixed points when $\sigma = \sigma_{\mathrm{c}}$. The determination of λ_{SR} itself is non-trivial, since it requires computation of the terms represented by ... in equation (285).

For $\sigma > \sigma_{\mathrm{c}}$, the scaling behaviour belongs to a new universality class, in which the growth exponent is unchanged but the scaling functions, for example $g_R(x)$, depend explicitly on σ. Note that the function $C(\mathbf{k}, t)$, the correlation with the initial condition, depends on σ for *any* $\sigma > 0$ through the $k^{-\sigma}$ term in the pre-factor $\Delta(k)$ in equation (280). Thus, in the scaling region,

$$C(\mathbf{k}, t) = \Delta_{\mathrm{LR}} k^{-\sigma} L^{\lambda} g_R(kL). \tag{288}$$

Summing this over k gives the autocorrelation function

$$A(t) \equiv \langle \vec{\phi}(\mathbf{r}, t) \cdot \vec{\phi}(\mathbf{r}, 0) \rangle \sim L^{-(d-\sigma-\lambda)}. \tag{289}$$

In the long-range regime, where $\lambda = (d - \sigma)/2$, this gives $A(t) \sim L^{-(d-\sigma)/2}$. Consider, as an example, the two-dimensional Ising model quenched from the equilibrium state at T_{C}. Then $\sigma = 2 - \eta = \frac{7}{4}$. Measurements of λ for the same model quenched from $T = \infty$, with non-conserved dynamics, give $\lambda_{\mathrm{SR}} \approx 0{\cdot}75$ [17, 19], as do experiments on twisted nematic liquid crystals, which are in the same universality class [21]. Therefore $\sigma > d - 2\lambda_{\mathrm{SR}}$ and this system is in the long-range universality class. It follows that $A(t) \sim L^{-1/8} \sim t^{-1/16}$, which has been confirmed by numerical simulations [81, 90].

The scaling function $g(x)$ for the equal-time structure-factor also has a different form in the long-range regime. For *any* $\sigma > 0$, $S(\mathbf{k}, t)$ has a long-range contribution $S_{\mathrm{LR}}(\mathbf{k}, t)$ varying as $k^{-\sigma}$ at small k. It is given by figure 25, where the open circle represents $\Delta(k)$ and the lines are exact response functions. Thus $S_{\mathrm{LR}}(\mathbf{k}, t) = \Delta_{\mathrm{LR}} k^{-\sigma} G(\mathbf{k}, t) G(-\mathbf{k}, t)$. Using the scaling form (94) for G gives $S_{\mathrm{LR}}(\mathbf{k}, t) = \Delta_{\mathrm{LR}} k^{-\sigma} L^{2\lambda} [g_R(kL)]^2$. Comparing this with the general scaling form $S(\mathbf{k}, t) = L^d g(kL)$, we see that, when $\sigma < \sigma_{\mathrm{c}}$ (i.e. in the short-range regime), S_{LR} is negligible in the scaling limit ($k \to 0, L \to \infty$, with kL fixed) and so does not contribute to the scaling function. Since the long-range correlations are

irrelevant in this case, the scaling function is identical with that for purely short-range correlations.

For $\sigma > \sigma_c$, the contribution S_{LR} survives in the scaling limit, and the full scaling function is long ranged, $g(x) \sim x^{-\sigma}$ for $x \to 0$. In real space, this means that the equal-time correlation function decays with the same power law as the initial-condition correlator, that is $C(\mathbf{r}, t) \sim (L/r)^{d-\sigma}$ for $r \gg L$. For the two-dimensional Ising model quenched from T_c, the predicted $(L/r)^{1/4}$ decay has been seen in simulations [90].

8.3.2. *Systems with quenched disorder*

The influence of quenched disorder on the motion of interfaces and other defects is of considerable current interest in a variety of contexts. The new ingredient when quenched disorder is present is that the defects can become pinned in energetically favourable configurations. At $T = 0$ this leads to a complete cessation of growth. For $T > 0$, thermal fluctuations can release the pins but, in general, growth is much slower than in 'pure' systems, typically logarithmic in time.

To see how logarithms arise, consider a single domain wall in a system with quenched random bonds. The typical transverse displacement of the wall over a length l, due to disorder roughening, is of order l^{ζ}, while the typical fluctuation of the wall energy around its mean value is of order l^{χ}. These exponents are related by the scaling law [135] $\chi = 2\zeta + d - 3$, which can be obtained by estimating the elastic energy of the deformed wall as $l^{d-1}(l^{\zeta}/l)^2$, and noting that the pinning and elastic energies should be comparable. The barrier to domain motion can be estimated by arguing [135–138] that the walls move in sections of length l, where l is the length scale at which the walls 'notice' their curvature, that is the disorder roughening l^{ζ} should be comparable with the distortion, of order $l^2/L(t)$, due to the curvature of walls with a typical radius $L(t)$ of curvature. This gives $l \sim L^{1/(2-\zeta)}$ and an activation barrier of order $l^{\chi} \sim L^{\chi/(2-\zeta)}$ (assuming that the energy *barriers* scale in the same way as the energy *fluctuations* between local equilibrium positions of the wall). Equating this barrier to T gives a growth law

$$L(t) \sim (T \ln t)^{(2-\zeta)/\chi}. \tag{290}$$

For $d = 2$, the exponents ζ and χ are exactly known [139]: $\zeta = \frac{2}{3}$ and $\chi = \frac{1}{3}$, giving $L(t) \sim (T \ln t)^4$. A number of attempts to measure $L(t)$ in computer simulations have been made [140–142], but it is difficult to obtain a sufficiently large range of $(\ln t)^4$ for a convincing test of the theoretical prediction. Recent experimental studies of the two-dimensional random-exchange Ising ferromagnet $Rb_2Cu_{0.89}Co_{0.11}F_4$, however, suggest that $L(t) \sim (\ln t)^{1/\psi}$ with $\psi = 0.20 \pm 0.05$ [143], consistent with the theoretical prediction $\psi = \frac{1}{4}$.

Perhaps of greater interest than the growth law itself is the universality class for the *scaling functions*. It can be argued [19] that, since $L \gg l \sim L^{1/(2-\zeta)}$ for $L \to \infty$ (note that $\zeta < 1$ for a system above its lower critical dimension; otherwise disorder-induced roughening would destroy the long-range order), on length scales of order L the driving force for domain growth is still the interface curvature; the pinning at smaller scales serves merely to provide the (scale-dependent) renormalization of the kinetic coefficient responsible for the logarithmic growth. This leads to the conclusion [19] that the scaling functions should be identical with those of the pure system, a prediction that is supported by numerical studies [141, 142]. The same prediction can be made for systems with random-field (i.e. local symmetry-breaking) disorder [19] and is supported by recent simulations [144].

It is interesting that the argument leading to equation (290) makes no reference to whether the order parameter is conserved or not. The time taken to surmount the pinning barriers dominates all other time scales in the problem. The argument outlined above suggests a scale-dependent kinetic coefficient $\Gamma(L) \sim \exp(-L^{\chi/(2-\eta)}/T)$. Putting this into the usual non-conserved growth law $L \sim [\Gamma(L)t]^{1/2}$ gives $L \sim [T \ln(t/L^2)]^{\chi/(2-\zeta)}$, which reduces to equation (290) asymptotically, since $\ln L \ll \ln t$ for $t \to \infty$. For conserved dynamics, the same argument just gives t/L^3 instead of t/L^2 inside the logarithm, and equation (290) is again recovered asymptotically.

While this physically based argument is certainly plausible, the RG makes a more powerful prediction; not only are the growth laws the same for conserved and non-conserved dynamics, but also they belong to the *same universality class*! This means, *inter alia*, that they have the *same scaling functions*! To see this, we simply note that, since the *fluctuations* in the free energy, $\delta F \sim L^{\chi}$, are asymptotically negligible compared with the *mean*, $\langle F \rangle \sim L^{d-1}$ (provided that the system supports an ordered phase at infinitesimal T), the strong-coupling exponent y is given by the same expression $y = d - 1$ as in the pure system. (Alternatively, and equivalently, the extra length of domain wall owing to disorder roughening of the interfaces in a volume L^d scales as $L^{d-3+2\zeta} \ll L^{d-1}$.) It follows from equation (273) that, *provided that the conservation law is relevant*, the growth law is $L(t) \sim t^{1/3}$ (for $\mu = 2$) as in the pure system. Since, however, equation (290) shows that $L(t)$ grows more slowly than $t^{1/3}$ for the non-conserved system, our previous arguments show that the conservation law is *irrelevant* for systems with quenched disorder. Therefore conserved and non-conserved systems are in the same universality class.

Numerical simulations [145, 146] allow us in principal to test this prediction. They certainly show logarithmic growth, but with an insufficient range of L for a definitive test of equation (290). The most striking conclusion of the RG is that the scaling functions are those of the non-conserved system. For example, a scaling plot for the structure factor, that is a plot of $L^{-d}S(k, t)$ against kL should give a non-zero intercept at $kL = 0$. For any fixed L, of course, the conservation law requires that S vanish at $k = 0$, but in the scaling limit ($k \to 0, L \to \infty$, with kL fixed) the region of small k where the conservation law is effective should shrink to zero faster than $1/L$ as $L \to \infty$. There are indeed indications of this in the small-k data of Iwai and Hayakawa [146], but the range of L explored is not sufficiently large to reach the true scaling limit. Indeed, this will always be difficult with growth as slow as in equation as (290).

8.4. *The renormalization group for binary liquids*

As a final application of the RG approach, we return to phase separation in binary liquids. The new element here is that the temperature T, although formally irrelevant, can enter scaling functions in cases where the minority phase consists of disconnected droplets, when the nominally dominant linear growth due to hydrodynamic flow is absent.

The analysis parallels that of model B, but including the extra hydrodynamic term of equation (51). In order to discuss the role of temperature, we have to include the thermal noise explicitly. The presence of the hydrodynamic term in equation (51) implies, via the fluctuation–dissipation theorem, that the noise correlator takes the form [38]

$$\langle \xi(\mathbf{r}, t)\xi(\mathbf{r}', t') \rangle = -2\lambda T \nabla^2 \delta(\mathbf{r} - \mathbf{r}')\delta(t - t') + 2T\nabla\phi(\mathbf{r}) \cdot T(\mathbf{r} - \mathbf{r}') \cdot \nabla'\phi(\mathbf{r}')\delta(t - t'). \quad (291)$$

Carrying out the RG step as before, the recurrence relations for λ and the viscosity η (implicit in the Oseen tensor (50)) become

$$\left(\frac{1}{\lambda}\right)' = b^{3-z}\left(\frac{1}{\lambda}\right), \tag{292}$$

$$\left(\frac{1}{\eta}\right)' = b^{z-1}\left(\frac{1}{\eta}\right). \tag{293}$$

Equation (292) is the same as equation (271) with $\zeta = d/2$ and $y = d-1$ inserted explicitly. The renormalization of the noise again gives equation (272), which we display again for convenience (with $y = d-1$):

$$T' = b^{1-d}T. \tag{294}$$

It is clear that the conventional conserved fixed point, $\lambda = \lambda^*$, which has $z = 3$, is unstable against the introduction of hydrodynamics, since $1/\eta$ (which measures the strength of the hydrodynamic interaction) scales up as b^2 at this fixed point. Rather, the 'hydrodynamic fixed point', with $\eta = \eta^*$, must have $z = 1$, recovering the dimension-analytical result obtained in section 2.7. At this fixed point, λ scales to zero, that is bulk diffusion of the order parameter is irrelevant at the largest scales. Temperature is also irrelevant, as expected.

The physical arguments of section 2.7 [38, 40], however, show that the linear growth (i.e. $z = 1$), which is a consequence of hydrodynamic flow along interfaces, is possible only when the minority phase is continuous. What happens if the minority phase consists of isolated droplets? Then $z > 1$, and the relevant fixed point must be $\eta^* = 0$. Let us consider the usual conserved (model B) fixed point in this light. This fixed point, with $\lambda = \lambda^*$ non-zero and finite, has $z = 3$, that is $t^{1/3}$ growth. At this fixed point the recursion relations for η and T are $\eta' = b^{-2}\eta$ and $T' = b^{1-d}T$. Therefore η and T both flow to zero, but their *ratio* remains fixed (for $d = 3$). Note that the ratio T/η is exactly what appears in the hydrodynamic part of the noise correlator (291). This means that, while the temperature is technically irrelevant, the hydrodynamic part of the noise cannot be discarded; it is just this part which drives the Brownian motion of the droplets that is responsible for coarsening by droplet coalescence. The ratio T/η is a *marginal* variable; so in principle we expect scaling functions to depend on it, reflecting the relative importance of evaporation–condensation and droplet coalescence to the coarsening (see, however, the discussion below).

To be more precise, we can use dimensional arguments to construct the important variables. The effect of thermal fluctuations on scales smaller than the correlation length ξ can be incorporated through the surface tension σ (which scales F) and the equilibrium order parameter M (which scales ϕ). The length scale associated with the Lifshitz–Slyozov mechanism is then [11, 25] $L(t) = (\lambda\sigma t/M^2)^{1/3}$, while the dimensionless marginal variable is $k_B TM^2/\sigma\lambda\eta$. The general form for $L(t)$ is therefore $L(t) = (\lambda\sigma t/M^2)^{1/3} f(k_B TM^2/\sigma\lambda\eta)$, where $f(x)$ is a cross-over function with $f(0) =$ constant. For large x, one must have $f(x) \sim x^{1/3}$ so that $L(t)$ is independent of λ, giving $L(t) \sim (k_B Tt/\eta)^{1/3}$ in this regime, in agreement with the Brownian motion argument of section 2.7. Note that the function f also depends implicitly on the volume fraction v of the minority phase.

This marginal behaviour is specific to $d = 3$. For general d, equations (293) and (294) give $(T/\eta)' = b^{z-d}(T/\eta)$. So for $d > 3$ the ratio T/η is irrelevant at the

Lifshitz–Slyozov fixed point, and the evaporation–condensation mechanism dominates asymptotically for all $T<T_C$, giving unique scaling functions for a given volume fraction. For $d<3$, on the other hand, T/η is *relevant* at the Lifshitz–Slyozov fixed point. The dynamics is therefore controlled by a 'coalescence fixed point', with T/η fixed, implying that $z=d$, and λ is an irrelevant variable. This agrees with the $d=2$ result of San Miguel *et al.* [147]. To summarize, for $d>3$ the Lifshitz–Slyozov mechanism dominates and $L\sim t^{1/3}$, for $d<3$ coalescence dominates and $z=d$, that is $L\sim t^{1/d}$, while for the physically relevant case $d=3$ both mechanisms operate and marginal behaviour is expected such that, even for a given volume fraction, scaling functions will depend continuously on the dimensionless ratio $k_BTM^2/\sigma\lambda\eta$.

It is important to note, however, that in the above discussion the transport coefficient λ in the equation of motion (51), and the viscosity η appearing in the Oseen tensor (50), have been treated as *independent variables*. While they can certainly be treated as independent in numerical simulations, in real binary liquids they are related [40]. Linearizing equation (51) around one of the bulk phases gives equation (21) as in model B dynamics (the hydrodynamic term in equation (51) drops out at linear order). Inserting the transport coefficient on the right-hand side (it was absorbed into the time scale in equation (21)) gives a bare diffusion constant $D_0=\lambda V''(1)\approx\lambda/\xi^2$, where ξ is the interface thickness. The diffusion constant for a drop of size L is $D(L)\sim D_0\xi/L\sim\mu k_BT\sim k_BT/\eta L$, using the Einstein relation, and the usual relation $\mu(L)\sim 1/\eta L$ for the mobility. This gives $\lambda\eta\sim k_BT\xi$. Using also $\sigma\sim M^2/\xi$, which follows from equation (11), for the surface tension gives the cross-over variable x as $k_BTM^2/\sigma\lambda\eta\approx 1$. A more careful calculation [40] shows that the evaporation–condensation and droplet coalescence mechanisms both lead to a mean droplet size $R(t)$ given by $R^3=k(k_BT/5\pi\eta)t$, with $k=0{\cdot}053$ for the Lifshitz–Slyozov mechanism and $k=12v$ for the droplet coalescence mechanism.

Effectively two-dimensional binary liquid systems can be achieved using the Hele–Shaw geometry, where the fluid is confined between parallel plates. The no-slip boundary conditions mean that the Navier–Stokes equation (47) simplifies, and the results are different from those obtained by simply putting $d=2$ in the previous paragraph, which correspond to using 'free' boundaries. In the Hele–Shaw geometry, $\nabla^2\mathbf{v}$ is dominated by the term $\partial^2\mathbf{v}/\mathrm{d}z^2$, owing to the rapid variation in $\mathbf{v}$ perpendicular to the plates (the z direction). This leads to the Darcy law form of the Navier–Stokes equation (the inertial terms can be neglected owing to the frictional effect of the boundaries):

$$\mathbf{v}=\frac{d^2}{12\eta}(-\nabla p-\phi\nabla\mu), \tag{295}$$

where d is the plate spacing and $\mathbf{v}(x,y)$ is now the velocity averaged over the z direction. Using the incompressibility condition $\nabla\cdot\mathbf{v}=0$ to eliminate p yields an equation of the form (50), but with the Oseen tensor replaced by its Hele–Shaw equivalent

$$T^{\mathrm{HS}}_{\alpha\beta}(\mathbf{k})=\frac{d^2}{12\eta}\left(\delta_{\alpha\beta}-\frac{k_\alpha k_\beta}{k^2}\right). \tag{296}$$

Our starting point for the RG analysis is therefore equations (47) and (291), with the Oseen tensor T replaced by T^{HS}.

Coarse graining in the x–y plane, holding the plate spacing d fixed, gives the recurrence relations

$$\lambda' = b^{z-3}\lambda,$$
$$\eta' = b^{3-z}\eta, \tag{297}$$
$$T' = b^{-1}T,$$

which have the same form as equations (292)–(294), with the extra factor b^2 in the η equation corresponding to the extra factor of k^2 in T^{HS}. Equations (297) still have the Lifshitz–Slyozov fixed point $\lambda = \lambda^*$, with $z = 3$ and T irrelevant, but now η (or the product $\lambda\eta$) is marginal, suggesting again a continuous family of universality classes reflecting the relative importance of bulk diffusion and hydrodynamic flow. In their numerical studies of critical quenches in the Hele–Shaw geometry, Shinozaki and Oono [148] verify the $t^{1/3}$ growth and find that the scaling functions do indeed depend systematically on the value of $\lambda\eta$ (and propose essentially the same explanation).

For any off-critical quench, fluid flow along the interfaces terminates when the droplets of minority phase become circular. Eventually, the Lifshitz–Slyozov mechanism dominates the coarsening, with $L(t) \sim t^{1/3}$ still, but unique scaling functions for a given volume fraction. In this geometry the ratio T/η, representing the hydrodynamic noise, flows to zero at the Lifshitz–Slyozov fixed point, $(T/\eta)' = b^{z-4}(T/\eta)$; so droplet coalescence is subdominant asymptotically in time. If the transport coefficient λ is sufficiently small, however, the coalescence fixed point, with $z = 4$ so that T/η is fixed, will dominate the coarsening for a range of times, giving $L(t) \sim (Tt/\eta)^{1/4}$.

This result may be derived heuristically by extending to the Hele–Shaw geometry the argument given in the final paragraph of section 2.7. For droplets of size R with areal number density $n \sim v/R^2$, where v is the volume fraction, the 'coalescence time' is given by the same expression, $t_c \sim R^2/vD$, as in the bulk case. In the Hele–Shaw geometry, however, the mobility of a droplet of size R is $\mu \sim d/\eta R^2$; so the Einstein relation $D = k_B T\mu$ for the diffusion constant gives $t_c \sim \eta R^4/vdk_B T$. This implies a time dependence $R \sim (vdk_B Tt/\eta)^{1/4}$ for the typical radius of a drop. Comparing this with the Lifshitz–Slyozov growth, $R \sim (\lambda\sigma t/M^2)^{1/3}$, shows that the cross-over from coalescence dominated to Lifshitz–Slyozov dominated regimes occurs when $R \sim vdk_B TM^2/\eta\lambda\sigma$. This length is just vd times the dimensionless cross-over variable x that we identified in the discussion of bulk binary liquids. For real binary liquids (as opposed to computer simulations) we have seen that x is of order unity; so the cross-over length is set by the product vd of the volume fraction and the plate spacing. Since this product is obviously less than d, it follows that a $t^{1/4}$ coalescence regime (which requires $R \gg d$) should be unobservable in real binary liquids.

9. Summary

In this article I have reviewed our current understanding of the dynamics of phase ordering and discussed some recent developments. The concept of topological defects provides a unifying framework for discussing the growth laws for the characteristic scale and motivates approximate treatments of the pair correlation function.

The most important consequence of the presence of topological defects in the system is the generalized Porod law, equation (70), for the large-kL tail of the structure factor. This power-law tail, whose existence has long been known for scalar systems, has recently been observed in computer simulations of various vector systems [100, 122, 149]. It should be stressed that the form of the tail depends only on the nature

of the dominant topological defects. In nematic liquid crystals, for example, the presence of disclinations [47], or '$\frac{1}{2}$ strings', implies a structure factor tail described by equation (70) with $n = 2$ [64], that is a k^{-5} tail for bulk systems. This tail has been seen in simulations [64, 65] and is not inconsistent [64] with experimental results [60, 61].

The Porod law (70), together with the scaling hypothesis, leads to a powerful and general technique for deriving growth laws [79]. The results are summarized in figure 24. Again, the technique is more general than the simple O(n) models to which it has been applied here. Nematic liquid crystals, for example, are described by the non-conserved dynamics of a traceless symmetric tensor field. However, the presence of dominant string defects implies the same growth law as for the O(2) model, namely $L(t) \sim t^{1/2}$, consistent with the simulations [65] (allowing for the predicted logarithmic corrections to scaling) and experiment [60, 61].

The dominant role of topological defects also motivates approximate treatments of the pair correlation scaling function $f(x)$ [55–58, 82], and the systematic treatment [87] discussed in section 5. All these theories lead to the same scaling function (131), with the OJK scaling function (126) corresponding to the special case $n = 1$. The form (131) is a direct consequence of the nonlinear mapping $\vec{\phi}(\vec{m})$, with $\vec{\phi} \to \hat{\mathbf{m}}$ for $|\vec{m}| \to \infty$, and the Gaussian distribution assumed for the field $\vec{m}$. The OJK-type theories [55, 56, 82, 87] and the Mazenko-type theories [57, 58, 85, 86] differ only in the equation for γ, the normalized pair correlation function for $\vec{m}$.

These approximate scaling functions all give good fits to experimental and simulation data (see for example figures 14 and 15). However, there is one important caveat. When fitting data to theoretical scaling functions, it is conventional to adjust the scale length $L(t)$ for the best fit. An *absolute* test can, however, be obtained by calculating two *different* scaling functions and plotting one against the other [101]. For example, the normalized correlator (176) of the square of the field can also be calculated within Gaussian theories of the OJK or Mazenko type [53]. The result depends only on γ, the normalized correlator of the Gaussian auxiliary field. Eliminating γ between $C(12)$ and $C_4(12)$ gives an absolute prediction for the function $C_4(C)$. When this prediction is compared with simulation results, however, the agreement is found to be rather poor (figure 17); C and C_4 can be fitted separately, as functions of $r/L(t)$, by choosing the scale length $L(t)$ independently for each fit but not simultaneously. However, the agreement improves with increasing d, in agreement with the idea that these theories based on a Gaussian auxiliary field become exact at large d [87]. Including the $1/N$ correction in the systematic approach of section 5.2 will presumably improve the fit at fixed d. Mazenko [98] has recently introduced an alternative way of including non-Gaussian corrections and finds improved agreement with the simulation results.

The calculation of scaling functions for *conserved fields* is a significantly greater challenge, especially for scalar fields, where even obtaining the correct $t^{1/3}$ growth law, within an approximate theory for the pair correlation function, is not straightforward. Mazenko [86] has extended his approximate theory to conserved scalar fields, but the agreement with high quality simulation data is not as good as for non-conserved fields [109]. There is an additional complication that a naive application of Mazenko's method gives $t^{1/4}$ growth, which Mazenko argues corresponds to surface diffusion only. In order to recover the $t^{1/4}$ growth he has to add an additional term to incorporate the effect of bulk diffusion. For conserved vector fields, the naive Mazenko approach gives the expected $t^{1/4}$ growth (see figure 24), but without the logarithmic correction expected for $n = 2$. The approximate analytical treatment [75, 110] (presented in section 5.5.1) of the

equation for $C(12)$, valid for $n \gg 1$, gives good agreement with scaling functions extracted from simulations [73]. A systematic approach for conserved fields, generalizing the treatment of section 5.2, would be very welcome, although it is far from straightforward. An even greater challenge is to develop good approximate scaling functions for binary liquids.

To summarize, we have focused on the role of topological defects as a general way of deriving, through the Porod law (70) and the scaling hypothesis (represented by equations (7) and (8)) the forms of the growth laws for phase ordering in various systems. The study of such defects also motivates, through the mapping to an auxiliary field that varies smoothly through the defect, approximate theories of scaling functions. For non-conserved fields, such methods are, in principle, systematically improvable (section 5). One of the challenges for the future is to try to develop comparable methods for conserved fields.

From a wider perspective, phase-ordering dynamics are, perhaps, the simplest example of a scaling phenomenon controlled by a strong-coupling RG fixed point (figure 4). It may not be too much to hope that techniques developed here will find useful applications in other branches of physics.

Acknowledgements

It is a pleasure to thank Rob Blundell, John Cardy, João Filipe, Nigel Goldenfeld, Khurram Humayun, David Jasnow, David Huse, Jürgen Kissner, Satya Majumdar, Gene Mazenko, Alan McKane, Mike Moore, Tim Newman, Yoshi Oono, Sanjay Puri, Andrew Rutenberg, Andres Somoza, Neil Turok and Martin Zapotocky for discussions. I also gratefully acknowledge the hospitality of the Isaac Newton Institute for Mathematical Sciences, where this work was completed.

References

[1] LIFSHITZ, I. M., 1962, *Zh. éksp. teor. Fiz.*, **42,** 1354 (Engl. Transl., 1962, *Sov. Physics JETP*, **15,** 939).
[2] LIFSHITZ, I. M., and SLYOZOV, V. V., 1961, *J. Phys. Chem. Solids*, **19,** 35.
[3] WAGNER, C., 1961, *Z. Elektrochem.*, **65,** 581.
[4] GUNTON, J. D., SAN MIGUEL, M., and SAHNI, P. S., 1983, *Phase Transitions and Critical Phenomena*, Vol. 8, edited by C. Domb and J. L. Lebowitz (New York: Academic Press), p. 267.
[5] BINDER, K., 1987, *Rep. Prog. Phys.*, **50,** 783.
[6] FURUKAWA, H., 1985, *Adv. Phys.*, **34,** 703.
[7] LANGER, J. S., 1992, *Solids Far From Equilibrium*, edited by C. Godrèche (Cambridge University Press), p. 297.
[8] KISSNER, J. G., 1992, Ph. D. Thesis, University of Manchester.
[9] HOHENBERG, P. C., and HALPERIN, B. I., 1977, *Rev. Mod. Phys.*, **49,** 435.
[10] BRAY, A. J., 1989, *Phys. Rev. Lett.*, **62,** 2841.
[11] BRAY, A. J., 1990, *Phys. Rev.* B, **41,** 6724.
[12] BINDER, K., and STAUFFER, D., 1974, *Phys. Rev. Lett.*, **33,** 1006.
[13] MARRO, J., LEBOWITZ, J. L., and KALOS, M. H., 1979, *Phys. Rev. Lett.*, **43,** 282.
[14] FURUKAWA, H., 1978, *Prog. theor. Phys., Osaka*, **59,** 1072; 1979, *Phys. Rev. Lett.*, **43,** 136.
[15] BRAY, A. J., 1990, *J. Phys.* A, **22,** L67; AMAR, J. G., and FAMILY, F., 1990, *Phys. Rev.* A, **41,** 3258; DERRIDA, B., GODRÈCHE, C., and YEKUTIELI, I., 1991, *Phys. Rev.* A, **44,** 6241.
[16] CONIGLIO, A., and ZANNETTI, M., 1989, *Europhys. Lett.*, **10,** 575.
[17] HUMAYUN, K., and BRAY, A. J., 1991, *J. Phys.* A, **24,** 1915.
[18] FURUKAWA, H., 1989, *J. Phys. Soc. Japan*, **58,** 216; 1989, *Phys. Rev.* B, **40,** 2341.
[19] FISHER, D. S., and HUSE, D. A., 1988, *Phys. Rev.* B, **38,** 373 (1988).
[20] NEWMAN, T. J., and BRAY, A. J., 1990, *J. Phys.* A, **23,** 4491.

[21] MASON, N., PARGELLIS, A. N., and YURKE, B., 1993, *Phys. Rev. Lett.*, **70,** 190; ORIHARA, H., and ISHIBASHI, Y., 1986, *J. phys. Soc. Japan*, **55,** 2151; NAGAYA, T., ORIHARA, H., and ISHIBASHI, Y., 1987, *J. phys. Soc. Japan*, **56,** 1898, 3086; 1990, *Ibid.*, **59,** 377.
[22] POROD, G., 1951, *Kolloid, Z.*, **124,** 83; 1952, *Ibid.*, **125,** 51.
[23] DEBYE, P., ANDERSON, H. R., and BRUMBERGER, H., 1957, *J. appl. Phys.*, **28,** 679; POROD, G., 1982, *Small-Angle X-ray Scattering*, edited by O. Glatter and O. Kratky (New York: Academic Press).
[24] ALLEN, S. M., and CAHN, J. W., 1979, *Acta metall.*, **27,** 1085.
[25] HUSE, D. A., 1986, *Phys. Rev.* B, **34,** 7845.
[26] AMAR, J., SULLIVAN, F., and MOUNTAIN, R., 1988, *Phys. Rev.* B, **37,** 196; ROGERS, T. M., ELDER, K. R., and DESAI, R. C., 1988, *Phys. Rev.* B, **37,** 9638; TORAL, R., CHAKRABARTI, A., and GUNTON, J. D., 1989, *Phys. Rev.* B, **39,** 4386; ROLAND, C., and GRANT, M., 1989, *Phys. Rev.* B, **39,** 11971.
[27] RUTENBERG, A. D., and BRAY, A. J., 1994, *Phys. Rev.* E (submitted).
[28] YAO, J. H., ELDER, K. R., GUO, H., and GRANT, M., 1993, *Phys. Rev.* B, **47,** 14110.
[29] ROGERS, T. M., and DESAI, R. C., 1989, *Phys. Rev.* B, **39,** 11956.
[30] MARQUSEE, J. A., and ROSS, J., 1984, *J. chem. Phys.*, **80,** 536.
[31] TOKUYAMA, M., and KAWASAKI, K., 1984, *Physica* A, **123,** 386; TOKUYAMA, M., KAWASAKI, K., and ENOMOTO, Y., 1986, *Physica*, A, **134,** 323; KAWASAKI, K., ENOMOTO, Y., and TOKUYAMA, M., 1986, *Physica*, A, **135,** 426; ENOMOTO, Y., TOKUYAMA, M., and KAWASAKI, K., 1986, *Acta Metall.*, **34,** 2119; TOKUYAMA, M., and ENOMOTO, Y., 1993, *Phys. Rev.* E, **47,** 1156.
[32] VOORHEES, P. W., and GLICKSMAN, M. E., 1984, *Acta metall.*, **32,** 2001; VOORHEES, P. W., 1985, *J. stat. Phys.*, **38,** 231.
[33] BEENAKKER, C. W. J., 1986, *Phys. Rev.* A, **33,** 4482.
[34] ARDELL, A. J., 1990, *Phys. Rev.* B, **41,** 2554; 1972, *Acta metall.*, **20,** 61.
[35] TSUMURAYA, K., and MIYATA, Y., 1983, *Acta metall.*, **31,** 437.
[36] BRAILSFORD, A. D., and WYNBLATT, P., 1979, *Acta metall.*, **27,** 489.
[37] MARDER, M., 1985, *Phys. Rev. Lett.*, **55,** 2953; 1987, *Phys. Rev.* A, **36,** 858.
[38] KAWASAKI, K., and OHTA, T., 1983, *Physica* A, **118,** 175.
[39] OHTA, T., 1984, *Ann. Phys. N.Y.*, **158,** 31.
[40] SIGGIA, E. D., 1979, *Phys. Rev.* A, **20,** 595.
[41] WONG, N. C., and KNOBLER, C. M., 1978, *J. chem. Phys.*, **69,** 725; 1981, *Phys. Rev.* A, **24,** 3205; CHOU, Y. C., and GOLDBURG, W. I., 1979, *Phys. Rev.* A, **20,** 2105; 1981, *Ibid.*, **23,** 858.
[42] PURI, S., and DUNWEG, B., 1992, *Phys. Rev.* A, **45,** 6977; VALLS, O. T., and FARRELL J. E., 1993, *Phys. Rev.* E., **47,** 36; KOGA, T., and KAWASAKI, K., 1993, *Physica* A, **196,** 389.
[43] SHINOZAKI, A., and OONO, Y., 1993, *Phys. Rev.* E., **48,** 2622.
[44] ALEXANDER, F. J., CHEN, S., and GRUNAU, D. W., 1993, *Phys. Rev.* B, **48,** 634.
[45] FURUKAWA, H., 1985, *Phys. Rev.* A., **31,** 1103.
[46] FARRELL, J. E., and VALLS, O. T., 1989, *Phys. Rev.* B, **40,** 7027; 1990, *Ibid.*, **42,** 2353; 1991, *Ibid.*, **43,** 630.
[47] KLÉMAN, M., 1983, *Points, Lines and Walls, in Liquid Crystals, Magnetic Systems, and Various Ordered Media* (New York: Wiley).
[48] OSTLUND, S., 1981, *Phys. Rev.* B, **24,** 485.
[49] PARGELLIS, A. N., FINN, P., GOODBY, J. W., PANNIZZA, P., YURKE, B., and CLADIS, P. E., 1992, *Phys. Rev.* A., **46,** 7765.
[50] YURKE, B., PARGELLIS, A. N., KOVACS, T., and HUSE, D. A., 1993, *Phys. Rev.* E, **47,** 1525.
[51] MUSNY, C. D., and CLARK, N. A., 1992, *Phys. Rev. Lett.*, **68,** 804; PLEINER, H., 1988, *Phys. Rev.* A, **37,** 3986; CLADIS, P. E., VAN SARLOOS, W., FINN, P. L., and KORTAN, A. R., 1987, *Phys. Rev. Lett.*, **58,** 222; RYSKIN, G., and KREMENETSKY, M., 1991, *Phys. Rev. Lett.*, **67,** 1574; PARGELLIS, A., TUROK, N., and YURKE, B., 1991, *Phys. Rev. Lett.*, **67,** 1570.
[52] PISMEN, L. M., and RUBINSTEIN, B. Y., 1992, *Phys. Rev. Lett.*, **69,** 96.
[53] BRAY, A. J., 1993, *Phys. Rev.* E, **47,** 228.
[54] BRAY, A. J., and HUMAYUN, K., 1993, *Phys. Rev.* E, **47,** R9.
[55] BRAY, A. J., and PURI, S., 1991, *Phys. Rev. Lett.*, **67,** 2670.
[56] TOYOKI, H., 1992, *Phys. Rev.* B, **45,** 1965.

[57] LIU, F., and MAZENKO, G. F., 1992, *Phys. Rev.* B, **45,** 6989.
[58] BRAY, A. J., and HUMAYUN, K., 1992, *J. Phys.* A, **25,** 2191.
[59] CHUANG, I., DURRER, R., TUROK, N., and YURKE, B., 1991, *Science*, **251,** 1336; CHUANG, I., TUROK, N., and YURKE, B., 1991, *Phys. Rev. Lett.*, **66,** 2472; YURKE, B., PARGELLIS, A. N., CHUANG, I., and TUROK, N., 1992, *Physica* B, **178,** 56.
[60] WONG, A. P. Y., WILTZIUS, P., and YURKE, B., 1992, *Phys. Rev. Lett.*, **68,** 3583.
[61] WONG, A. P. Y., WILTZIUS, P., LARSON, R. G., and YURKE, B., 1993, *Phys. Rev.* E, **47,** 2683.
[62] DE GENNES, P. G., 1974, *The Physics of Liquid Crystals* (Oxford: Clarendon).
[63] PARGELLIS, A. N., GREEN, S., and YURKE, B., 1994, *Phys. Rev.* E, **49,** 4250.
[64] BRAY, A. J., PURI, S., BLUNDELL, R. E., and SOMOZA, A. M., 1993, *Phys. Rev.* E, **47,** 2261.
[65] BLUNDELL, R. E., and BRAY, A. J., 1992, *Phys. Rev.* A, **46,** R6154.
[66] MAZENKO, G. F., and ZANNETTI, M., 1984, *Phys. Rev. Lett.*, **53,** 2106; 1985, *Phys. Rev.* B, **32,** 4565; ZANNETTI, M., and MAZENKO, G. F., 1987, *Phys. Rev.* B, **35,** 5043. DE PASQUALE, F., 1984, *Nonequilibrium Cooperative Phenomena in Physics and Related Topics*, edited by M. G. Velarde (New York: Plenum), p. 529. DE PASQUALE, F., FEINBERG, D., and TARTAGLIA, P., 1987, *Phys. Rev.* B, **36,** 2220.
[67] CONIGLIO, A., RUGGIERO, P., and ZANNETTI, M., 1994, *Phys. Rev.* E, **50,** 1046.
[68] NEWMAN, T. J., BRAY, A. J., and MOORE, M. A., 1990, *Phys. Rev.* B, **42,** 4514.
[69] KISSNER, J. G., and BRAY, A. J., 1993, *J. Phys.* A, **26,** 1571.
[70] JANSSEN, H. K., SCHAUB, B., and SCHMITTMAN, B., 1989, *Z. Phys.*, **73,** 539.
[71] CONIGLIO, A., OONO, Y., SHINOZAKI, A., and ZANNETTI, M., 1992, *Europhys. Lett.*, **18,** 59.
[72] MONDELLO, M., and GOLDENFELD, N., 1993, *Phys. Rev.* E, **47,** 2384.
[73] SIEGERT, M., and RAO, M., 1993, *Phys. Rev. Lett.*, **70,** 1956.
[74] RAO, M., and CHAKRABARTI, A., 1994, *Phys. Rev.* E, **49,** 3727.
[75] BRAY, A. J., and HUMAYUN, K., 1992, *Phys. Rev. Lett.*, **68,** 1559.
[76] NAGAI, T., and KAWASAKI, K., 1986, *Physica* A, **134,** 483; RUTENBERG, A. D., and BRAY, A. J., 1994, *Phys. Rev.* E, **50,** 1900.
[77] BRAY, A. J., DERRIDA, B., and GODRÈCHE, C., 1994, *Europhys. Lett.*, **27,** 175.
[78] DERRIDA, B., BRAY, A. J., and GODRÈCHE, C., 1994, *J. Phys.* A, **27,** L357.
[79] BRAY, A. J., and RUTENBERG, A. D., 1994, *Phys. Rev.* E, **49,** R27.
[80] KAY, M., RUTENBERG, A. D., and BRAY, A. J., 1994, unpublished.
[81] BRAY, A. J., HUMAYUN, K., and NEWMAN, T. J., 1991, *Phys. Rev.* B, **43,** 3699.
[82] OHTA, T., JASNOW, D., and KAWASAKI, K., 1982, *Phys. Rev. Lett.*, **49,** 1223.
[83] KAWASAKI, K., YALABIK, M. C., and GUNTON, J. D., 1978, *Phys. Rev.* A, **17,** 455.
[84] MAZENKO, G. F., 1989, *Phys. Rev. Lett.*, **63,** 1605.
[85] MAZENKO, G. F., 1990, *Phys. Rev.* B, **42,** 4487.
[86] MAZENKO, G. F., 1991, *Phys. Rev.* B, **43,** 5747.
[87] BRAY, A. J., and HUMAYUN, K., 1993, *Phys. Rev.* E, **48,** 1609.
[88] YEUNG, C., and JASNOW, D., 1990, *Phys. Rev.* B, **42,** 10 523.
[89] OONO, Y., and PURI, S., 1988, *Mod. Phys. Lett.* B, **2,** 861.
[90] HUMAYUN, K., and BRAY, A. J., 1993, *Phys. Rev.* B, **46,** 10 594.
[91] SUZUKI, M., 1976, *Prog. theor. Phys., Osaka*, **56,** 77, 477.
[92] PURI, S., and ROLAND, C., 1990, *Phys. Lett.* A, **151,** 500.
[93] LIU, F., and MAZENKO, G. F., 1991, *Phys. Rev.* B, **44,** 9185.
[94] BRAY, A. J., and HUMAYUN, K., 1990, *J. Phys.* A, **23,** 5897.
[95] LIU, F., and MAZENKO, G. F., 1992, *Phys. Rev.* B, **45,** 4656.
[96] TOMITA, H., 1984, *Prog. Theor. Phys., Osaka*, **72,** 656; 1986, *Ibid.*, **75,** 482.
[97] YEUNG, C., OONO, Y., and SHINOZAKI, A., 1994, *Phys. Rev.* E, **49,** 2693.
[98] MAZENKO, G. F., 1994, *Phys. Rev.* E, **49,** 3717.
[99] ABRAMOWITZ, M., and STEGUN, I., 1968, *Handbook of Mathematical Functions* (New York: Dover Publications).
[100] BLUNDELL, R. E., and BRAY, A. J., 1994, *Phys. Rev.* E, **49,** 4925.
[101] BLUNDELL, R. E., BRAY, A. J., and SATTLER, S., 1993, *Phys. Rev.* E, **48,** 2476.
[102] BRAY, A. J., and KISSNER, J. G., 1992, *J. Phys.* A, **25,** 31.
[103] OONO, Y., and PURI, S., 1987, *Phys. Rev. Lett.*, **58,** 836; 1988, *Phys. Rev.* A, **38,** 434.
[104] LIU, F., and MAZENKO, G. F., 1992, *Phys. Rev.* B, **46,** 5963.
[105] OHTA, T., and NOZAKI, H., 1989, *Space–Time Organization in Macromolecular Fluids*, edited by F. Tanaka, M. Doi and T. Ohta (Berlin: Springer), p. 51.

[106] TOMITA, H., 1993, *Prog. theor. Phys., Osaka*, **90,** 521.
[107] KRAMER, E., and MAZENKO, G. F., 1993, unpublished.
[108] MAZENKO, G. F., 1994, preprint.
[109] SHINOZAKI, A., and OONO, Y., 1991, *Phys. Rev. Lett.*, **66,** 173.
[110] ROJAS INIGUEZ, F., and BRAY, A. J., 1994, *Phys. Rev.* E, in press.
[111] YEUNG, C., 1988, *Phys. Rev. Lett.*, **61,** 1135.
[112] FURUKAWA, H., 1989, *Prog. theor. Phys., Osaka, Suppl.*, **99,** 358.
[113] TOMITA, H., 1991, *Prog. theor. Phys., Osaka*, **85,** 47.
[114] FRATZL, P., LEBOWITZ, J. L., PENROSE, O., and AMAR, J., 1991, *Phys. Rev.* B, **44,** 4794.
[115] FRATZL, P., and LEBOWITZ, J. L., 1989, *Acta metall.*, **37,** 3245.
[116] MAZENKO, G. F., 1992, unpublished.
[117] BRAY, A. J., and PURI, S., 1993, unpublished. RUTENBERG, A. D., and BRAY, A. J. 1994, *Phys. Rev.* E, submitted.
[118] HUMAYUN, K., and BRAY, A. J., 1992, unpublished.
[119] TOYOKI, H., 1993, *Mod. Phys. Lett.* B, **7,** 397; 1994, *Formation, Dynamics and Statistics of Patterns*, Vol. 2, edited by K. Kawasaki, M. Suzuki, and A. Onuki (Singapore: World Scientific).
[120] ONUKI, A., 1992, *Phys. Rev.* A, **45,** 3384.
[121] MONDELLO, M., and GOLDENFELD, N., 1992, *Phys. Rev.* A, **45,** 657.
[122] TOYOKI, H., 1991, *J. phys. Soc. Japan*, **60,** 1433.
[123] BRAY, A. J., 1993, *Phys. Rev.* E, **47,** 3191.
[124] ONUKI, A., 1985, *Prog. theor. Phys.*, Osaka, **74,** 1155.
[125] SIEGERT, M., 1994, private communication.
[126] RUTENBERG, A. D., and BRAY, A. J., 1994, *Phys. Rev.* E, **50,** 1900.
[127] ROLAND, C., and GRANT, M., 1990, *Phys. Rev.* B, **41,** 4663.
[128] JEPPESEN, C., and MOURITSEN, O. G., 1993, *Phys. Rev.* B, **47,** 14724.
[129] LAI, Z. W., MAZENKO, G. F., and VALLS, O. T., 1988, *Phys. Rev.* B, **37,** 9481.
[130] MAZENKO, G. F., VALLS, O. T., and ZHANG, F. C., 1985, *Phys. Rev.* B, **32,** 5807.
[131] VIÑALS, J., GRANT, M., SAN MIGUEL, M., GUNTON, J. D., and GAWLINSKI, E. T., 1985, *Phys. Rev. Lett.*, **54,** 1264; KUMAR, S., VIÑALS, J., and GUNTON, J. D., 1986, *Phys. Rev.* B, **34,** 1908; ROLAND, C., and GRANT, M., 1988, *Phys. Rev. Lett.*, **60,** 2657.
[132] CARDY, J. L., 1992, *J. Phys.* A, **25,** 2765.
[133] HALPERIN, B. I., HOHENBERG, P. C., and MA, S.-K., 1976, *Phys. Rev.* B, **13,** 4119.
[134] BRAY, A. J., 1991, *Phys. Rev. Lett.*, **66,** 2048.
[135] HUSE, D. A., and HENLEY, C. L., 1985, *Phys. Rev. Lett.*, **54,** 2708.
[136] VILLAIN, J., 1984, *Phys. Rev. Lett.*, **52,** 1543.
[137] BRUINSMA, R., and AEPPLI, G., 1984, *Phys. Rev. Lett.*, **52,** 1543.
[138] NATTERMANN, T., 1985, *Phys. Stat. sol.* (b), **132,** 125.
[139] HUSE, D. A., HENLEY, C. L., and FISHER, D. S., 1985, *Phys. Rev. Lett.*, **5,** 2924.
[140] GREST, G. S., and SROLOVITZ, D. J., 1985, *Phys. Rev.* B, **32,** 3014; CHOWDHURY, D., GRANT, M., and GUNTON, J. D., 1985, *Phys. Rev.* B, **35,** 6792; CHOWDHURY, D., and KUMAR, S., 1987, *J. statist. Phys.*, **49,** 855; OH, J. H., and CHOI, D. I., 1986, *Phys. Rev.* B, **33,** 3448; CHOWDHURY, D., 1990, *J. Phys., Paris*, **51,** 2681.
[141] BRAY, A. J., and HUMAYUN, K., 1991, *J. Phys.* A, **24,** L1185.
[142] PURI, S., CHOWDHURY, D., and PAREKH, N., 1991, *J. Phys.* A, **24,** L1087.
[143] SCHINS, A. G., ARTS, A. F. M., and DE WIJN, H. W., 1993, *Phys. Rev. Lett.*, **70,** 2340.
[144] RAO, M., and CHAKRABARTI, A., 1993, *Phys. Rev. Lett.*, **71,** 3501.
[145] PURI, S., and PAREKH, N., 1992, *J. Phys.* A, **15,** 4127.
[146] IWAI, T., and HAYAKAWA, H., 1993, *J. Phys. Soc., Japan*, **62,** 1583; HAYAKAWA, H., and IWAI, T., 1992, *Pattern Formation in Complex Dissipative Systems*, edited by S. Kai, (Singapore: World Scientific), p. 62.
[147] SAN MIGUEL, M., GRANT, M., and GUNTON, J. D., 1985, *Phys. Rev.* A, **31,** 1001.
[148] SHINOZAKI, A., and OONO, Y., 1992, *Phys. Rev.* A, **45,** R2161.
[149] TOYOKI, H., 1991, *J. phys. Soc. Japan*, **60,** 1153.